UNIVERSITY OF CALIFORNIA
RIVERSIDE

# Complex Dimensions of Self-Similar Systems

A Dissertation submitted in partial satisfaction
of the requirements for the degree of

Doctor of Philosophy

in

Mathematics

by

Erin Peter James Pearse

June 2006

Dissertation Committee:

Dr. Michel Lapidus, Chairperson
Dr. John Baez
Dr. Qi Zhang

**Acknowledgements**

Obviously, I would like to thank my advisor for the diligence, enthusiasm, guidance, and energy without which this dissertation would never have been completed. I would also like to thank my fellow graduate students, especially the members of the Fractal Research Group, for their encouragement and friendship, and for making a lively research environment. I would especially like to thank Britta Daudert for providing an invaluable audience and sounding board.

I am indebted to the members of my committee for taking out of their busy schedules, as well as to the members of the department who always had time for my questions.

Several helpful ideas arose from discussions with Machiel van Frankenhuijsen, Bob Strichartz, Martina Zähle, and Steffen Winter. Accordingly, I am very grateful for their time and insights.

I would also like to thank the London Mathematical Society for allowing me to include most of the paper [LaPe1], which will shortly be appearing in the Journal of the London Mathematical Society, as Chapter 2 of this dissertation.

Finally, and most especially, I would like to thank my wife for her unwavering support. With a thousand little caring details, she has made graduate school a most wonderful experience.

This dissertation is dedicated to my parents and my uncle, for encouraging me to be curious about everything, and for guiding me toward the academic path.

ABSTRACT OF THE DISSERTATION
Complex Dimensions of Self-Similar Systems
by

Erin Peter James Pearse
Doctor of Philosophy, Graduate Program in Mathematics
University of California, Riverside, June 2006
Dr. Michel Lapidus, Chairperson

The theory of complex dimensions of self-similar subsets of $\mathbb{R}$ is studied in some detail in [La-vF4]. This dissertation extends that theory to self-similar sets of $\mathbb{R}^d$. The major themes of this work (as reflected in the title) are: (i) the unification of different aspects of mathematics via the theory of *complex dimensions*, and (ii) that when studying self-similarity, it is necessary to take the defining system of mappings as the primary object of study.

A self-similar set $F$ (or *attractor*) is one satisfying

$$F = \Phi(F) := \bigcup_{j=1}^{J} \Phi_j(F)$$

for some family of contraction similarities $\Phi = \{\Phi_j\}$, henceforth called a *self-similar system*. In order to define the zeta functions which lie at the heart of this study, we first define a *self-similar tiling*; a canonical decomposition of the complement of the attractor $F$ of the self-similar system $\Phi$, within its convex hull. The tiling shares key properties of the system itself and allows for the extension of the theory of complex dimensions to higher-dimensional fractal sets. The tiles constitute a certain neighbourhood of the fixed point $F$; by examining the dynamics of $\Phi$ on them, we study more than just the fixed point of the system.

A zeta function, a generating function for the geometry of the object, is defined in terms of the action of $\Phi$ on the tiling. The *complex dimensions* of the system (or tiling) are the poles of this zeta function.

A key result of [La-vF4] is the (explicit) tube formula for fractal strings (i.e., 1-dimensional tilings). This dissertation obtains a higher-dimensional analogue of this result and exposes connections to geometric measure theory in the process. It turns out that the tube formula for tilings is also a fractal extension of the classical Steiner formula. Instead of being a polynomial in $\varepsilon$ summed over the integers

$\{0, \ldots, d\}$, however, the tube formula for tilings is a power series which also includes one term for each complex dimension. This further justifies the term ‘complex dimensions’ and takes a step toward defining curvature for a fractal.

This dissertation should have applications to spectral asymptotics on domains which are fractal or have fractal boundaries. It may also lead to a robust notion of curvature (measures) for self-similar sets.

# Contents

# List of Figures

# Chapter 1

# Introduction

## 1.1 Background

In [La-vF4], Lapidus and van Frankenhuijsen lay the foundations for a theory of complex dimensions with a rather thorough investigation of the theory of fractal strings. The essential strategy is to study fractal subsets of $\mathbb{R}$ by studying their complements.[1] Such an object may be represented by a sequence of bounded open intervals $L = \{L_n\}_{n=1}^{\infty}$ with lengths

$$\mathcal{L} := \{\ell_n\}_{n=1}^{\infty}, \quad \text{with } \sum_{n=1}^{\infty} \ell_n < \infty. \tag{1.1}$$

The positive numbers $\ell_n$ are the lengths of the connected components (open intervals) of $L$, written in nonincreasing order.

The authors of [La-vF4] are able to relate geometric and physical properties of such objects through the use of zeta functions which contain geometric and spectral information about the given string. This information includes the dimension and measurability of the fractal under consideration, which we now recall.

For a nonempty bounded open set $L \subseteq \mathbb{R}$, $V_L(\varepsilon)$ is defined to be the volume (length, or 1-dimensional Lebesgue measure) of the *inner $\varepsilon$-neighborhood* of $L$:

$$V_L(\varepsilon) := \mathrm{vol}_1\{x \in L \,\vdots\, dist(x, \partial L) < \varepsilon\}, \tag{1.2}$$

[1]For supplementary references on fractal strings, see [LaPo1–2,LaMa,La1–3, HeLa1–2,La-vF2–3].

where $\mathrm{vol}_1$ denotes 1-dimensional Lebesgue measure. In general, a *tube formula* is an explicit expression for $V_L(\varepsilon)$ as a function of $\varepsilon$. As it is shown in [LaPo1] that $V_L$ depends exclusively on $V_{\mathcal{L}}$, the tube formula for a fractal string is defined to be

$$V_{\mathcal{L}}(\varepsilon) := V_L(\varepsilon). \tag{1.3}$$

The *Minkowski dimension* of the boundary $\partial L$ (or of the fractal string $\mathcal{L}$) is

$$D = D_{\partial L} = \inf\{t \geq 0 \,\vdots\, V_{\mathcal{L}}(\varepsilon) = O\left(\varepsilon^{1-t}\right) \text{ as } \varepsilon \to 0^+\}. \tag{1.4}$$

The set $\partial L$ is *Minkowski measurable* if and only if the limit

$$\mathcal{M} = \mathcal{M}(D; \partial L) = \lim_{\varepsilon \to 0+} V_{\mathcal{L}}(\varepsilon)\varepsilon^{-(1-D)} \tag{1.5}$$

exists, and lies in $(0, \infty)$. In this case, $\mathcal{M}$ is called the Minkowski content of $\partial L$. $\mathcal{M}$ is not a measure as it is not countably additive. Minkowski–Bouligand dimension (also called 'box dimension' and other names) and Minkowski content are discussed extensively in the literature. See, e.g., [Man,Tr,La1, LaPo1–2,Mat, La-vF4,HeLa1–2] and the relevant references therein for further information.

A primary goal of this dissertation is to extend much of the 1-dimensional theory of fractal strings to fractal subsets of higher-dimensional Euclidean spaces. Reconsidering the above definitions, if $L$ is an open subset of $\mathbb{R}^d$, then analogous statements hold if $1$ is replaced by $d$ in (1.2)–(1.5). In this case, $\mathrm{vol}_d$ denotes the $d$-dimensional Lebesgue measure (which is area for $d = 2$) in the counterpart of (1.2).

Much of the geometric information about a fractal string is encoded in its *geometric zeta function*, defined to be the meromorphic extension of

$$\zeta_{\mathcal{L}}(s) = \sum_{n=1}^{\infty} \ell_n^s. \tag{1.6}$$

It is shown in [La-vF4, Thm. 1.10] that

$$D = \inf\{\sigma \geq 0 \,\vdots\, \textstyle\sum_{n=1}^{\infty} \ell_n^\sigma < \infty\}, \tag{1.7}$$

i.e., that the Minkowski dimension of a fractal string is the abscissa of convergence of its geometric zeta function [La2]. In accordance with this result, the *complex dimensions of* $\mathcal{L}$ are defined to be the set

$$\mathcal{D}_{\mathcal{L}} = \{\omega \in \mathbb{C} \,\vdots\, \zeta_{\mathcal{L}} \text{ has a pole at } \omega\}. \tag{1.8}$$

One reason why these complex dimensions are important is the explicit tubular formula for fractal strings, a key result of [La-vF4]. Namely, under suitable conditions on the string $\mathcal{L}$, one has the following *tube formula*:

$$V_{\mathcal{L}}(\varepsilon) = \sum_{\omega \in \mathcal{D}_{\mathcal{L}}} \operatorname{res}\left(\zeta_{\mathcal{L}}(s); \omega\right) \frac{(2\varepsilon)^{1-\omega}}{\omega(1-\omega)} + \mathcal{R}(\varepsilon), \tag{1.9}$$

where the sum is taken over the complex dimensions $\omega$ of $\mathcal{L}$, and the error term $\mathcal{R}(\varepsilon)$ is of lower order than the sum as $\varepsilon \to 0^+$. (See [La-vF4, Thm. 8.1].) For the present discussion, the important thing about this formula is its general form:

$$V_{\mathcal{L}}(\varepsilon) = \sum_{\omega \in \mathcal{D}_{\mathcal{L}}} c_\omega \varepsilon^{1-\omega} + \text{ error}, \tag{1.10}$$

In the case when $\mathcal{L}$ is a self-similar string i.e., when $\partial\mathcal{L}$ is a self-similar subset of $\mathbb{R}$, one distinguishes two complementary cases:

(1) In the *lattice case*, i.e., when the underlying scaling ratios have rationally dependent logarithms, the error term vanishes identically and the complex dimensions lie periodically on finitely many vertical lines (including the line $\operatorname{Re} s = D$). In this case, there are infinitely many complex dimensions with real part $D$.

(2) In the *nonlattice case*, the complex dimensions are quasiperiodically distributed and $s = D$ is the only complex dimension with real part $D$. Also, $\mathcal{L}$ is Minkowski measurable if and only if it is nonlattice. Nonlattice dimensions appear in such a way as to have infinitely many with different real parts, but all lying in a horizontally bounded strip $D_l \leq \operatorname{Re} s \leq D$.

This is described in greater detail in Remark 4.3.1. See also [La-vF4, Chap. 2–3] for a discussion of quasiperiodicity, and see [L,La3] and [La-vF4, §2.4] for further discussion of the lattice/nonlattice dichotomy.

The results described above hold only for fractal subsets of $\mathbb{R}$. It is the goal of this dissertation to develop the higher-dimensional analogues of these results and ideas. The primary goal is the tube formula $V_{\mathcal{T}}(\varepsilon)$ for self-similar tilings (1.13) obtained in Chapter 5 which is analogous to (1.10). This result is central to the others (as it incorporates aspects of all the other notions discussed), and has the advantage of being independently verifiable; this is carried out for the Koch tiling in Remark 6.3.2 of Example 6.3.

## 1.2 Overview

Chapter 2 gives a computation of the tube formula for the Koch snowflake curve by hand, i.e., via basic geometric considerations and much computation. The result is a formula of the form

$$V_{\mathrm{Kc}}(\varepsilon) = \sum_{n\in\mathbb{Z}} \varphi_n \varepsilon^{2-D-\mathbb{i}n\mathbf{p}} + \sum_{n\in\mathbb{Z}} \psi_n \varepsilon^{2-\mathbb{i}n\mathbf{p}}, \tag{1.11}$$

for some constant coefficients $\varphi_n$ and $\psi_n$, and some $\mathbf{p} \in \mathbb{R}$, given in full detail in §2.5. This preliminary result serves as a guide and a way to check the theory of the ensuing chapters; the general tube formula should match this one when applied to the Koch curve. Indeed, from (1.11), one sees that the possible complex dimensions of the Koch curve are

$$\mathcal{D}_{\partial L} = \{D + \mathbb{i}n\mathbf{p} \,\vdots\, n \in \mathbb{Z}\} \cup \{\mathbb{i}n\mathbf{p} \,\vdots\, n \in \mathbb{Z}\}.$$

See Remark 2.5.2 for why the word "possible" is used here.

Additionally, the investigations leading to the results obtained in this chapter suggest a different approach for the general case. As described in §2.7, it becomes apparent that one ought to consider the function system which generates the Koch curve as the primary object, rather than the curve itself.

Chapter 3 concerns the development of a framework suitable for the general analysis of self-similar objects, the self-similar tiling constructed in [Pe]. The self-similar tiling $\mathcal{T}$ is the the natural higher-dimensional counterpart of the *self-similar* fractal strings studied in [La-vF4].

To get the flavour of the self-similar tilings, it may be helpful to preview some of the examples given in §3.4; especially Fig. 3.1–3.2. Roughly speaking, the tiling $\mathcal{T}$ is obtained in 4 steps. (1) Begin with an iterated function system (IFS) where the functions are contraction similitudes $\{\Phi_j\}$. (2) Take the convex hull of the attractor of this system. (3) The image of the hull under these mappings is a subset of the hull itself. The components of the complement of this subset will be the generators of the tiling. (4) The successive iteration of the mappings $\{\Phi_j\}$ on the generators produces a tiling of the original attractor. The details of the construction are given in §3.2.

Chapter 4 develops the notion of inradius, the higher-dimensional analogue of the length $\ell_n$. The scaling measure and geometric measure are then defined using the inradius. More precisely, the *scaling measure* encodes all the scaling ratios that occur under iteration of the self-similar system (a type of iterated function system defined in Definition 3.2.1); and the *geometric measure* comes from the scaling measure and encodes the sizes of all the tiles via the inradius; see §4.2. The geometric measure gives the density of geometric states of the tiling; it records the size and type of tiles occurring in the tiling $\mathcal{T}$.

Also, a given tiling has a *scaling zeta function* $\zeta_{\mathfrak{s}}$ which is defined as the Mellin transform of the scaling measure; and a *tiling zeta function* $\zeta_{\mathcal{T}}$ which is defined in terms of the scaling zeta function and (several properties of) the generators of the tiling. The scaling zeta function is defined entirely in terms of the scaling ratios of the similarity transformations $\{\Phi_j\}$ and consequently is formally identical to the geometric zeta function of a (normalized) ordinary fractal string as given in (1.6). The *scaling complex dimensions* $\mathcal{D}_{\mathfrak{s}}$ is defined to be the set of poles of the scaling zeta function $\zeta_{\mathfrak{s}}$. It turns out that the structure of the set of scaling complex dimensions is identical to the structure of the set of complex dimensions of a fractal string, as studied in [La-vF4]. In particular, the lattice/nonlattice dichotomy still holds, as does the structure theorem [La-vF4, Thm. 2.17]. The tiling zeta function $\zeta_{\mathcal{T}}$ is closely related, but is actually a generating function for the entire geometry of the tiling; i.e., it encodes all pertinent geometric data of the tiling. Accordingly, the tiling zeta function $\zeta_{\mathcal{T}}$ is meromorphic and distribution-valued and appears as a sum over the complex dimensions of the tiling. The set of complex dimensions of the tiling $\mathcal{T}$ is defined to be $\mathcal{D}_\mathcal{T} := \mathcal{D}_\mathfrak{s} \cup \{0, 1, \ldots, d-1\}$. Thus, that is, $\zeta_\mathcal{T}$ has a term for each scaling complex dimension in $\mathcal{D}_\mathfrak{s}$, and for each integral dimension $0, 1, \ldots, d-1$.

Chapter 5 uses the self-similar tiling and associated zeta functions to develop a tube formula for self-similar tilings. §5.2 describes how the pieces of the puzzle fit together, i.e., how the tube formula $V_\mathcal{T}(\varepsilon)$ is understood as a distribution, and the general strategy for assembling the tube formula from the various ingredients (measures, zeta functions, etc.). The generality of the theory of distributional explicit formulas developed in [La-vF4] makes it perfectly suitable for self-similar tilings. Although the main result of this chapter is obtained for fractal sprays (a slightly more general object), we are primarily interested in its applications to self-similar tilings.

The extended distributional formula [La-vF4, Thm. 5.26] is used to obtain an expression for the distributional action of the geometric measure $\eta_\mathfrak{g}$ on a test function $\varphi$. This test function is not required to be smooth on $(0, \infty)$; these technicalities are discussed in Theorem 5.3.4. We apply the extended distributional formula to a specific test function $\gamma_G$ which gives the tube formula for a tile of $\mathcal{T}$ that has inradius $1/x$. This will produce a tube formula for the tiling:

$$V_\mathcal{T}(\varepsilon) = \langle \eta_\mathfrak{g}, \gamma_G \rangle. \tag{1.12}$$

Development of this expression produces the higher-dimensional tube formula given in Theorem 5.4.5:

$$V_\mathcal{T}(\varepsilon) = \sum_{\omega \in \mathcal{D}_\mathfrak{s} \cup \{0,1,\ldots,d-1\}} c_\omega \varepsilon^{d-\omega} + \mathcal{R}(\varepsilon), \tag{1.13}$$

where $\omega \in \mathcal{D}_\mathfrak{s}$ is a scaling dimension (i.e., a pole of the scaling zeta function $\zeta_\mathfrak{s}$), and each coefficient $c_\omega$ in (1.13) is defined in terms of the residue of the tiling zeta function at the complex dimension $\omega$. Theorem 5.5.1 shows how the error term $\mathcal{R}$ vanishes for self-similar tilings.

It is clear that (1.13) is an extension of (1.10), it is shown in §5.6 precisely how the two coincide for $d = 1$. However, much more is true. When the tileset nontriviality condition (defined in Definition 3.2.7) is not satisfied, the self-similar system has a convex or 'trivially self-similar' attractor, and the tube formula (1.13) devolves into a close relative of Steiner's classical tube formula for convex or polyconvex sets; this is discussed in Remark 5.4.7. Steiner's formula is discussed in more detail in Remark 4.4.5 and Remark 4.4.6, but it is essentially a polynomial in $\varepsilon$ of the form

$$V_A(\varepsilon) = \sum_{i \in \{0,1,\ldots,d-1\}} c_i \varepsilon^{d-i}. \tag{1.14}$$

Thus, the investigations described in this dissertation have uncovered connections between fractal geometry and geometric measure theory!While these two fields are thematically intimate, there has not previously been much overlap in the way of formulas or specific results. The relationships discovered in the course of the research leading to this dissertation yield new insights into the 1-dimensional theory of fractal strings and provide new geometric interpretations for previous results. Additionally, some of the ideas developed herein may allow for the development of a rigourous notion of fractal curvature in the near future; this is the subject [LaPe3]. In particular the coefficients $c_\omega$ appearing in (1.13) are almost exactly equal to those in (1.14) for $\omega = \{0, 1, \ldots, d-1\}$, as one might expect by comparison with the tube formulas of Steiner, Weyl, and Federer; see [Schn2,We,Fed]. This leads one to believe that the other coefficients $c_\omega$ (which are defined in terms of residues of the tiling zeta function $\zeta_{\mathcal{T}}$ at $\omega$) may also have an interpretation in terms of curvature. In particular, the role played by the complex dimensions in the tube formula for the tiling gives further justification for calling these objects "dimensions".

A selection of examples is given in Chapter 6. Tilings are presented for the Cantor set, Koch curve, Sierpinski gasket, Sierpinski carpet, pentagasket, and Menger sponge. For each example, the tiling is given, along with the associated measures, zeta functions, complex dimensions, and tube formulas.

Finally, Chapter 7 contains some concluding remarks, including some reflections on the results of this dissertation and how they mesh with previous results, and some ideas for future directions of research.

*Remark* 1.2.1 (A note on the references). The primary reference for this dissertation is the research monograph "Fractal Geometry, Complex Dimensions and Zeta

Functions: Geometry and spectra of fractal strings" by Lapidus and van Frankenhuijsen [La-vF4]. This volume is essentially a revised and much expanded version of "Fractal Geometry and Number Theory: Complex dimensions of fractal strings and zeros of zeta functions" [La-vF1], by the same authors. The present paper cites [La-vF4] almost exclusively, so we provide the following partial correspondence between chapters for the aid of the reader, as [La-vF4] has not yet appeared at the time of this writing.

| [La-vF1] | Ch. 2 | Ch. 3 | Ch. 4 | Ch. 6 |
|---|---|---|---|---|
| [La-vF4] | Ch. 2–3 | Ch. 4 | Ch. 5 | Ch. 8 |

*Remark* 1.2.2. Throughout, we reserve the symbol $\mathbb{i} = \sqrt{-1}$ for the imaginary number.

# Chapter 2

# The Koch Tube Formula

## 2.1 Introduction

In this chapter, the tube formula $V_{\mathrm{Kc}}(\varepsilon)$ is computed for a well-known (and well-studied) example, the Koch snowflake.[1] This curve provides an example of a *lattice self-similar fractal* and a nowhere differentiable plane curve. The Koch snowflake can be viewed as the boundary $\partial L$ of a bounded and simply connected open set $L \subseteq \mathbb{R}^2$ and that it is obtained by fitting together three congruent copies of the Koch curve $K$, as shown in Fig. 2.1. A general discussion of the Koch curve may be found in [Man, §II.6] or [Fal1, Intro. and Chap. 9].

The Koch curve is a self-similar fractal with dimension $D := \log_3 4$ (Hausdorff and Minkowski dimensions coincide for the Koch curve) and may be constructed by means of its self-similar structure (as in [Kig, §1.2] or [Fal1, Chap. 9])

[1]I gratefully acknowledge the London Mathematical Society for allowing me to include in this chapter material from [LaPe1], a paper which is to be published shortly in the Journal of the London Mathematical Society.

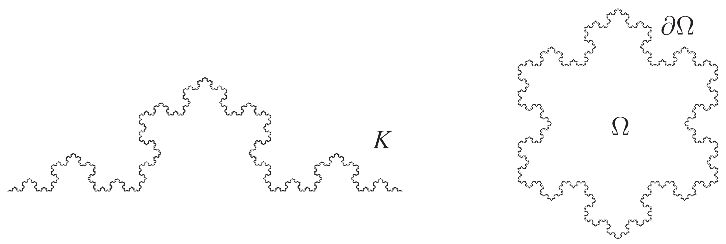


Figure 2.1: The Koch curve $K$ and Koch snowflake domain $L$.

as follows: let $\xi = \frac{1}{2} + \frac{1}{2\sqrt{3}}\mathbb{i}$, with $\mathbb{i} = \sqrt{-1}$, and define two maps on $\mathbb{C}$ by

$$\Phi_1(z) := \xi\bar{z} \quad \text{and} \quad \Phi_2(z) := (1-\xi)(\bar{z}-1)+1.$$

Then the Koch curve is the self-similar set of $\mathbb{R}^2$ with respect to $\{\Phi_1, \Phi_2\}$; i.e., the unique nonempty compact set $K \subseteq \mathbb{R}^2$ satisfying $K = \Phi_1(K) \cup \Phi_2(K)$. See Definition 3.2.4 and the examples of §3.4 for more on this.

The main result of this chapter is the following new result.

**Theorem 2.1.1.** *The area of the inner $\varepsilon$-neighbourhood of the Koch snowflake is given by the following tube formula:*

$$V_{Kc}(\varepsilon) = G_1(\varepsilon)\varepsilon^{2-D} + G_2(\varepsilon)\varepsilon^2, \tag{2.1}$$

*where $D = \log_3 4$ is the Minkowski dimension of $\partial L$, $\mathbf{p} := 2\pi/\log 3$ is the oscillatory period, and $G_1$ and $G_2$ are periodic functions (of multiplicative period 3) which are discussed in full detail in Theorem 2.5.1. This formula may also be written*

$$V_{Kc}(\varepsilon) = \sum_{n\in\mathbb{Z}} \varphi_n \varepsilon^{2-D-\mathbb{i}n\mathbf{p}} + \sum_{n\in\mathbb{Z}} \psi_n \varepsilon^{2-\mathbb{i}n\mathbf{p}}, \tag{2.2}$$

*for suitable constants $\varphi_n, \psi_n$ which depend only on $n$. These constants are expressed in terms of the Fourier coefficients $g_\alpha$ of a multiplicative function which bears structural similarities to the classical Cantor–Lebesgue function described in more detail in §2.6.*

While this formula is new, it should be noted that a previous approximation has been obtained in [La-vF1, §10.3]; see (2.13) in Rem. 2.2.3 below. The present formula, however, is exact. By reading off the powers of $\varepsilon$ appearing in (2.2), one immediately obtains the following corollary:

**Corollary 2.1.2.** *The possible*[2] *complex dimensions of the Koch snowflake are*

$$\mathcal{D}_{\partial L} = \{D + \mathbb{i}n\mathbf{p} \,\vdots\, n \in \mathbb{Z}\} \cup \{\mathbb{i}n\mathbf{p} \,\vdots\, n \in \mathbb{Z}\}. \tag{2.3}$$

This is illustrated in Fig. 2.8. Also, for more precision regarding Cor. 2.1.2, see Remark 2.5.3 below, as well as the discussion surrounding (2.42).

[2] *The reason for the word "possible" is discussed in Remark 2.5.2.*

*Remark* 2.1.3. The significance of the tube formula (2.1) is that it gives a detailed account of the oscillations that are intrinsic to the geometry of the Koch snowflake curve. More precisely, the *real part* $D$ yields the order of the *amplitude* of these oscillations (as a function of $\varepsilon$) while the imaginary part $n\mathbf{p} = 2\pi n/\log 3$ $(n = 0, 1, 2, \dots)$ gives their *frequencies*. This is in agreement with the 'philosophy' of the mathematical theory of the complex dimensions of fractal strings as developed in [La-vF4]. Additionally, if one can show the existence of a complex dimension with real part $D$ and imaginary part $\mathbb{i}n\mathbf{p}, n \neq 0$, then Theorem 2.1.1 immediately implies that the Koch curve is not Minkowski measurable, as conjectured in [La3, Conj. 2&3, pp. 159,163–4].

The rest of this chapter is dedicated to the proof of Theorem 2.1.1 (stated more precisely as Theorem 2.5.1). More specifically, §2.2 gives an approximation to the area $V_{\text{Kc}}(\varepsilon)$ of the inner $\varepsilon$-neighborhood. In §2.3, the 'error' resulting from this approximation is taken into account. The form of this error is studied further in §2.3.1, and the amount of it in §2.3.2. Results from §2.2 and §2.3 are combined in §2.4 to deduce the tube formula Theorem 2.5.1. There are also some comments on the interpretation of Theorem 2.5.1 included in §2.5. Finally, §2.6 discusses some of the properties of the Cantor-like and multiplicatively periodic function $h(\varepsilon)$, the Fourier coefficients of which occur explicitly in the expansion of $V_{\text{Kc}}(\varepsilon)$ stated in Theorem 2.5.1.

## 2.2 Estimating the area

Consider an approximation to the inner $\varepsilon$-neighbourhood of the Koch curve, as shown in Fig. 2.3. Although the eventual goal is to compute the neighborhood

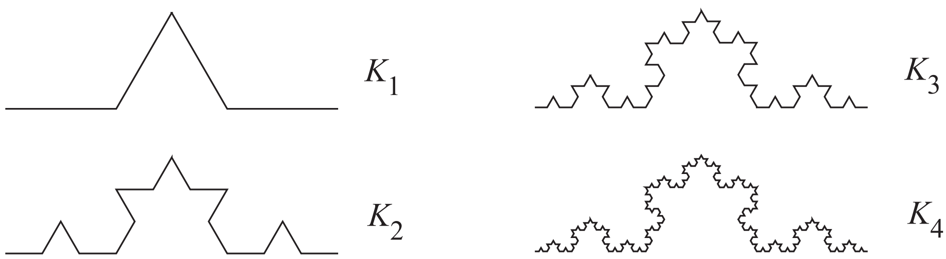


Figure 2.2: The first four stages in the geometric construction of $K$.

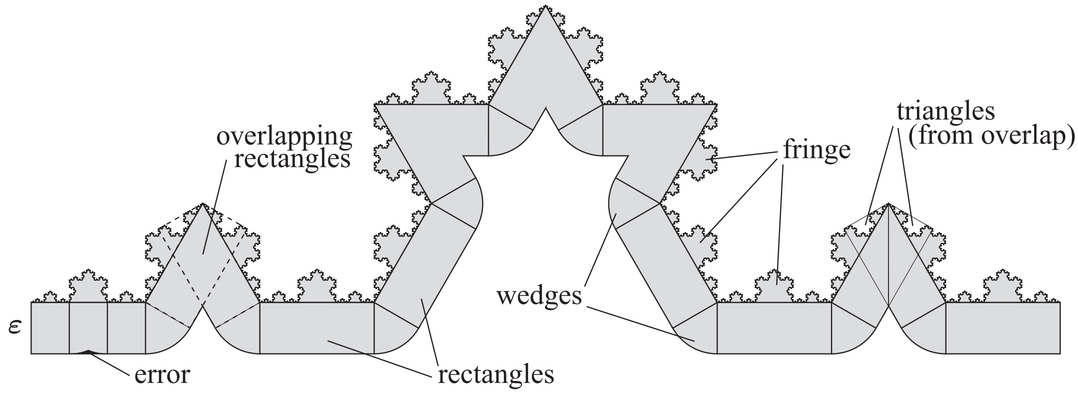


Figure 2.3: An approximation to the inner $\varepsilon$-neighbourhood of the Koch curve, with $\varepsilon \in I_2$. The refinement level here is based on the graph $K_2$, the second stage in the geometric construction of the Koch curve (see Fig. 2.2).

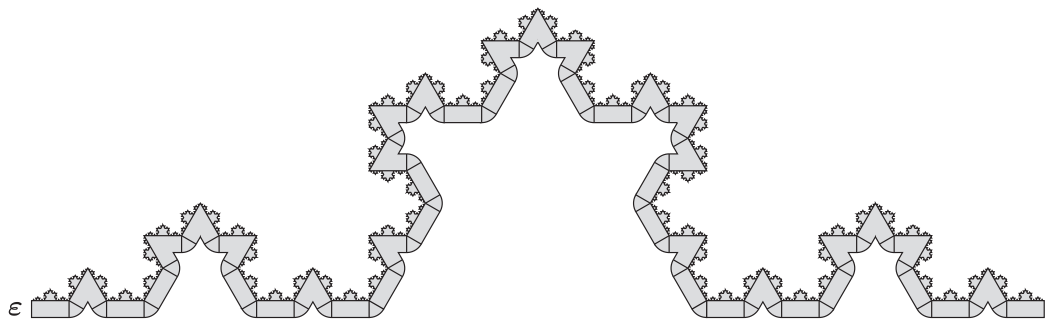


Figure 2.4: A smaller $\varepsilon$-neighbourhood of the Koch curve, for $\varepsilon \in I_3$. This refinement level is based on the graph $K_3$, the third stage in the construction of the Koch curve.

for the entire snowflake, it will be more convenient to work with one third of it throughout the sequel (as depicted in the figure).

A first step is to determine the area of the $\varepsilon$-neighbourhood with functions that give the area of each kind of piece (rectangle, wedge, fringe, as shown in the figure) in terms of $\varepsilon$, and functions that count the number of each of these pieces, in terms of $\varepsilon$. As seen by comparing Fig. 2.3 to Fig. 2.4, the number of such pieces increases exponentially.

The base of the Koch curve has length 1. The approximation is carried out for different values of $\varepsilon \in [0, 1]$, as the main concern will be the behavior of $V_{\mathrm{Kc}}(\varepsilon)$ as $\varepsilon \to 0^+$. In particular, let

$$I_n := (3^{-(n+1)}/\sqrt{3}, 3^{-n}/\sqrt{3}]. \tag{2.4}$$

Whenever $\varepsilon = 3^{-n}/\sqrt{3}$, the approximation shifts to the next level of refinement. For example, Fig. 2.3 shows $\varepsilon \in I_2$, and Fig. 2.4 shows $\varepsilon \in I_3$. Consequently, for $\varepsilon \in I_0$, it suffices to consider an $\varepsilon$-neighbourhood of the prefractal curve $K_0$ , and for $\varepsilon \in I_1$, it suffices to consider an $\varepsilon$-neighbourhood of the prefractal curve $K_1$, etc. Fig. 2.2 shows these prefractal approximations.

For a neighbourhood of $K_n$, the function

$$n = n(\varepsilon) := \left[\log_3 \frac{1}{\varepsilon\sqrt{3}}\right] = [x] \tag{2.5}$$

gives the $n$ for which $\varepsilon \in I_n$. Here, the square brackets indicate the floor function (integer part) and

$$x := -\log_3(\varepsilon\sqrt{3}), \tag{2.6}$$

a notation which will frequently prove convenient in the sequel. Further, let

$$\{x\} := x - [x] \in [0, 1) \tag{2.7}$$

denote the fractional part of $x$.

Observe that for $\varepsilon \in I_n$, $n$ is fixed even as $\varepsilon$ is changing. To see how this is useful, consider that for all $\varepsilon$ in this interval, the number of rectangles (including those which overlap in the corners) is readily seen to be the fixed number

$$r_n := 4^n. \tag{2.8}$$

Also, each of these rectangles has area $\varepsilon 3^{-n}$, where $n$ is fixed as $\varepsilon$ traverses $I_n$. Continuing in this constructive manner, one obtains the following lemma.

**Lemma 2.2.1.** *For $\varepsilon \in I_n$, there are*

*(i) $r_n = 4^n$ rectangles, each with area $\varepsilon 3^{-n}$,*

*(ii) $w_n = \frac{2}{3}(4^n - 1)$ wedges, each with area $\frac{\pi\varepsilon^2}{6}$,*

*(iii) $u_n = \frac{2}{3}(4^n + 2)$ triangles, each with area $\frac{\varepsilon^2\sqrt{3}}{2}$, and*

*(iv) $4^n$ components of fringe, each with area $\frac{\sqrt{3}}{20}9^{-n}$.*

*Proof.* Part (i) is already established. For (ii), exploit the self-similarity of the

Koch curve $K$ to obtain the recurrence relation $w_n = 4w_{n-1} + 2$, which can be solved to find the number of wedges

$$w_n := \sum_{j=0}^{n-1} 2 \cdot 4^j = \tfrac{2}{3}\left(4^n - 1\right). \tag{2.9}$$

The area of each wedge is clearly $\pi\varepsilon^2/6$, as the angle is always fixed at $\pi/3$.

(iii) To prevent double-counting, it will be necessary to keep track of the number of rectangles that overlap in the acute angles so that the appropriate number of triangles may be subtracted. This quantity is

$$u_n := 4^n - \sum_{j=1}^{n-1} 4^j = \tfrac{2}{3}\left(4^n + 2\right), \tag{2.10}$$

and each of these triangles has area $\varepsilon^2\sqrt{3}/2$.

(iv) To measure the area of the fringe, note that the area under the entire Koch curve is given by $\sqrt{3}/20$, so the fringe of $K_n$ will be this number scaled by $\left(3^{-n}\right)^2$. There are $4^n$ components, one atop each rectangle (see Fig. 2.3). $\square$

Lemma 2.2.1 gives a preliminary area formula for the $\varepsilon$-neighbourhood. Here, 'preliminary' indicates the absence of the 'error estimate' developed in §2.3.

**Lemma 2.2.2.** *The $\varepsilon$-neighbourhood of the Koch curve has approximate area*

$$\widetilde{V}_{Kc}(\varepsilon) = \varepsilon^{2-D} 4^{-\{x\}} \left( \tfrac{3\sqrt{3}}{40} 9^{\{x\}} + \tfrac{\sqrt{3}}{2} 3^{\{x\}} + \tfrac{1}{6}\left(\tfrac{\pi}{3} - \sqrt{3}\right)\right) - \tfrac{\varepsilon^2}{3}\left(\tfrac{\pi}{3} + 2\sqrt{3}\right). \tag{2.11}$$

This formula is *approximate* in the sense that it measures a region slightly larger than the actual $\varepsilon$-neighbourhood. This discrepancy is accounted for and analyzed in detail in §3.

*Proof of Lemma 2.2.2.* Using (2.5) and (2.6), we obtain:

$$4^x = \tfrac{1}{2}\varepsilon^{-D}, \qquad 9^{-x} = 3\varepsilon^2, \qquad \left(\tfrac{4}{3}\right)^x = \tfrac{\sqrt{3}}{2}\varepsilon^{1-D}, \qquad \left(\tfrac{4}{9}\right)^x = \tfrac{3}{2}\varepsilon^{2-D}. \tag{2.12}$$

Now using $n = [x] = x - \{x\}$, we compute the contributions of the rectangles, wedges, triangles, and fringe, respectively, as

$$\begin{aligned}
\widetilde{V}^r_{\mathrm{Kc}}(\varepsilon) &= \varepsilon\left(\tfrac{4}{3}\right)^n = \varepsilon^{2-D}\tfrac{\sqrt{3}}{2}\cdot 4^{-\{x\}}3^{\{x\}},\\
\widetilde{V}^w_{\mathrm{Kc}}(\varepsilon) &= \tfrac{\pi\varepsilon^2}{9}(4^n-1) = \varepsilon^{2-D}\tfrac{\pi}{18}\cdot 4^{-\{x\}} - \varepsilon^2\tfrac{\pi}{9},\\
\widetilde{V}^u_{\mathrm{Kc}}(\varepsilon) &= \tfrac{\varepsilon^2\sqrt{3}}{3}(4^n+2) = \varepsilon^{2-D}\tfrac{\sqrt{3}}{6}\cdot 4^{-\{x\}} + \varepsilon^2\tfrac{2\sqrt{3}}{3}, \text{ and}\\
\widetilde{V}^{\mathrm{f}}_{\mathrm{Kc}}(\varepsilon) &= \left(\tfrac{4}{9}\right)^n\left(\tfrac{\sqrt{3}}{20}\right) = \varepsilon^{2-D}\tfrac{3\sqrt{3}}{40}\cdot 4^{-\{x\}}9^{\{x\}}.
\end{aligned}$$

Putting all this together, $\widetilde{V}_{\mathrm{Kc}} = \widetilde{V}^r_{\mathrm{Kc}} + \widetilde{V}^w_{\mathrm{Kc}} - \widetilde{V}^u_{\mathrm{Kc}} + \widetilde{V}^{\mathrm{f}}_{\mathrm{Kc}}$ gives the result. $\square$

*Remark* 2.2.3. It is pleasing to find that this is in agreement with earlier predictions of what $\widetilde{V}_{\mathrm{Kc}}(\varepsilon)$ should look like. In particular, [La-vF1, p. 209] gives the estimate

$$V_{\mathrm{Kc}}(\varepsilon) \approx \varepsilon^{2-D}\frac{\sqrt{3}}{4}4^{-\{x\}}\left(\frac{3}{5}9^{\{x\}} + 6\cdot 3^{\{x\}} - 1\right), \tag{2.13}$$

which differs only from $\widetilde{V}_{\mathrm{Kc}}(\varepsilon)$ in (2.11) by some constant coefficients and the final term of order $\varepsilon^2$.

The Fourier series of the periodic function $\varepsilon^{-(2-D)}\widetilde{V}_{\mathrm{Kc}}(\varepsilon)$ will be required in (2.26). Recall the formula (computed in Appendix A)

$$a^{-\{x\}} = \frac{a-1}{a}\sum_{n\in\mathbb{Z}}\frac{e^{2\pi\mathbb{i}nx}}{\log a + 2\pi\mathbb{i}n}. \tag{2.14}$$

This formula is valid for $a > 0, a \neq 1$ and has been used repeatedly in [La-vF4]. Note that it follows from Dirichlet's Theorem and thus holds in the sense of Fourier series. In particular, the series in (2.14) converges pointwise; this is also true in (2.16) and (2.17) below.

The following identity will be of frequent use throughout this chapter:

$$e^{2\pi\mathbb{i}nx} = \left(\varepsilon\sqrt{3}\right)^{-\mathbb{i}n\mathbf{p}} = (-1)^n\varepsilon^{-\mathbb{i}n\mathbf{p}}, \qquad \text{for } n\in\mathbb{Z}, \tag{2.15}$$

where $\mathbf{p} = 2\pi/\log 3$ is the oscillatory period as in Theorem 2.1.1. Using the notation $x = -\log_3(\varepsilon\sqrt{3})$, the Fourier expansion of $a^{-\{x\}}$ given in (2.14) becomes

$$a^{-\{x\}} = \frac{a-1}{a\log 3}\sum_{n\in\mathbb{Z}}\frac{(-1)^n\varepsilon^{-\mathbb{i}n\mathbf{p}}}{\log_3 a + \mathbb{i}n\mathbf{p}}. \tag{2.16}$$

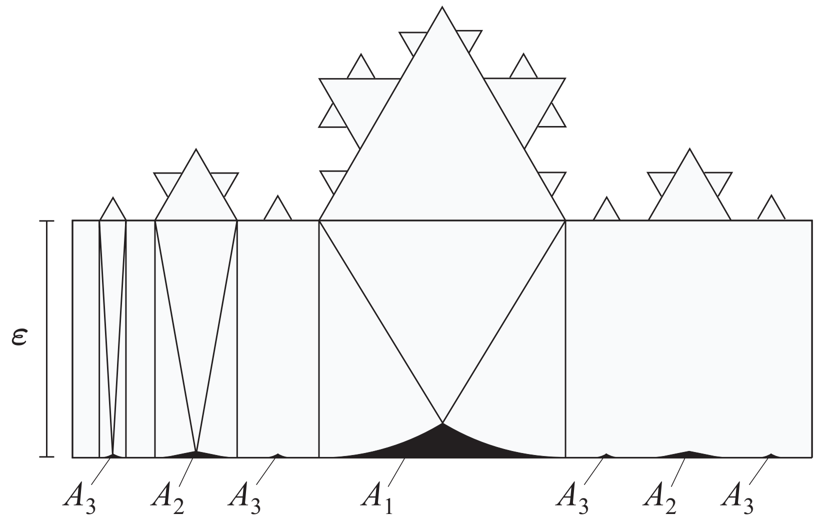


Figure 2.5: An error block for $\varepsilon \in I_n$. The central third of the block contains one large isosceles triangle, two wedges, and the trianglet $A_1$.

Recall that $\{x\} = x - [x]$ denotes the fractional part of $x$. If one uses the notation $D = \log_3 4$, (2.11) can be expressed in terms of (2.16) as a pointwise convergent Fourier series in $\varepsilon$:

$$\widetilde{V}_{\mathrm{Kc}}(\varepsilon) = \tfrac{1}{3\log 3}\sum_{n\in\mathbb{Z}} \left(\tfrac{-3^{5/2}}{2^5(D-2+\mathbb{i}n\mathbf{p})} + \tfrac{3^{3/2}}{2^3(D-1+\mathbb{i}n\mathbf{p})} + \tfrac{\pi-3^{3/2}}{2^3(D+\mathbb{i}n\mathbf{p})}\right)(-1)^n\varepsilon^{2-D-\mathbb{i}n\mathbf{p}} - \tfrac{1}{3}\left(\tfrac{\pi}{3}+2\sqrt{3}\right)\varepsilon^2. \tag{2.17}$$

## 2.3 Computing the error

Now one must account for all the little 'trianglets', the small regions shaped like a crest of water on an ocean wave. These regions were included in the original calculation, but now must be subtracted. This error appeared in each of the rectangles counted earlier, and so the error from one of these rectangles will be referred to as an 'error block'. Fig. 2.5 shows how this error is incurred and how it inherits a Cantoresque structure from the Koch curve. Actually, in §2.3.2 this 'error' will be shown to have several terms, some of which are of the same order as the leading term in $\widetilde{V}_{\mathrm{Kc}}(\varepsilon)$, which is proportional to $\varepsilon^{2-D}$ by (2.17). Hence, caution should be exercised when carrying out such computations and one should not be

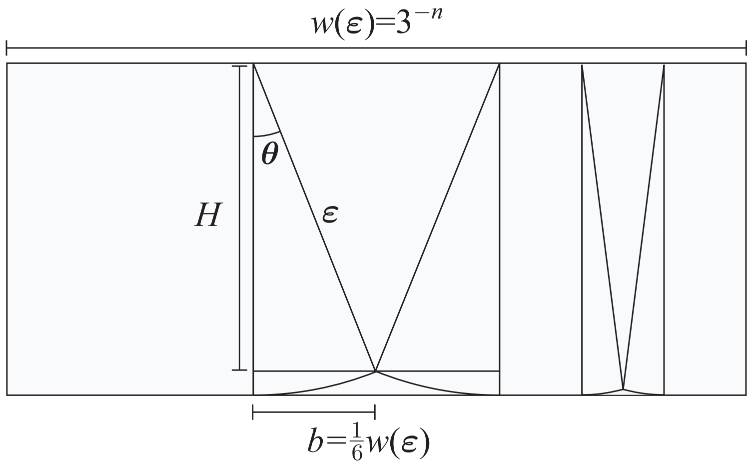


Figure 2.6: Finding the height of the central triangle.

too quick to set aside terms that appear negligible.

### 2.3.1 Finding the area of an 'error block'

In calculating the error, the first step is to find the area of one of these error blocks. Later, the number of these error blocks will be counted, as a function of $\varepsilon$. Note that $n$ is fixed throughout §2.3.1, but $\varepsilon$ varies within $I_n$. Define the function

$$w = w(\varepsilon) := 3^{-n} = 3^{-[x]}. \tag{2.18}$$

This function $w(\varepsilon)$ gives the width of one of the rectangles, as a function of $\varepsilon$ (see Fig. 2.6). Note that $w(\varepsilon)$ is constant as $\varepsilon$ traverses $I_n$, as is $n = n(\varepsilon)$. From Fig. 2.6, one can work out that the area of both wedges adjacent to $A_k$ is

$$\varepsilon^2 \sin^{-1}\left(\tfrac{w}{2\cdot 3^k \varepsilon}\right),$$

and that the area of the triangle above $A_k$ is

$$\varepsilon \tfrac{w}{2\cdot 3^k}\sqrt{1 - \left(\tfrac{w}{2\cdot 3^k \varepsilon}\right)^2}.$$

Then for $k = 1, 2, \ldots$, the area of the trianglet $A_k$ is given by

$$A_k(\varepsilon) = \varepsilon \frac{w(\varepsilon)}{3^k} - \varepsilon^2 \sin^{-1}\left(\frac{w(\varepsilon)}{2 \cdot 3^k \varepsilon}\right) - \varepsilon \frac{w(\varepsilon)}{2 \cdot 3^k} \sqrt{1 - \left(\frac{w(\varepsilon)}{2 \cdot 3^k \varepsilon}\right)^2}, \tag{2.19}$$

and appears with multiplicity $2^{k-1}$, as in Fig. 2.5. Using (2.18) and (2.6), one can write $w(\varepsilon) = 3^{-x} 3^{\{x\}} = \varepsilon\sqrt{3}(\frac{1}{3})^{-\{x\}}$, and define

$$3_k^x := \tfrac{w}{3^k \varepsilon} = 3^{\{x\}-k+1/2}. \tag{2.20}$$

Hence the entire contribution of one error block may be written as

$$B(\varepsilon) := \sum_{k=1}^{\infty} 2^{k-1} \left( 3_k^x - \sin^{-1}\left(\tfrac{3_k^x}{2}\right) - \tfrac{3_k^x}{2}\sqrt{1 - \left(\tfrac{3_k^x}{2}\right)^2} \right) \varepsilon^2. \tag{2.21}$$

Recall the power series expansions

$$\sin^{-1} u = \sum_{m=0}^{\infty} \tfrac{(2m)!\, u^{2m+1}}{2^{2m}(m!)^2(2m+1)} \quad \text{and} \quad \sqrt{1-u^2} = 1 - \sum_{m=0}^{\infty} \tfrac{(2m)!\, u^{2m+2}}{2^{2m+1} m!(m+1)!},$$

which are valid for $|u| < 1$. Apply these formulae to $u = \frac{w}{2 \cdot 3^k \varepsilon}$, so convergence is guaranteed by

$$0 \le \tfrac{w}{2 \cdot 3^k \varepsilon} = \tfrac{3^{\{x\}}\sqrt{3}}{2 \cdot 3^k} \le \tfrac{\sqrt{3}}{2} < 1,$$

and the fact that the series in (2.21) starts with $k = 1$. Then (2.21) becomes

$$\begin{aligned}
B(\varepsilon) &= \sum_{k=1}^{\infty} 2^{k-1} \left[ \tfrac{3_k^x}{2} + \sum_{m=0}^{\infty} \tfrac{(2m)!\,(3_k^x)^{2m+3}}{2^{4m+4} m!(m+1)!} - \sum_{m=0}^{\infty} \tfrac{(2m)!\,(3_k^x)^{2m+1}}{2^{4m+1}(m!)^2(2m+1)} \right] \varepsilon^2 \\
&= \sum_{k=1}^{\infty} 2^{k-1} \left[ \sum_{m=1}^{\infty} \tfrac{(2m-2)!\,(3_k^x)^{2m+1}}{2^{4m}(m-1)!m!} - \sum_{m=1}^{\infty} \tfrac{(2m)!\,(3_k^x)^{2m+1}}{2^{4m+1}(m!)^2(2m+1)} \right] \varepsilon^2 \\
&= \sum_{m=1}^{\infty} \sum_{k=1}^{\infty} \tfrac{2^{k-1}}{(3^{2m+1})^k} \tfrac{(2m-2)!\,(3^{\{x\}+1/2})^{2m+1}}{2^{4m}(m-1)!m!} \left(1 - \tfrac{(2m-1)2m}{2m(2m+1)}\right) \varepsilon^2 \\
&= \sum_{m=1}^{\infty} \tfrac{1}{3^{2m+1}} \left( \tfrac{1}{(3^{2m+1}-2)/3^{2m+1}} \right) \tfrac{(2m-2)!\,(\sqrt{3})^{2m+1}}{2^{4m-1}(m-1)!m!(2m+1)} \left(\tfrac{1}{3^{2m+1}}\right)^{-\{x\}} \varepsilon^2 \\
&= \sum_{m=1}^{\infty} \tfrac{(2m-2)!}{2^{4m-1}(m-1)!m!(2m+1)(3^{2m+1}-2)} \left(\tfrac{1}{3^{2m+1}}\right)^{-\{x\}} \varepsilon^2.
\end{aligned} \tag{2.22}$$

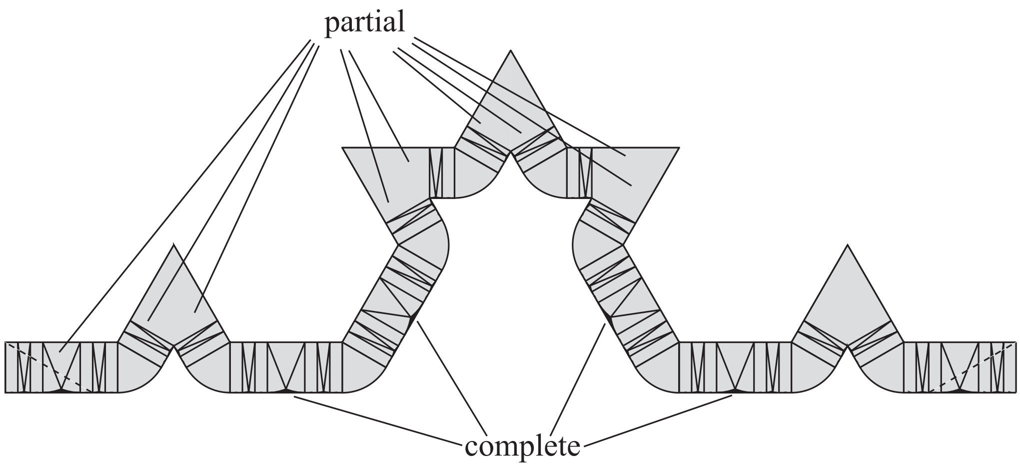


Figure 2.7: Error block formation. The ends are counted as partial because three of these pieces will be added together to make the entire snowflake.

The interchange of sums is validated by checking absolute convergence of the final series via the ratio test, and then applying Fubini's Theorem to retrace the steps of the derivation above.

### 2.3.2 Counting the error blocks

Some blocks are present in their entirety as $\varepsilon$ traverses an interval $I_n$, while others are in the process of forming: two in each of the peaks and one at each end (see Fig. 2.7). Using the same notation as previously in Lemma 2.2.1, count the complete and partial error blocks with

$$c_n = r_n - u_n = \tfrac{1}{3}\left(4^n - 4\right), \quad \text{and} \quad p_n = u_n = \tfrac{2}{3}\left(4^n + 2\right).$$

By means of (2.5)–(2.7), convert $c_n$ and $p_n$ into functions of the continuous variable $\varepsilon$, where $\varepsilon > 0$:

$$c(\varepsilon) = \tfrac{1}{3}\left(\tfrac{\varepsilon^{-D}}{2}4^{-\{x\}} - 4\right) \quad \text{and} \quad p(\varepsilon) = \tfrac{2}{3}\left(\tfrac{\varepsilon^{-D}}{2}4^{-\{x\}} + 2\right). \tag{2.23}$$

With $B(\varepsilon)$ given by (2.22), the total error is thus

$$E(\varepsilon) := B(\varepsilon)\left[c(\varepsilon) + p(\varepsilon)h(\varepsilon)\right]. \tag{2.24}$$

*Remark* 2.3.1. The function $h(\varepsilon)$ in (2.24) is some periodic function that oscillates multiplicatively in a region bounded between 0 and 1, indicating what portion of the partial error block has formed; see Fig. 2.5 and Fig. 2.7. The function $h(\varepsilon)$ is not known explicitly, but by the self-similarity of $K$, it has multiplicative period 3; i.e., $h(\varepsilon) = h(\frac{\varepsilon}{3})$. Using (2.15), the Fourier expansion

$$h(\varepsilon) = \sum_{\alpha\in\mathbb{Z}} g_\alpha(-1)^\alpha \varepsilon^{-\mathrm{i}\alpha\mathbf{p}} = \sum_{\alpha\in\mathbb{Z}} g_\alpha e^{2\pi i\alpha x} = g(x) \tag{2.25}$$

shows that one may also consider $h(\varepsilon)$ as an *additively* periodic function of the variable $x = -\log_3(\varepsilon\sqrt{3})$, with additive period 1. The interested reader may wish to see §2.6 for a further discussion of $h(\varepsilon)$, including a sketch of its graph, justification of the convergence of (2.25), and a brief discussion of some of its properties.

Back to the computation; substituting (2.22) and (2.23) into (2.24) gives

$$\begin{aligned}
E(\varepsilon) &= B(\varepsilon)\left[\tfrac{\varepsilon^{-D}}{3}4^{-\{x\}}\left(\tfrac{1}{2}+h(\varepsilon)\right)+\tfrac{4}{3}\left(h(\varepsilon)-1\right)\right] \\
&= \tfrac{1}{3}\sum_{m=1}^{\infty}\tfrac{(2m-2)!(h(\varepsilon)+1/2)}{2^{4m-1}(m-1)!m!(2m+1)(3^{2m+1}-2)}\left(\tfrac{4}{3^{2m+1}}\right)^{-\{x\}}\varepsilon^{2-D} \\
&\qquad + \tfrac{1}{3}\sum_{m=1}^{\infty}\tfrac{(2m-2)!(h(\varepsilon)-1)}{2^{4m-3}(m-1)!m!(2m+1)(3^{2m+1}-2)}\left(\tfrac{1}{3^{2m+1}}\right)^{-\{x\}}\varepsilon^{2} \\
&= \tfrac{1}{3\log 3}\sum_{m=1}^{\infty}\sum_{n\in\mathbb{Z}}\tfrac{(2m-2)!(4-3^{2m+1})(-1)^n(h(\varepsilon)+1/2)}{2^{4m+1}(m-1)!m!(2m+1)(3^{2m+1}-2)(D-2m-1+\mathrm{i}n\mathbf{p})}\varepsilon^{2-D-\mathrm{i}n\mathbf{p}} \\
&\qquad + \tfrac{1}{3\log 3}\sum_{m=1}^{\infty}\sum_{n\in\mathbb{Z}}\tfrac{(2m-2)!(1-3^{2m+1})(-1)^n(h(\varepsilon)-1)}{2^{4m-3}(m-1)!m!(2m+1)(3^{2m+1}-2)(-2m-1+\mathrm{i}n\mathbf{p})}\varepsilon^{2-\mathrm{i}n\mathbf{p}} \\
&= \tfrac{1}{3\log 3}\sum_{n\in\mathbb{Z}}(h(\varepsilon)+1/2)(-b_n)(-1)^n\varepsilon^{2-D-\mathrm{i}n\mathbf{p}} \\
&\qquad + \tfrac{1}{3\log 3}\sum_{n\in\mathbb{Z}}(h(\varepsilon)-1)(-\tau_n)(-1)^n\varepsilon^{2-\mathrm{i}n\mathbf{p}},
\end{aligned} \tag{2.26}$$

where the constants $b_n$ and $\tau_n$ have been written in the shorthand notation as follows:

$$b_n := \sum_{m=1}^{\infty}\tfrac{(2m-2)!(3^{2m+1}-4)}{2^{4m+1}(m-1)!m!(2m+1)(3^{2m+1}-2)(D-2m-1+\mathrm{i}n\mathbf{p})}, \tag{2.27}$$

$$\text{and } \tau_n := \sum_{m=1}^{\infty} \tfrac{(2m-2)!(3^{2m+1}-1)}{2^{4m-3}(m-1)!m!(2m+1)(3^{2m+1}-2)(-2m-1+\mathbb{i}n\mathbf{p})}. \tag{2.28}$$

In the third equality of (2.26), formula (2.16) has been applied to $a = 4/3^{2m+1}$ and to $a = 1/3^{2m+1}$, respectively. By the ratio test, the complex numbers $b_n$ and $\tau_n$ given by (2.27) and (2.28) are well-defined. This (and Fubini's Theorem) justifies the interchange of sums in the last equality of (2.26).

## 2.4 Computing the area

With estimate (2.17) for the area of the neighbourhood of the Koch curve $\widetilde{V}_{\mathrm{Kc}}(\varepsilon)$, and formula (2.26) for the 'error' $E(\varepsilon)$, the exact area of the inner neighbourhood of the full Koch snowflake can be found as follows:

$$\begin{aligned}
V_{\mathrm{Kc}}(\varepsilon) &= 3\left(\widetilde{V}_{\mathrm{Kc}}(\varepsilon) - E(\varepsilon)\right) \\
&= \tfrac{1}{\log 3}\sum_{n\in\mathbb{Z}}\left(\tfrac{-3^{5/2}}{2^5(D-2+\mathbb{i}n\mathbf{p})} + \tfrac{3^{3/2}}{2^3(D-1+\mathbb{i}n\mathbf{p})} + \tfrac{\pi-3^{3/2}}{2^3(D+\mathbb{i}n\mathbf{p})}\right)(-1)^n\varepsilon^{2-D-\mathbb{i}n\mathbf{p}} \\
&\quad + \tfrac{1}{\log 3}\sum_{n\in\mathbb{Z}}(h(\varepsilon)+1/2)(-1)^n b_n \varepsilon^{2-D-\mathbb{i}n\mathbf{p}} \\
&\quad - \left(\tfrac{\pi}{3}+2\sqrt{3}\right)\varepsilon^2 + \tfrac{1}{\log 3}\sum_{n\in\mathbb{Z}}(h(\varepsilon)-1)(-1)^n\tau_n\varepsilon^{2-\mathbb{i}n\mathbf{p}} \\
&= \tfrac{1}{\log 3}\sum_{n\in\mathbb{Z}}\left(\tfrac{-3^{5/2}}{2^5(D-2+\mathbb{i}n\mathbf{p})} + \tfrac{3^{3/2}}{2^3(D-1+\mathbb{i}n\mathbf{p})} + \tfrac{\pi-3^{3/2}}{2^3(D+\mathbb{i}n\mathbf{p})}\right. \\
&\qquad\qquad\qquad \left. + \tfrac{b_n}{2} + h(\varepsilon)b_n\right)(-1)^n\varepsilon^{2-D-\mathbb{i}n\mathbf{p}} \\
&\quad + \tfrac{1}{\log 3}\sum_{n\in\mathbb{Z}}\left(-\tau_n - \log 3\left(\tfrac{\pi}{3}+2\sqrt{3}\right)\delta_0^n + h(\varepsilon)\tau_n\right)(-1)^n\varepsilon^{2-\mathbb{i}n\mathbf{p}},
\end{aligned} \tag{2.29}$$

where $\delta_0^n$ is the Kronecker delta. Therefore,

$$V_{\mathrm{Kc}}(\varepsilon) = G_1(\varepsilon)\varepsilon^{2-D} + G_2(\varepsilon)\varepsilon^2, \tag{2.30}$$

where the periodic functions $G_1$ and $G_2$ are given by

$$G_1(\varepsilon) := \frac{1}{\log 3} \sum_{n\in\mathbb{Z}} \left(a_n + b_n h(\varepsilon)\right)(-1)^n \varepsilon^{-\mathbb{i}n\mathbf{p}} \tag{2.31}$$

$$\text{and} \quad G_2(\varepsilon) := \frac{1}{\log 3} \sum_{n\in\mathbb{Z}} \left(\sigma_n + \tau_n h(\varepsilon)\right)(-1)^n \varepsilon^{-\mathbb{i}n\mathbf{p}}. \tag{2.32}$$

This expression uses (2.27) and (2.28), and introduces the notation $a_n$ and $\sigma_n$ (stated explicitly in (2.40)). The series must be rearranged so as to collect all factors of $\varepsilon$. First, split the sum in (2.31) as

$$G_1(\varepsilon) = \frac{1}{\log 3} \sum_{n\in\mathbb{Z}} a_n(-1)^n \varepsilon^{-\mathbb{i}n\mathbf{p}} + \frac{h(\varepsilon)}{\log 3} \sum_{n\in\mathbb{Z}} b_n(-1)^n \varepsilon^{-\mathbb{i}n\mathbf{p}} \tag{2.33}$$

because $a(\varepsilon) := \sum_{n\in\mathbb{Z}} a_n(-1)^n \varepsilon^{-\mathbb{i}n\mathbf{p}}$ and $b(\varepsilon) := \sum_{n\in\mathbb{Z}} b_n(-1)^n \varepsilon^{-\mathbb{i}n\mathbf{p}}$ are each convergent: $a(\varepsilon)$ converges for the same reason as (2.17), and one can show that

$$b(\varepsilon) = \sum_{m=0}^{\infty} \tfrac{(4\log 3)(2m-2)!}{2^{4m+1}3^{m-1/2}(m-1)!m!(2m+1)(3^{2m+1}-2)} \left(\tfrac{4}{3^{2m+1}}\right)^{-\{x\}} \tag{2.34}$$

converges to a well-defined distribution induced by a locally integrable function; one proves directly that $|b_n| \le c/|n|$ by writing (2.27) as

$$b_n = \sum_{m=1}^{\infty} \tfrac{\beta_m}{D-2m-1+\mathbb{i}n\mathbf{p}}, \qquad \text{with} \qquad \sum_{m=1}^{\infty} \beta_m < \infty. \tag{2.35}$$

Then the rearrangement leading to (2.34) is justified via the "descent method" with $q = 2$, as described in Remark 2.4.1 below. Note that the right-hand side of (2.34) converges by the ratio test and is thus defined pointwise on $\mathbb{R} \sim \mathbb{Z}$. Therefore, this also indicates that $b(\varepsilon)$ and $h(\varepsilon)$ are periodic functions. Considered as functions of the variable $x = \log_3(1/\varepsilon\sqrt{3})$, both have period 1 with $b$ continuous for $0 \le x < 1$ and $h$ continuous for $0 < x \le 1$. Further, each is monotonic on its period interval, and possesses a bounded jump discontinuity only at the endpoint. This may be seen for $b(\varepsilon)$ from (2.34) and for $h(\varepsilon)$ from §6.

Although distributional arguments have been used to obtain (2.34), the right-hand side of (2.34) is locally integrable and has a representation as a piecewise continuous function. Thus the distributional equality in (2.34) actually holds pointwise in the sense of Fourier series and all results are still valid pointwise. Recall that the Dirichlet–Jordan Theorem [Zy, Thm. II.8.1] states that if $f$ is periodic and (locally) of bounded variation, its Fourier series converges pointwise to $\left(f(x-) + f(x+)\right)/2$. As described above, $b(\varepsilon)$ and $h(\varepsilon)$ are each of bounded variation and therefore [Zy, Thm. II.4.12] implies that $b_n = O(1/n)$ and $g_n = O(1/n)$ as $n \to \pm\infty$. Finally, [Zy, Thm. IX.4.11] may be applied to yield the pointwise equality

$$b(\varepsilon)h(\varepsilon) = \sum_{n\in\mathbb{Z}} \sum_{\alpha\in\mathbb{Z}} b_\alpha g_{n-\alpha} (-1)^n \varepsilon^{-\mathbb{i}n\mathbf{p}}. \tag{2.36}$$

The theorem applies because (2.34) shows that $b(\varepsilon)$ is bounded away from 0.

Now that all the $\varepsilon$'s are combined, we substitute (2.36) back into (2.33) and rewrite $G_1(\varepsilon) = \left(a(\varepsilon) + b(\varepsilon)h(\varepsilon)\right) / \log 3$ as in (2.39a):

$$G_1(\varepsilon) = \frac{1}{\log 3} \sum_{n\in\mathbb{Z}} \left( a_n + \sum_{\alpha\in\mathbb{Z}} b_\alpha g_{n-\alpha} \right) (-1)^n \varepsilon^{-\mathbb{i}n\mathbf{p}}. \tag{2.37}$$

Manipulating $G_2(\varepsilon)$ similarly, Eqn. (2.32) can be rewritten in its final form (2.39b), and thereby complete the proof of Theorem 2.5.1.

*Remark* 2.4.1. The convergence of the Fourier series associated to a periodic distribution is proved via the *descent method* by integrating both sides $q$ times (for sufficiently large $q$) so that one has pointwise convergence. After enough integrations, the distribution will be a smooth function, the series involved will converge absolutely, and the Weierstrass theorem can be applied pointwise. At this point, rearrangements or interchanges of series are justified pointwise, and one obtains a pointwise formula for the $q^{\text{th}}$ antiderivative of the desired function. Then one takes the distributional derivative $q$ times to obtain the desired formula. See [LavF4, Rem. 5.20]. How large the positive integer $q$ needs to be depends on the order of polynomial growth of the Fourier coefficients. Recall that the Fourier series of a periodic distribution converges distributionally if and only if the Fourier coefficients are of slow growth, i.e., do not grow faster than polynomially. Moreover, from the point of view of distributions, there is no distinction to be made between convergent trigonometric series and Fourier series. See [Sch, §VII,I]. The descent method is used again in Appendix D; see especially Theorem D.1.21

and Theorem D.1.23.

## 2.5 The Koch tube formula: main results

Theorem 2.5.1 summarizes the results of the previous 4 sections. It is the main result of this chapter, and the more precise form of Theorem 2.1.1, discussed in the introductory section §2.1.

**Theorem 2.5.1.** *The area of the inner $\varepsilon$-neighbourhood of the Koch snowflake is given pointwise by the following tube formula:*

$$V_{Kc}(\varepsilon) = G_1(\varepsilon)\varepsilon^{2-D} + G_2(\varepsilon)\varepsilon^2, \tag{2.38}$$

*where $G_1$ and $G_2$ are periodic functions of multiplicative period 3, given by*

$$G_1(\varepsilon) := \frac{1}{\log 3}\sum_{n\in\mathbb{Z}}\left(a_n + \sum_{\alpha\in\mathbb{Z}} b_\alpha g_{n-\alpha}\right)(-1)^n\varepsilon^{-\mathbb{i}n\mathbf{p}} \tag{2.39a}$$

$$\text{and}\ \ G_2(\varepsilon) := \frac{1}{\log 3}\sum_{n\in\mathbb{Z}}\left(\sigma_n + \sum_{\alpha\in\mathbb{Z}} \tau_\alpha g_{n-\alpha}\right)(-1)^n\varepsilon^{-\mathbb{i}n\mathbf{p}}, \tag{2.39b}$$

*where $a_n, b_n, \sigma_n$, and $\tau_n$ are the complex numbers given by*

$$\begin{aligned}
a_n &= -\frac{3^{5/2}}{2^5(D-2+\mathbb{i}n\mathbf{p})} + \frac{3^{3/2}}{2^3(D-1+\mathbb{i}n\mathbf{p})} + \frac{\pi-3^{3/2}}{2^3(D+\mathbb{i}n\mathbf{p})} + \frac{1}{2}b_n,\\
b_n &= \sum_{m=1}^{\infty}\frac{(2m)!\,(3^{2m+1}-4)}{4^{2m+1}(m!)^2(4m^2-1)(3^{2m+1}-2)(D-2m-1+\mathbb{i}n\mathbf{p})},\\
\sigma_n &= -\log 3\left(\frac{\pi}{3}+2\sqrt{3}\right)\delta_0^n - \tau_n,\ \textit{and}\\
\tau_n &= \sum_{m=1}^{\infty}\frac{(2m)!\,(3^{2m+1}-1)}{4^{2m-1}(m!)^2(4m^2-1)(3^{2m+1}-2)(-2m-1+\mathbb{i}n\mathbf{p})},
\end{aligned} \tag{2.40}$$

*where $\delta_0^0 = 1$ and $\delta_0^n = 0$ for $n \neq 0$ is the Kronecker delta.*

In Theorem 2.5.1, $D = \log_3 4$ is the Minkowski dimension of the Koch snowflake $\partial L$ and $\mathbf{p} = 2\pi/\log 3$ is its oscillatory period, following the terminology of [La-vF4]. The numbers $g_\alpha$ appearing in (2.39) are the Fourier coefficients of the periodic function $h(\varepsilon)$, a suitable nonlinear analogue of the Cantor–

Lebesgue function, defined in Rem. 2.3.1 and further discussed in §2.6 below.

*Remark* 2.5.2. The reader may easily check that formula (2.38) can also be written

$$V_{\mathrm{Kc}}(\varepsilon) = \sum_{n\in\mathbb{Z}} \varphi_n \varepsilon^{2-D-\mathbb{i}n\mathbf{p}} + \sum_{n\in\mathbb{Z}} \psi_n \varepsilon^{2-\mathbb{i}n\mathbf{p}}, \tag{2.41}$$

for suitable constants $\varphi_n, \psi_n$ which depend only on $n$. Now by analogy with the tube formula (1.9) from [La-vF4], the exponents of $\varepsilon$ in (2.41) may be interpreted as the 'complex co-dimensions' of $\partial L$. Hence, we can simply read off the possible complex dimensions, and as depicted in Fig. 2.8, we obtain a set of possible complex dimensions

$$\mathcal{D}_{\partial L} = \{D + \mathbb{i}n\mathbf{p} \,\vdots\, n \in \mathbb{Z}\} \cup \{\mathbb{i}n\mathbf{p} \,\vdots\, n \in \mathbb{Z}\}. \tag{2.42}$$

One caveat should be mentioned: this is assuming that none of the coefficients $\varphi_n$ or $\psi_n$ vanishes in (2.41). Indeed, in that case the actual complex dimensions would only form a subset of the right-hand side of (2.42). This is the reason for using the adjective "possible" in the previous paragraph. Following the 'approximate tube formula' obtained in [La-vF4], it is to be expected that the set of complex dimensions should contain all numbers of the form $D + \mathbb{i}n\mathbf{p}$. Keeping (1.13) and (2.42) in mind, we can rewrite (2.41) as

$$V_{\mathrm{Kc}}(\varepsilon) = \sum_{\omega\in\mathcal{D}_{\partial L}} c_\omega \varepsilon^{2-\omega}. \tag{2.43}$$

In fact, it is (2.43) that guided intuition in the research that lead to (1.13), stated more precisely in Theorem 5.4.5.

*Remark* 2.5.3. It should be emphasized that in this chapter, there is no direct definition of the complex dimensions of the Koch snowflake curve $\partial L$ (or of other fractals in $\mathbb{R}^2$). Instead, the complex dimensions are given by analogy with formula (1.9) above to deduce the possible complex dimensions of $\partial L$ (or of $K$) from the tube formula (2.38). As is seen in the proof of Theorem 2.5.1, the tube formula for the Koch curve $K$ is of the same form as for that of the snowflake curve $\partial L$ (they differ only be a factor of 3). It follows that $K$ and $\partial L$ have the

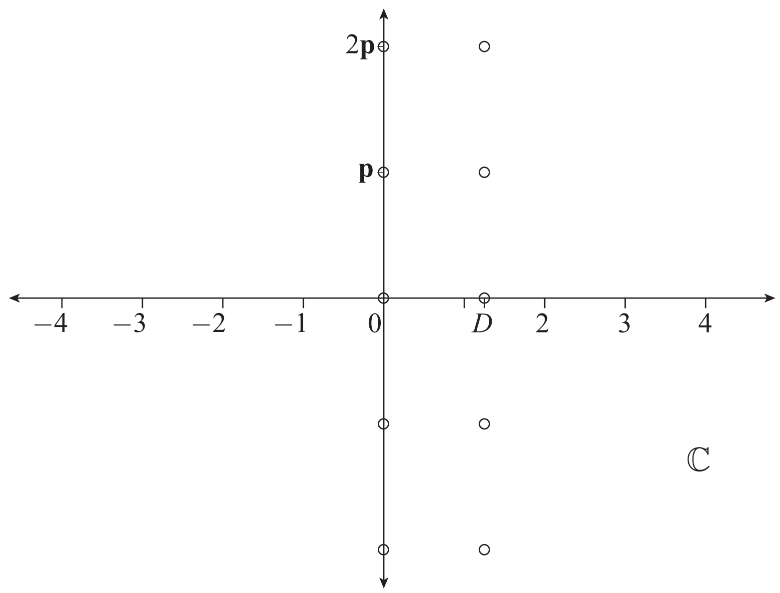


Figure 2.8: The possible complex dimensions of $K$ and $\partial L$. The Minkowski dimension is $D = \log_3 4$ and the oscillatory period is $\mathbf{p} = \frac{2\pi}{\log 3}$.

same possible complex dimensions (see Cor. 2.1.2).

In Chapter 5 below, the tiling zeta function $\zeta_{\mathcal{K}}(s)$ of the Koch curve is defined. This allows the complex dimensions to be deduced directly as the poles of the meromorphic continuation of $\zeta_{\mathcal{K}}$. Indeed, the poles of $\zeta_{\mathcal{K}}$ turn out to be the points $\{D + \mathbb{i}n\mathbf{p} \,\vdots\, n \in \mathbb{Z}\}$, in agreement with (2.42).

*Remark* 2.5.4. In the long-term, by analogy with J. Steiner's tube formula for convex bodies [Schn2], or H. Weyl's tube formula [We] for smooth Riemannian submanifolds (see [Gr]), the coefficients $a_n, b_n, \sigma_n, \tau_n$ of the tube formula (2.38) should be interpreted as an appropriate substitute of the intrinsic curvature measures or 'Weyl curvatures' in this context. This is mentioned again in §4.4.5. See the corresponding discussion in [La-vF4, §8.2 and §12.3] for fractal strings; also see [La-vF3]. This is a very difficult open problem and is still far from being resolved, even in the one-dimensional case of fractal strings. The curvature interpretation of the coefficients of the tube formula for a self-similar tiling is discussed in Remark 4.4.5 and Remark 5.4.7, and is under further investigation in [LaPe3]. Also see [Wi] for recent results in defining curvature measures on fractals.

*Remark* 2.5.5. (Reality principle.) As is the case for the complex dimensions of self-similar strings (see [La-vF4, Chap. 2–3] and [La-vF2–3]), the *possible com-*

*plex dimensions of $\partial L$ come in complex conjugate pairs, with attached complex conjugate coefficients*. Indeed, since $\overline{g_\alpha} = g_{-\alpha}$ (see §2.6), a simple inspection of the formulas in (2.40) shows that for every $n \in \mathbb{N}$,

$$\overline{a_n} = a_{-n}, \overline{b_n} = b_{-n}, \overline{\sigma_n} = \sigma_{-n}, \text{ and } \overline{\tau_n} = \tau_{-n}. \tag{2.44}$$

It follows that $a_0, b_0, \sigma_0$, and $\tau_0$ are reals and that $G_1$ and $G_2$ in (2.39) are *real*-valued, in agreement with the fact that $V_{\mathrm{Kc}}(\varepsilon)$ represents an *area*. This observation will be repeated for the tube formula of a self-similar tiling, in Remark 5.4.9.

## 2.6 The Cantor-like function $h(\varepsilon)$

Let us briefly discuss the semi-mysterious Cantor-like function

$$h(\varepsilon) = \sum_{\alpha \in \mathbb{Z}} g_\alpha (-1)^\alpha \varepsilon^{-\mathrm{i}\alpha\mathbf{p}} = \sum_{\alpha \in \mathbb{Z}} g_\alpha e^{2\pi\mathrm{i}\alpha x} = g(x), \tag{2.45}$$

introduced in (2.25). It is shown in [LlWi] that for a self-similar set $F$, there is a dichotomy: either every $\varepsilon$-neighbourhood of $F$ is polyconvex, or no $\varepsilon$-neighbourhood of $F$ is polyconvex.[3] It follows that for any set of the latter type, there will be a function analogous to $h(\varepsilon)$ which expresses the difference between the volume of the $\varepsilon$-neighbourhood and the volume of the convex hull of the $\varepsilon$-neighbourhood.

Note that since $h$ is real-valued (in fact, $0 \leq h < \mu < 1$), it is the case that $g_{-\alpha} = \overline{g_\alpha}$ for all $\alpha \in \mathbb{Z}$. Further, recall from §2.3.2 that in view of the self-similarity of $K$, $h(\varepsilon)$ is multiplicatively periodic with period 3, i.e., $h(\varepsilon) = h(\frac{\varepsilon}{3})$. Alternatively, (2.45) shows that it can be thought of as an additively periodic function of $x$ with period 1, i.e., $g(x) = g(x+1)$. In virtue of its geometric definition, the function $h(\varepsilon)$ is continuous and even monotonic when restricted to one of its period intervals $I_n := \left(3^{-n-3/2}, 3^{-n-1/2}\right]$. Since $h$ is of bounded variation, its Fourier series converges pointwise by [Zy, Thm. II.8.1] and its Fourier coefficients satisfy

$$g_\alpha = O(1/\alpha), \text{ as } \alpha \to \pm\infty \tag{2.46}$$

by [Zy, Thm. II.4.12], as discussed at the very end of §2.4.

[3] A set is defined to be polyconvex iff it is a finite union of convex compact sets.

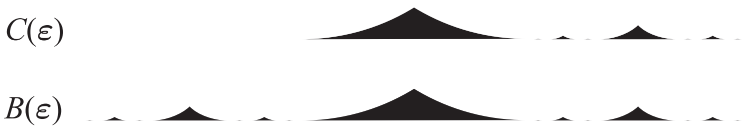


Figure 2.9: $\mu$ is the ratio $\mathrm{vol}_2(C(\varepsilon))/\,\mathrm{vol}_2(B(\varepsilon))$.

Further, since $h(\varepsilon)$ is defined as a ratio of areas (see Remark 2.3.1), it is clear that $h(\varepsilon) \in [0, \mu)$ for all $\varepsilon > 0$. Note that $h(\varepsilon) \leq \mu < 1$ and so $h(\varepsilon)$ does not attain the value 1; the error blocks being formed are never complete. The partial error blocks only form across the first $\frac{2}{3}$ of the line segment beneath them. They reach this point precisely when $\varepsilon = 3^{-n}/\sqrt{3}$ for some $n \geq 1$. Back in (2.21), the error of a single error block was found to be given by

$$B(\varepsilon) = \sum_{k=1}^{\infty} 2^{k-1} A_k(\varepsilon),$$

where $A_k(\varepsilon)$ is given by (2.19). Thus the supremum of $h(\varepsilon)$ will be the ratio

$$\left(\tfrac{B(\varepsilon_k)-A_1(\varepsilon_k)}{2} + A_1(\varepsilon_k)\right)/B(\varepsilon_k),$$

which will be the same constant for each $\varepsilon_k = 3^{-k-1/2}, \quad k = 1, 2, \ldots$ (see Fig. 2.9). In other words, the number sought is

$$\mu := \frac{A_1(\varepsilon_k) + \frac{1}{2}\sum_{k=2}^{\infty} 2^{k-1} A_k(\varepsilon_k)}{\sum_{k=1}^{\infty} 2^{k-1} A_k(\varepsilon_k)} = \frac{A_1(\varepsilon_k) + \sum_{k=2}^{\infty} 2^{k-2} A_k(\varepsilon_k)}{\sum_{k=1}^{\infty} 2^{k-1} A_k(\varepsilon_k)} \in (0, 1).$$

Note that although this definition of $\mu$ initially appears to depend on $k$, the ratio in question is between two areas which have exactly the same proportion at each $\varepsilon_k$; this is a direct consequence of the lattice self-similarity of the Koch curve. In other words, if $C(\varepsilon)$ is the area indicated in Fig. 2.9, then the relations

$$3C(\tfrac{\varepsilon}{3}) = C(\varepsilon) \text{ and } 3B(\tfrac{\varepsilon}{3}) = B(\varepsilon)$$

show that $\mu$ is well-defined.

Using again the notation $x = -\log_3(\varepsilon\sqrt{3})$ and $\{x\} = x - [x]$, it may be

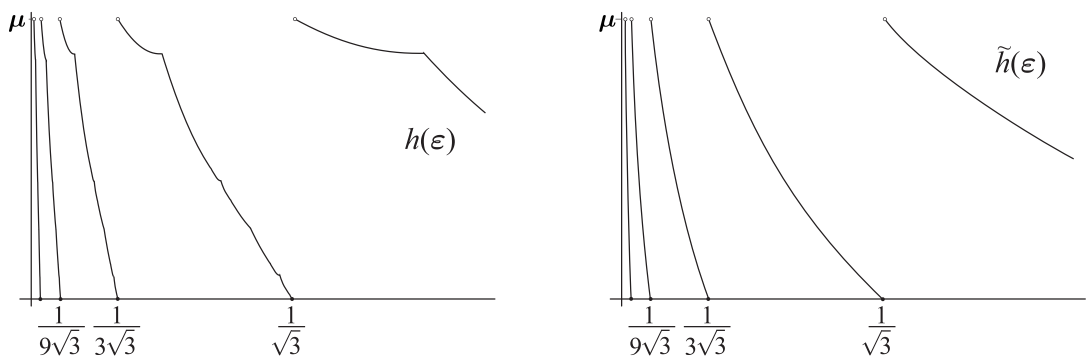


Figure 2.10: A comparison between the graph of the Cantor-like function $h$ and the graph of its approximation $\tilde{h}$.

helpful to consider the function

$$\tilde{h}(\varepsilon) = \mu \cdot \{-[x] - x\}. \tag{2.47}$$

This function is an approximation to $h(\varepsilon)$ which shares two essential properties of $h(\varepsilon)$ but has the advantage of having an explicit form. The two essential properties are

(i) $h(\varepsilon_k) = \lim_{\vartheta \to 0^-} h(\varepsilon_k + \vartheta) = 0$,

(ii) $\lim_{\vartheta \to 0^+} h(\varepsilon_k + \vartheta) = \mu$,

where $\varepsilon_k = 1/3^k\sqrt{3}$, for every $k \in \mathbb{N}$, as shown in Fig. 2.10. That is, $h(\varepsilon)$ goes from 0 to $\mu$ as $\varepsilon$ goes from $3^{-k}$ to $3^{-(k+1)}$. The function $\tilde{h}(\varepsilon)$ shares both of these properties but is much smoother. Indeed, $\tilde{h}(\varepsilon)$ only has points of nondifferentiability at each $\varepsilon_k$ and is otherwise a smooth logarithmic curve. The true $h(\varepsilon)$, by contrast, is a much more complex object that deserves further study in later work.

## 2.7 Remarks about the Koch tube formula

The methods used above should work for all lattice self-similar fractals (i.e., those for which the underlying scaling ratios have rationally dependent logarithms) as well as for other examples considered in [La-vF1]. This would even include the Cantor–Lebesgue curve, a self-affine fractal. For example, the counterpart of Theorem 2.5.1 for the square (rather than triangular) snowflake curve has already been obtained. By applying density arguments (as in [La-vF1, Chap. 2]), these methods may also yield information about the complex dimensions of nonlattice fractals.

The general idea is that the periodicity with which the scaling ratios appear gives a natural sequence of scales at which to perform the calculations. In the present case, for example, the scaling ratios of the function system generating the Koch curve were both $\sqrt{3}$. Hence, the computations were all performed with regard to a scale of approximation given by $\varepsilon$ moving through intervals whose endpoints are powers of $\sqrt{3}$; see (2.4). The inherent difficulty of studying nonlattice fractals as in this chapter lies in the absence of natural approximation levels, and the associated lack of periodicity. One can think of the Koch snowflake as being generated geometrically; take a hexagon and remove a succession of scaled equilateral triangles; see Fig. 3.1 and Fig. 3.2. Each time function $h(\varepsilon)$ passes through one of its periods, it corresponds to the approximation shifting to the scale of the next removed triangle. For a nonlattice fractal, this shift does not occur discretely, nor with any regularity. Indeed, in the general (not necessarily self-similar) case, the shift towards increasing accuracy may even be continuous.

The peculiarities of the geometry of the Koch curve derive from the properties of the system of functions for which it is the attractor. In other words, rather than focusing on the Koch curve as a geometric object constructed via union or intersection of certain sets, we will consider it instead to be generated by a system of mappings. In fact, it is the system of mappings which is fundamental; the Koch curve is one geometric manifestation of the system, but there may also be others. In fact, we construct such an object in the next chapter.

In what follows, attention is focused on the system of mappings which generate a self-similar set, rather than the set itself. However, the set is certainly not ignored entirely. By analogy, one includes an examination of the fixed points of dynamical systems while studying the system, but one does not restrict attention entirely to the fixed points. Restricting attention to just this small amount of data would lead one to lose sight of other (often more subtle and complex) qualities of the system. Indeed, this is perhaps more than just an analogy. As discussed in §3.2, a self-similar set is essentially the fixed point of a mapping

$$\Phi = \bigcup_{j=1}^{J} \Phi_j : \mathbb{K}^d \to \mathbb{K}^d$$

defined on the metric space $(\mathbb{K}^d, \delta)$ of nonempty compact subsets of $\mathbb{R}^d$ with Hausdorff metric $\delta$, where the $\Phi_j$ are contraction similarity transformations (see Definition 3.2.1 and especially (3.3)). Then the map $\Phi$ is a contraction mapping, and the self-similar set $F$ is its unique fixed point. Studying the Koch curve without considering $\Phi$ is like hoping to understand a dynamical system by focusing entirely on its fixed points. The rest of this dissertation will perhaps provide one step towards understanding the general dynamics of $\Phi$, by studying the behavior of $\Phi$ near $F$.

This shift in perspectives from geometric to dynamical systems is in marked contrast to previous work, e.g., [La-vF1, Chap. 2]. However, it leads to a natural framework for the study of self-similar objects in higher dimensions. It also agrees with physical ideas stemming from considerations of the spectral problem and inverse spectral problem for fractal domains (and domains with fractal boundary).

# Chapter 3

# The Self-Similar Tiling

## 3.1 Introduction

This chapter presents the construction of a self-similar tiling which is canonically associated to a given self-similar system $\Phi$, as defined in Definition 3.2.1. The term "self-similar tiling" is used here in a sense quite different from the one often encountered in the literature. In particular, the region being tiled is the complement of the self-similar set $F$ within its convex hull, rather than all of $\mathbb{R}^d$. Moreover, the tiles themselves are neither self-similar nor are they all of the same size; in fact, the tiles may even be simple polyhedra. However, the name "self-similar tiling" is appropriate because we will have a tiling of the convex hull: the union of the closures of the tiles is the entire convex hull, and the interiors of the tiles intersect neither each other, nor the attractor $F$. While the tiles themselves are not self-similar, the overall structure of the tiling is.[1] The tiles appear in stages, and this gives insight into the dynamics of $\Phi$; see the end of §2.7.

The construction of the tiling begins with definition of the generators, a collection of open sets obtained from the convex hull of $F$. The rest of the tiles will be images of these generators under the action of the original self-similar system. Thus, the tiling $\mathcal{T}$ essentially arises as a spray on the generators, in the sense of [LaPo2] and [La-vF4]. The tiles thus obtained form a collection of sets whose geometry is typically much simpler than that of $F$, yet retains key information about both $F$ and $\Phi$. In particular, the tiles encode all the scaling data of $\Phi$.

[1]Technically, the tiling is *subselfsimilar* in that $\Phi(\mathcal{T}) \subseteq \mathcal{T}$; see Cor. 3.5.16.

Section §3.2 gives the tiling construction and illustrates the method with several familiar examples, including the Koch snowflake curve, Sierpinski gasket and pentagasket. Section §3.5 describes the basic properties of the tiling.

It is shown in Chapters 4 that the tiles allow one to define a zeta function $\zeta_{\mathcal{T}}$ for $\Phi$ which is essentially a generating function for the geometry of $F$. In Chapter 5, this geometric zeta function will allow for computation of an explicit tube formula for $\mathcal{T}$. Moreover, one may define the complex dimensions of $\mathcal{T}$ as the poles of $\zeta_{\mathcal{T}}$. The tube formula $V_{\mathcal{T}}(\varepsilon)$ of Chapter 5 is thus defined entirely in terms of the self-similar tiling constructed in this section.

## 3.2 Basic terms

**Definition 3.2.1.** A *self-similar system* is a family $\Phi := \{\Phi_j\}_{j=1}^J$ (with $J \geq 2$) of contraction similitudes

$$\Phi_j(x) := r_j A_j x + p_j, \quad j = 1, \dots, J. \tag{3.1}$$

For $j = 1, \dots, J$, we have $0 < r_j < 1, p_j \in \mathbb{R}^d$, and $A_j \in O(d)$, the orthogonal group of rigid rotations in $d$-dimensional Euclidean space $\mathbb{R}^d$. Thus, each $\Phi_j$ is the composition of an (affine) isometry and a homothety (scaling).

*Remark* 3.2.2. Note that different self-similar systems may give rise to the same self-similar set. In this paper, the emphasis is placed on the self-similar system and its corresponding dynamical system, rather than on the self-similar set; see §2.7.

**Definition 3.2.3.** The numbers $r_j$ are referred to as the *scaling ratios* of $\Phi$. For convenience, we may take the scaling ratios in nonincreasing order, i.e., reindex $\{\Phi_j\}$ so that

$$1 > r_1 \geq r_2 \geq \dots \geq r_J > 0. \tag{3.2}$$

**Definition 3.2.4.** A self-similar system is thus just a particular type of iterated function system (IFS). It is well known[2] that for such a family of maps, there is a

[2]See [Hut], as described in [Fal1] or [Kig], for example.

unique and self-similar set $F$ satisfying the fixed-point equation

$$F = \Phi(F) := \bigcup_{j=1}^{J} \Phi_j(F). \tag{3.3}$$

We call $F$ the *attractor* of $\Phi$, or the *self-similar set* associated with $\Phi$. The *action of* $\Phi$ is the set map defined by (3.3). Thus, one says that $F$ is invariant under the action of $\Phi$.

**Definition 3.2.5.** We fix some notation for later use. Let

$$C := [F] \tag{3.4}$$

be the *convex hull* of the attractor $F$, that is, the intersection of all convex sets containing $F$. Since $F$ is a compact set, it follows that $C$ is also compact, by [Schn2, Thm. 1.1.10]. Further, let

$$C^o := \operatorname{int}(C) = C \sim \partial C. \tag{3.5}$$

*Remark* 3.2.6. For this paper, it will suffice to work with the ambient dimension

$$d = \dim C, \tag{3.6}$$

restricting the maps $\Phi_j$ as appropriate. In (3.6), $\dim C$ is defined to be the usual topological dimension of the smallest affine space containing $C$. An appropriate change of coordinates allows one to think of this convention as using a minimal subspace $\mathbb{R}^d$; if $F$ is a Cantor set in $\mathbb{R}^3$, we study it as if the ambient space were the line containing it, rather than $\mathbb{R}^3$. Note that this means $C^o$ is open in the standard topology; and so we have $C^o \neq \varnothing$. This remark is intended to allay any fears about possibly needing to use relative interior instead of interior (see [KlRo] or [Schn2]) and other unnecessary complications.

**Definition 3.2.7.** A self-similar system satisfies the *tileset condition* iff for $j \neq \ell$,

$$\operatorname{int} \Phi_j(C) \cap \operatorname{int} \Phi_\ell(C) = \varnothing. \tag{3.7}$$

It is shown in Cor. 3.5.10 that because $C = \overline{\operatorname{int} C}$, (3.7) implies that the images

$\Phi_j(C)$ and $\Phi_\ell(C)$ can intersect only on their boundaries:

$$\Phi_j(C) \cap \Phi_\ell(C) \subseteq \partial\Phi_j(C) \cap \partial\Phi_\ell(C).$$

Here, $\partial A := \overline{A} \cap \overline{A^c}$, where $A^c$ is the complement of $A$ and $\overline{A}$ denotes the (topological) closure of $A$. To avoid trivialities, we also require

$$C^o \nsubseteq \Phi(C). \tag{3.8}$$

The *nontriviality condition* (3.8) disallows the case $C^o \sim \Phi(C) = \varnothing$, and hence guarantees the existence of the tiles in §3.3.

*Remark* 3.2.8. The tileset condition is a restriction on the overlap of the images of the mappings, comparable to the *open set condition* (OSC). The OSC requires a nonempty bounded open set $U$ such that the sets $\Phi_j(U)$ are disjoint but $\Phi(U) \subseteq U$. See, e.g., [Fal1, Chap. 9]. If one takes $U = \operatorname{int} C$, then it will be clear from Cor. 3.5.3 of §3.5 that the OSC follows from (3.7); see Remark 3.5.4.

**Definition 3.2.9.** Denote the *words of length $k$* (of $\{1, 2, \ldots, J\}$) by

$$\begin{aligned} W_k = W_k^J &:= \{1, 2, \ldots, J\}^k \\ &= \{w = w_1 w_2 \ldots w_k \vdots w_j \in \{1, 2, \ldots, J\}\}, \end{aligned} \tag{3.9}$$

and the set of all (finite) words by $W := \bigcup_k W_k$. Generally, the dependence of $W_k^J$ on $J$ is suppressed. For $w$ as in (3.9), we use the standard IFS notation

$$\Phi_w(x) := \Phi_{w_k} \circ \ldots \circ \Phi_{w_2} \circ \Phi_{w_1}(x) \tag{3.10}$$

to describe compositions of maps from the self-similar system.

**Definition 3.2.10.** For a set $A \subseteq \mathbb{R}^d$, a *tiling* of $A$ is a sequence of sets $\{A_n\}_{n=1}^\infty$ such that

(i) $A = \bigcup_{n=1}^N A_n$, and

(ii) $A_n \cap A_m = \partial A_n \cap \partial A_m$ for $n \neq m$.

We then say that the sets $A_n$ *tile* $A$. Further, define a *tiling of $A$ by open sets* to be a sequence of *open* sets $\{A_n\}$ satisfying $\overline{A} = \bigcup_{n=1}^N \overline{A_n}$, where $A_n \cap A_m = \varnothing$

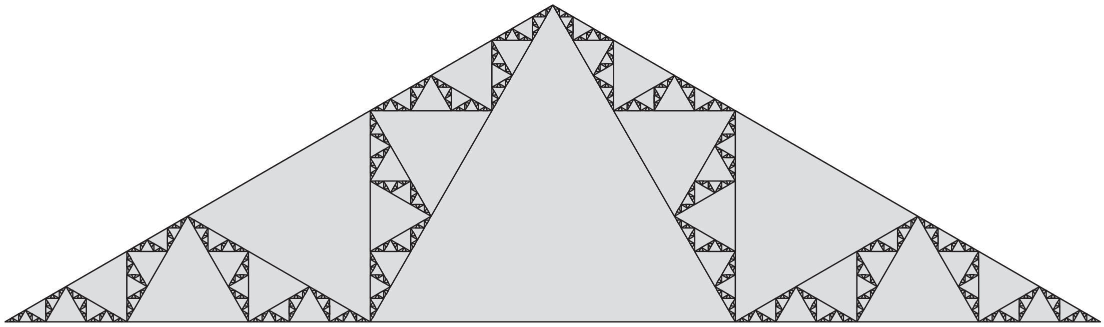

Figure 3.1: Tiling the complement of the Koch curve $K$. The equilateral triangles form an open tiling of the convex hull $C = [K]$, in the sense of Definition 3.2.10.

for $n \neq m$. In general, $N$ may be taken to be $\infty$. Fig. 3.1 shows an example of a tiling by open sets with $N = \infty$.

## 3.3 The construction

In this section, we construct a *self-similar tiling*, that is, a tiling which is constructed via the mappings of a self-similar system. Such a tiling will consequently have a self-similar structure, and is defined precisely in Definition 3.3.3 below. The reader is invited to look ahead at Figure 3.2, where the construction is illustrated step-by-step for the illuminative example of the Koch curve.

For the system $\{\Phi_j\}$ with attractor $F$, denote the hull of the attractor by

$$C_0 = C := [F]. \tag{3.11}$$

Denote the image of $C$ under the action of $\Phi$ (in accordance with (3.3)) by

$$C_k := \Phi^k(C) = \bigcup_{w \in W_k} \Phi_w(C), \quad k = 1, 2, \ldots . \tag{3.12}$$

Note that this is equivalent to the inductive definition

$$C_k := \Phi(C_{k-1}), \quad k = 1, 2, \ldots . \tag{3.13}$$

**Definition 3.3.1.** The *tilesets* are the sets

$$T_k := \overline{C_{k-1} \sim C_k}, \quad k = 1, 2, \dots \tag{3.14}$$

**Definition 3.3.2.** The *generators* $G_q$ of the aforementioned tiling $\mathcal{T}$ are the connected components of the open set

$$\operatorname{int}(C \sim \Phi(C)) = G_1 \sqcup G_2 \sqcup \dots \sqcup G_Q. \tag{3.15}$$

The symbol $\sqcup$ is used to indicate *disjoint* union.

As will be shown in Theorem 3.5.11, it follows from the tileset conditions (3.7)–(3.8) (and some other facts) that the tilesets and tiles are nonempty, and that each tileset is the closure of its interior. Also, Theorem 3.5.14 will justify the terminology "generators" by showing

$$T_k = \bigsqcup_{q=1}^{Q} \overline{\Phi^{k-1}(G_q)}, \tag{3.16}$$

that is, that any difference $C_{k-1} \sim C_k$ is (modulo some boundary points) the image of the generators under the action of $\Phi$. The number $Q$ of generators depends on the specific geometry of $C$ and on the self-similar system $\Phi$. It is conceivable that $Q = \infty$ for some systems $\Phi$, but no such examples are known. This possibility will be investigated further in [LaPe3].

**Definition 3.3.3.** The *self-similar tiling* of $F$ is

$$\mathcal{T} := \left( \{\Phi_j\}_{j=1}^{J}, \{G_q\}_{q=1}^{Q} \right). \tag{3.17}$$

We may also abuse the notation a little, and use $\mathcal{T}$ to denote the set of corresponding *tiles*:

$$\mathcal{T} = \{R_n\}_{n=1}^{\infty} = \{\Phi_w(G_q) \vdots w \in W, q = 1, \dots, Q\}, \tag{3.18}$$

where the sequence $\{R_n\}$ is an enumeration of the tiles. Clearly, each tile is nonempty and $d$-dimensional. Furthermore, Theorem 3.5.15 will confirm that (3.18) is an open tiling in the sense of Definition 3.2.10. The motivation for

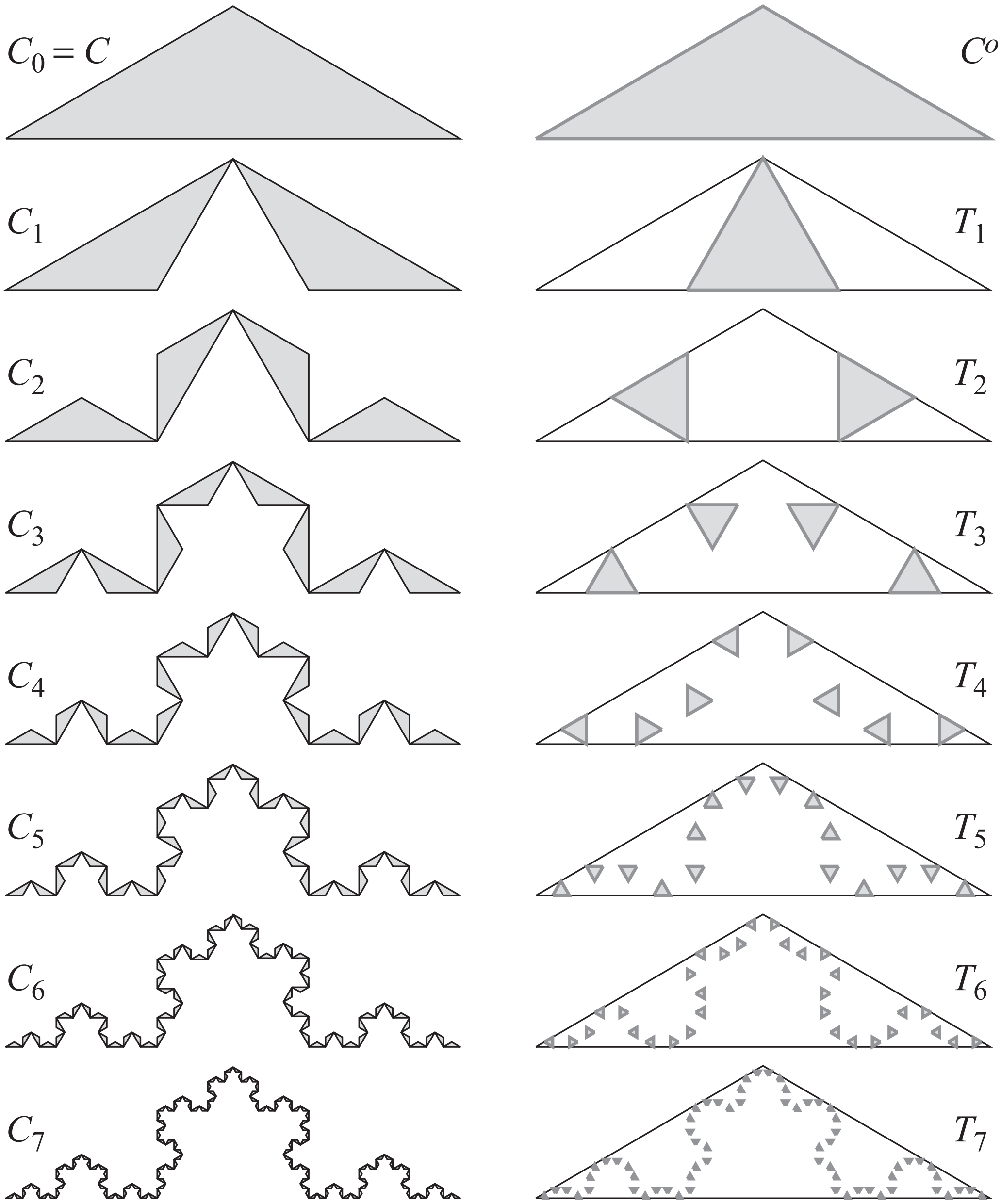


Figure 3.2: The left column shows images of the convex hull $C$ under successive applications of $\Phi$. The right column shows how the $T_k$ tile the complement; they are overlaid in Fig. 3.1. This tiling has one generator $G_1 = \operatorname{int} T_1$.

definining tiles as images of the generators in (3.18) becomes apparent in Remark 4.4.3.

## 3.4 Tiling Examples

All examples this section have polyhedral generators, but this is not the general case. In fact, generators may have boundaries that are continuously differentiable, although it is not possible that they be twice continuously differentiable. This was observed to be true for the convex hull of an attractor in [StWa], and it immediately carries over to the generators as well. This is studied further in [LaPe3]; see also §3.6.1.

### 3.4.1 The Koch tiling

Figure 3.1 shows the self-similar tiling of the Koch curve; the steps of the construction are illustrated in Figure 3.2. In this case, the tiling is $\mathcal{K} = \big(\{\Phi_j\}_{j=1}^2, \{G\}\big)$, and it is easiest to write down the similarities as maps $\Phi_j : \mathbb{C} \to \mathbb{C}$, with the natural identification of $\mathbb{C}$ and $\mathbb{R}^2$:

$$\Phi_1(z) := \xi\bar{z} \quad \text{and} \quad \Phi_2(z) := (1-\xi)(\bar{z}-1)+1 \tag{3.19}$$

for $\xi = \frac{1}{2} + \frac{1}{2\sqrt{3}}\mathbb{i}$. For this example, $r_1 = r_2 = 1/\sqrt{3}$ and the single generator $G$ is the equilateral triangle of side length $\frac{1}{3}$ depicted as $T_1$ in Fig. 3.2. Here and henceforth, we reserve the symbol $\mathbb{i} = \sqrt{-1}$ for the imaginary number.

### 3.4.2 The 1-parameter family of Koch tilings

There is an entire family of Koch curves generalizing the standard Koch curve. We use the same system as above:

$$\Phi_1(z) := \xi\bar{z} \quad \text{and} \quad \Phi_2(z) := (1-\xi)(\bar{z}-1)+1,$$

but now $\xi$ may be any complex number satisfying

$$|\xi|^2 + |1-\xi|^2 < 1, \tag{3.20}$$

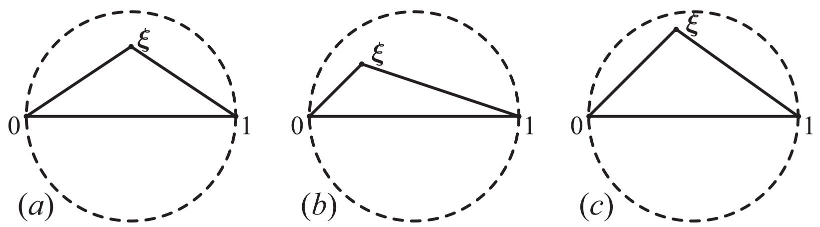


Figure 3.3: $(a)$ The parameter $\xi$ for the standard Koch curve, as depicted in Fig. 3.1 and Fig. 3.2. $(b)$ $\xi$ for a skinny Koch, as in Fig. 3.4. $(c)$ $\xi$ for a chunky Koch, as in Fig. 3.5.

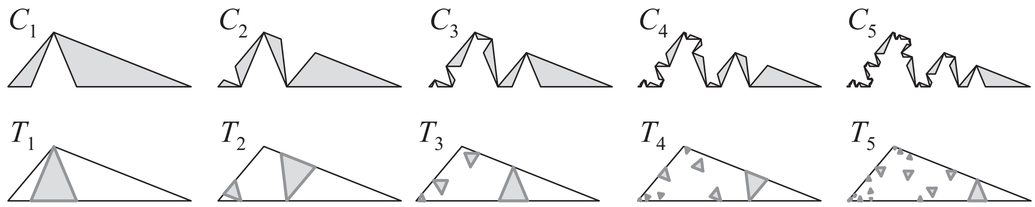


Figure 3.4: Self-similar tiling of nonstandard Koch curve $(b)$.

as shown in Figure 3.3. Geometric considerations show that (3.20) must be satisfied in order for the tileset condition (3.7) to be met.

For any member of this family, we have one isoceles triangle $G = G_1 = \operatorname{int} T_1$ for a generator. A key point of interest in this example is that, in the language of [La-vF4], curves from this family will generally be nonlattice, i.e., the logarithms of the scaling ratios will not be rationally dependent. Thus, one may use this example to construct tilings where the scaling ratios involved satisfy certain number-theoretic conditions, as studied in [La-vF4].

### 3.4.3 The one-sided Koch tiling

Occasionally, one may wish to consider a set which is not self-similar, but which has a (piecewise) self-similar boundary. The Koch snowflake is an example of

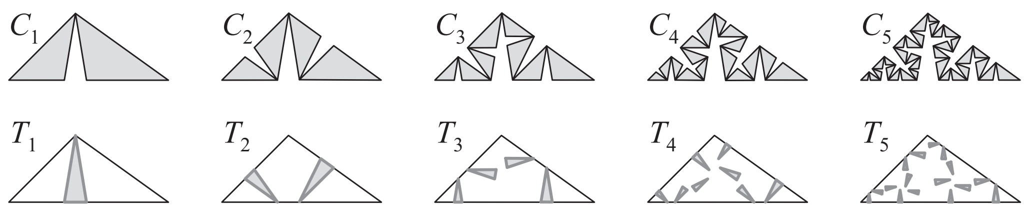


Figure 3.5: Self-similar tiling of nonstandard Koch curve $(c)$.

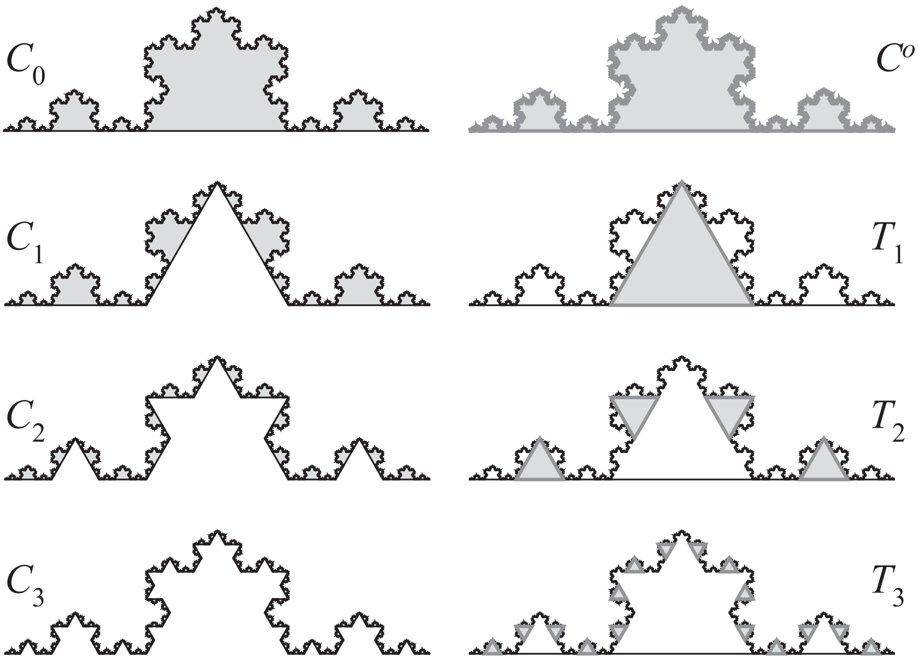


Figure 3.6: Self-similar tiling of the interior Koch curve.

such a domain. When considering the area of the interior of the Koch curve, one is interested in tiling only the region on one side of the curve. This perspective is motivated by mimicking the calculation of the interior $\varepsilon$-neighbourhood of the snowflake, as opposed to a 2-sided $\varepsilon$-neighbourhood.

For this approach, the previous IFS will not work; its alternating nature maps portions of the interior to the exterior and vice versa. We can, however, view the Koch curve as the self-similar set generated by an IFS consisting of 4 maps, each with scaling ratio $\frac{1}{3}$, in the obvious manner. Since we want each stage of the construction to generate only those triangles which lie inside the curve, it behooves us to take the intersection of the convex hull with the interior of the Koch curve, as seen in the shaded region of $C_0$ in Figure 3.6. The Koch curve may now be constructed using the 4-map IFS depicted in Figure 3.6 (note how $C_1 = \bigcup_{j=1}^{4} \Phi_j(C_0)$, etc).

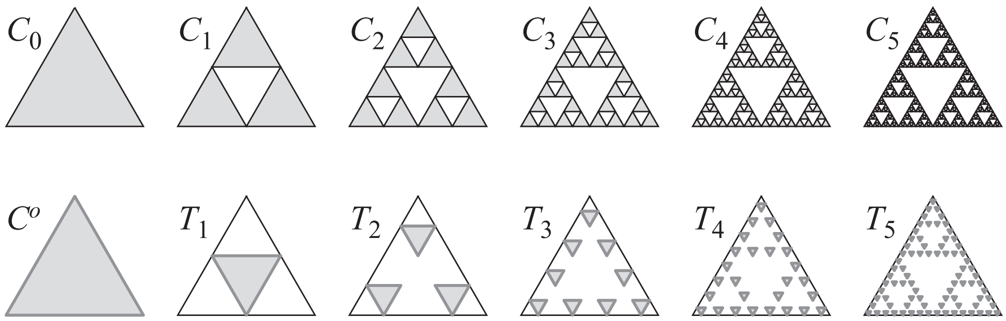


Figure 3.7: Self-similar tiling of the Sierpinski gasket.

### 3.4.4 The Sierpinski gasket

The Sierpinski gasket system consists of the three maps

$$\Phi_j(x) = \frac{1}{2}x + \frac{p_j}{2},$$

where the $p_j$ are the vertices of an equilateral triangle; the standard example is $p_1 = 0, p_2 = 1,$ and $p_3 = (1 + \mathbb{i}\sqrt{3})/2$.

The convex hull of the gasket is the triangle with vertices $p_1, p_2, p_3$. The generator $G$ is the 'middle fourth' of the hull (the interior of $T_1$ in Figure 3.7).

### 3.4.5 The Pentagasket

The pentagasket is constructed via five maps

$$\Phi_j(x) = \phi^{-2}x + p_j,$$

where the $p_j$ form the vertices of a pentagon of side length 1, and $\phi = \frac{1+\sqrt{5}}{2}$ is the golden ratio, so that the scaling ratio of each mapping is

$$r_j = \phi^{-2} = \tfrac{3-\sqrt{5}}{2}, \quad j = 1, \dots, 5.$$

The pentagasket is the first example of multiple generators $G_q$. In fact, we have the generators $\operatorname{int} T_1 = G_1 \sqcup \cdots \sqcup G_6$ where $G_1$ is a pentagon and $G_2, \dots, G_6$ are triangles.

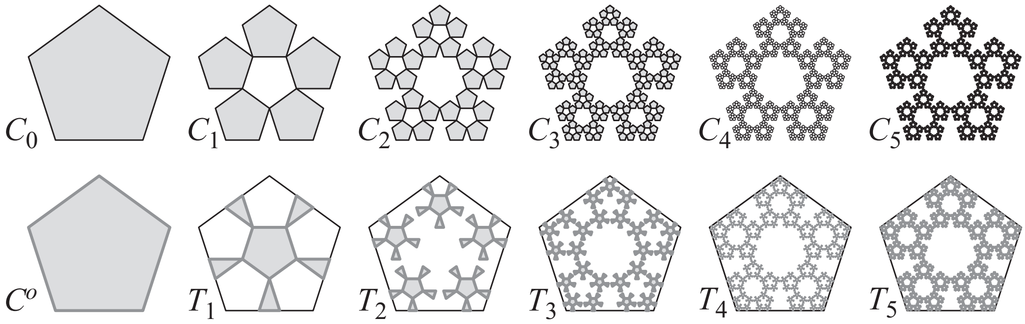


Figure 3.8: Self-similar tiling of the pentagasket.

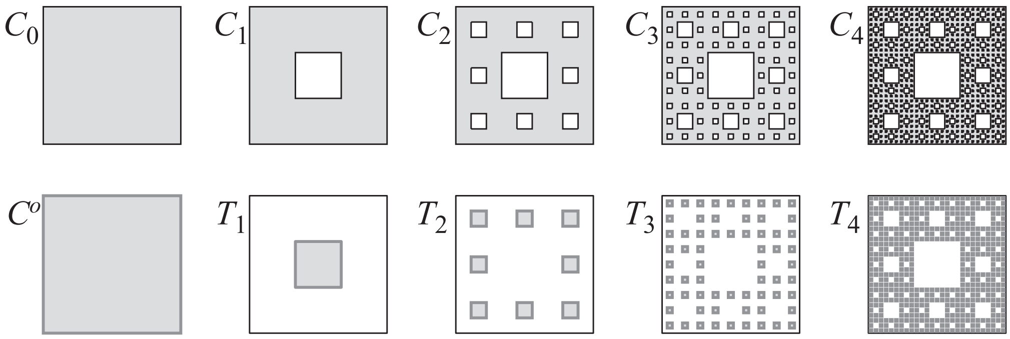


Figure 3.9: Self-similar tiling of the Sierpinski carpet.

### 3.4.6 The Sierpinski carpet

The Sierpinski carpet is constructed via eight maps

$$\Phi_j(x) = \tfrac{x}{3} + p_j,$$

where $p_j = (a_j, b_j)$ for $a_j, b_j \in \{0, \frac{1}{3}, \frac{2}{3}\}$, excluding the single case $(1/3, 1/3)$. The Sierpinski carpet is an example which is not finitely ramified; indeed, it is not even post-critically finite (see [Kig]).

### 3.4.7 The Menger sponge

The Menger sponge is constructed via twenty maps

$$\Phi_j(x) = \tfrac{x}{3} + p_j,$$

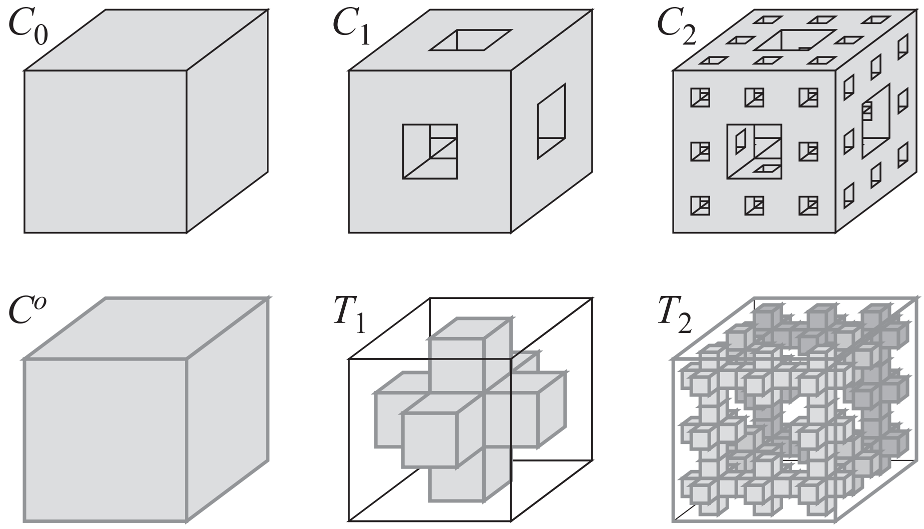


Figure 3.10: Self-similar tiling of the Menger sponge.

where $p_j = (a_j, b_j, c_j)$ for $a_j, b_j, c_j \in \{0, \frac{1}{3}, \frac{2}{3}\}$, except for the six cases when exactly two coordinate are $1/3$, and the single case when all three coordinates are $1/3$.

The Menger sponge system is the first example with an generator of dimension greater than 2, also the first example with a nonconvex generator.

### 3.4.8 A preview of later examples

Each of the examples of this section will be revisited in greater detail in Chapter 6, where their tube formulas (and other associated objects) will also be given.

## 3.5 Properties of the tiling

The results of this section indicate that a self-similar tiling may be constructed for any self-similar system satisfying the tileset condition of Definition 3.2.7. Throughout, we will use the fact that $\overline{A} = \operatorname{int} A \sqcup \partial A$, where we denote the closure of $A$ by $\overline{A}$, the interior of $A$ by $\operatorname{int} A$, and the boundary of $A$ by $\partial A = \overline{A} \cap \overline{A^c}$, where $A^c = \mathbb{R}^d \sim A$. Recall that $\sqcup$ indicates *disjoint* union.

**Theorem 3.5.1.** *For each $k \in \mathbb{N}$, one has $C_{k+1} \subseteq C_k \subseteq C$.*

*Proof.* Any point $x \in C$ is a convex combination of points in $F$. Since similarity transformations preserve convexity, $\Phi_j(x)$ will be a convex combination of points in $\Phi_j(F) \subseteq F$. Hence $\Phi_j(C) \subseteq [F] = C$ for each $j$, so $\Phi(C) \subseteq C$. By iteration of this argument, we immediately have $\Phi^k(C) \subseteq C$ for any $k \in \mathbb{N}$. From (3.13), it is clear that

$$C_{k+1} = \Phi(C_k) = \Phi^{k+1}(C) = \Phi^k(\Phi(C)) \subseteq \Phi^k(C) = C_k, \tag{3.21}$$

where the inclusion follows by $\Phi(C) \subseteq C$, as established initially. □

**Corollary 3.5.2.** *The tileset condition is preserved under the action of* $\Phi$*, i.e.,*

$$\operatorname{int} \Phi_j(C_k) \cap \operatorname{int} \Phi_\ell(C_k) = \varnothing, \quad \forall k \in \mathbb{N}. \tag{3.22}$$

*Proof.* From Theorem 3.5.1 we have $\operatorname{int} \Phi_j(C_k) \subseteq \operatorname{int} \Phi_j(C)$, and similarly for $\Phi_\ell$. The disjointness of $\operatorname{int} \Phi_j(C_k)$ and $\operatorname{int} \Phi_\ell(C_k)$ follows from the tileset condition (3.7). □

**Corollary 3.5.3.** *For $A \subseteq C_k$, we have $\Phi_w(A) \subseteq C_k$, for all $w \in W$. In particular, $F \subseteq C_k, \forall k$.*

*Proof.* By iteration of (3.21), it is immediate that $C_m \subseteq C_k$ for any $m \geq k$. Since $\Phi(A) \subseteq \Phi(C_k) = C_{k+1} \subseteq C_k$ by Theorem 3.5.1, the first conclusion follows. The special case follows by induction on $k$ with basis case $A = F \subseteq C = C_0$. The inductive step is

$$F \subseteq C_k \quad \Longrightarrow \quad F = \Phi(F) \subseteq \Phi(C_k) = C_{k+1}.$$ □

*Remark* 3.5.4. With $k = 0$ and $A = \operatorname{int} C$, Cor. 3.5.3 shows that any system $\Phi$ satisfying the tileset condition (3.7) must also satisfy the open set condition (OSC); see Remark 3.2.8.

**Corollary 3.5.5.** *The decreasing sequence of sets $\{C_k\}$ converges to $F$.*

*Proof.* Cor. 3.5.3 shows $F \subseteq C_k$ for every $k$, so it is clear that $F \subseteq \bigcap C_k$. For the reverse inclusion, suppose $x \notin F$, so that $x$ must be some positive distance $\varepsilon$ from $F$. Recall that $r_1$ is the largest scaling ratio of the maps $\{\Phi_j\}$, and that $0 < r_1 < 1$.

For $w \in \mathcal{W}_k$, we have $diam(\Phi_w(C)) \leq r_1^k diam(C)$, which clearly tends to 0 as $k \to \infty$. Therefore, we can find $k$ for which all points of $C_k = \Phi^k(C)$ lie within $\varepsilon/2$ of $F$. Thus $x$ cannot lie in $C_k$ and hence $x \notin \bigcap C_k$. □

*Remark* 3.5.6. Convergence also holds in the sense of Hausdorff metric, by a theorem of [Hut]; see also [Fal1] or [Kig] for a nice discussion. Hutchinson showed that $\Phi$ is a contraction mapping on the metric space of compact subsets of $\mathbb{R}^d$, which is complete when endowed with the Hausdorff metric. An application of the contraction mapping principle then shows that $\Phi$ has a unique fixed point (as stated in Definition 3.2.4) and that any other point tends towards it under iteration of the action of $\Phi$. This phenomenon is especially apparent in Figures 3.2, 3.7, 3.8, and 3.9.

**Lemma 3.5.7.** *The action of* $\Phi$ *commutes with set closure, i.e.,* $\Phi\left(\overline{A}\right) = \overline{\Phi(A)}$

*Proof.* It is well known that closure commutes with finite unions, i.e., for any sets $A, B$, one has $\overline{A} \cup \overline{B} = \overline{(A \cup B)}$. See, e.g., [Mu, Chap. 2, §17]. Also, each $\Phi_j$ is a homeomorphism, and is thus a closed, continuous map. Therefore,

$$\Phi\left(\overline{A}\right) = \bigcup_{j=1}^{J} \Phi_j\left(\overline{A}\right) = \bigcup_{j=1}^{J} \overline{\Phi_j(A)} = \overline{\bigcup_{j=1}^{J} \Phi_j(A)} = \overline{\Phi(A)}. \qquad \square$$

**Theorem 3.5.8.** *If* $A$ *is the closure of its interior, then so is* $\Phi(A)$.

*Proof.* Let $x \in \Phi(A)$ so that $x \in \Phi_j(A)$ for some $j = 1, \ldots, J$. Because each map $\Phi_j$ is a homeomorphism, we know that $\Phi_j(A)$ is the closure of its interior, and hence that $x \in \overline{\operatorname{int} \Phi_j(A)} \subseteq \overline{\operatorname{int} \Phi(A)}$. The reverse inclusion $\overline{\operatorname{int} \Phi(A)} \subseteq \Phi(A)$ is immediate because $A$ is closed by hypothesis (and thus $\Phi(A)$ is also closed). □

**Corollary 3.5.9.** *Each set* $C_k$ *is the closure of its interior.*

*Proof.* The set $C = [F]$ is convex by definition, and compact by [Schn2, Thm. 1.1.10]. Therefore, $C$ is the closure of its interior by [Schn2, Thm. 1.1.14]. The conclusion follows by iteration of Theorem 3.5.8. □

**Corollary 3.5.10.** *The tileset condition implies that images of the hull can only overlap on their boundaries:*

$$\Phi_j(C) \cap \Phi_\ell(C) \subseteq \partial\Phi_j(C) \cap \partial\Phi_\ell(C), \quad \textit{for } j \neq \ell. \tag{3.23}$$

*Proof.* Let $x \in \Phi_j(C) \cap \partial\Phi_\ell(C)$. Suppose, by way of contradiction, that $x \in \operatorname{int}\Phi_j(C)$. Then we can find an open neighbourhood $U$ of $x$ which is contained in $\operatorname{int}\Phi_j(C)$. Since $x \in \partial\Phi_\ell(C)$, there must be some $z \in U \cap \operatorname{int}\Phi_\ell(C)$, by Cor. 3.5.9. But then $z \in \operatorname{int}\Phi_j(C) \cap \operatorname{int}\Phi_\ell(C)$, in contradiction to the tileset condition. □

**Theorem 3.5.11** (Nondegeneracy of tilesets)**.** *Each tileset is the closure of its interior.*

*Proof.* We need only show $T_k \subseteq \overline{\operatorname{int} T_k}$, since the reverse containment is clear by the closedness of $T_k$. Since $\overline{A} = \operatorname{int} A \sqcup \partial A$, take $x \in \operatorname{int}(C_{k-1} \sim C_k)$ to begin. Using Cor. 3.5.9, we have equality in the first step of the following derivation:

$$\begin{aligned}
C_{k-1} \sim C_k &= \overline{\operatorname{int}(C_{k-1})} \sim \overline{C_k} \\
&\subseteq \overline{\operatorname{int}(C_{k-1}) \sim C_k} \\
&\subseteq \overline{\operatorname{int}(C_{k-1} \sim C_k)} \qquad (3.24)\\
&\subseteq \overline{\operatorname{int}\left(\overline{C_{k-1} \sim C_k}\right)}.
\end{aligned}$$

The containment (3.24) follows from

$$\operatorname{int}(C_{k-1}) \sim C_k = \operatorname{int}(\operatorname{int}(C_{k-1}) \sim C_k) \subseteq \operatorname{int}(C_{k-1} \sim C_k),$$

where one has the equality because the difference of an open and closed set is open, and the containment because $\operatorname{int}(C_{k-1}) \subseteq C_{k-1}$.

Now consider the case when $x \in \partial(C_{k-1} \sim C_k)$. Pick an open set $U$ and find $z \in U \cap (C_{k-1} \sim C_k)$. Then $z \in \overline{\operatorname{int}\left(\overline{C_{k-1} \sim C_k}\right)}$ by the same argument as above. This means that $x$ is a limit point of the closed set $\overline{\operatorname{int}\left(\overline{C_{k-1} \sim C_k}\right)}$, and hence must lie within it. □

The following corollary will be useful in the proof of Theorem 3.5.14.

**Corollary 3.5.12.** *For $j = 1, \ldots, J$, $\overline{\Phi_j(C_{k-1}) \sim \Phi_j(C_k)}$ is the closure of its interior.*

*Proof.* Because each $\Phi_j$ is a homeomorphism, the set $\Phi_j(\overline{C_{k-1} \sim C_k})$ will be the closure of its interior by Theorem 3.5.11. However, we have

$$\Phi_j(\overline{C_{k-1} \sim C_k}) = \overline{\Phi_j(C_{k-1} \sim C_k)} = \overline{\Phi_j(C_{k-1}) \sim \Phi_j(C_k)}, \tag{3.25}$$

since $\Phi_j$ is closed and injective. $\square$

We are now ready to prove the main result of this section.

**Theorem 3.5.13.** *Each tileset is the image under $\Phi$ of its predecessor, i.e.,*

$$\Phi(T_k) = T_{k+1}, \quad \textit{for } k \in \mathbb{N}. \tag{3.26}$$

*Proof.* Using using Definition 3.3.1 and (3.25), we have the identities

$$\Phi(T_k) = \bigcup_{j=1}^{J} \overline{\Phi_j(C_{k-1} \sim C_k)}, \text{ and} \tag{3.27}$$

$$T_{k+1} = \overline{C_k \sim C_{k+1}}. \tag{3.28}$$

($\subseteq$) To see that (3.27) is a subset of (3.28), pick $x \in \Phi(T_k)$, so that

$$x \in \overline{\Phi_j(C_{k-1} \sim C_k)} = \overline{\Phi_j(C_{k-1}) \sim \Phi_j(C_k)} \tag{3.29}$$

for some $j = 1, \dots, J$. Since $\overline{A} = \operatorname{int} A \sqcup \partial A$, we proceed by cases. Here again, $\sqcup$ denotes the disjoint union.

(i) Let $x \in \operatorname{int}(\Phi_j(C_{k-1}) \sim \Phi_j(C_k))$. Then let $U \subseteq \Phi_j(C_{k-1}) \sim \Phi_j(C_k)$ be an open neighbourhood of $x$. Since $x \in U \subseteq \Phi_j(C_{k-1})$, we have $x \in \operatorname{int} \Phi_j(C_{k-1}) \subseteq C_k$.

By way of contradiction, suppose that $x \in C_{k+1}$. Then $x \in \Phi_\ell(C_k)$ for some $\ell$. Note that $\ell \neq j$, since $x \notin \Phi_j(C_k)$ by initial choice of $x$. Inasmuch as Theorem 3.5.1 gives $x \in \Phi_\ell(C_{k-1})$, Cor. 3.5.10 implies

$$x \in \partial\Phi_j(C_{k-1}) \cap \partial\Phi_\ell(C_{k-1}), \tag{3.30}$$

contradicting the fact that $x \in \operatorname{int} \Phi_j(C_{k-1})$. So we may conclude that

$$x \in C_k \sim C_{k+1} \subseteq \overline{C_k \sim C_{k+1}}. \tag{3.31}$$

(ii) Now consider $x \in \partial(\Phi_j(C_{k-1}) \sim \Phi_j(C_k))$. Again, let $U$ be an open neighbourhood of $x$. By Cor. 3.5.12, we can find $w \in U \cap \operatorname{int}(\Phi_j(C_{k-1}) \sim \Phi_j(C_k))$. By applying the arguments of part (i), we obtain $w \in \overline{C_k \sim C_{k+1}}$ and hence that $x$ is a limit point of $\overline{C_k \sim C_{k+1}}$. Since this latter set is closed, we have shown that $x \in \overline{C_k \sim C_{k+1}}$ in case (ii), and completed the forward inclusion.

($\supseteq$) Now we need to show that (3.28) is a subset of (3.27). Since

$$x \in \overline{C_k \sim C_{k+1}} = \operatorname{int}(C_k \sim C_{k+1}) \sqcup \partial(C_k \sim C_{k+1}), \tag{3.32}$$

this will again require two parts.

(iii) Let $x \in \operatorname{int}(C_k \sim C_{k+1}) \subseteq \Phi(C_{k-1}) \sim \Phi(C_k)$. Then $x \in \Phi(C_{k-1})$ means that $x \in \Phi_j(C_{k-1})$ for some $j = 1, \dots, J$. Furthermore, there must be some $y \in C_{k-1}$ with $\Phi_j(y) = x$. We know $y \notin C_k$, because otherwise

$$y \in C_k \quad \implies \quad x = \Phi_j(y) \in \Phi_j(C_k) \subseteq C_{k+1}, \tag{3.33}$$

which contradicts the initial choice $x \notin C_{k+1}$. Thus $y \in C_{k-1} \sim C_k$, which implies

$$x = \Phi_j(y) \in \Phi_j(C_{k-1} \sim C_k) \subseteq \overline{\Phi_j(C_{k-1} \sim C_k)}. \tag{3.34}$$

(iv) Now consider $x \in \partial(C_k \sim C_{k+1})$, and again let $U$ be an open neighbourhood of $x$. Then there is some $z \neq x$ with $z \in U \cap \operatorname{int}(C_k \sim C_{k+1})$. By applying the arguments of part (iii) to $z$, we see

$$z \in \operatorname{int}(C_k \sim C_{k+1}) \quad \implies \quad z \in \overline{\Phi_j(C_{k-1} \sim C_k)}. \tag{3.35}$$

Therefore, we have shown that $x$ is a limit point of $\overline{\Phi_j(C_{k-1} \sim C_k)}$, and is hence contained in it. This completes the proof of the equality (3.26). □

**Theorem 3.5.14.** *The tilesets can be recovered as the closure of the images of the generators under the action of* $\Phi$, *that is,*

$$T_k = \overline{\bigsqcup_{q=1}^{Q} \Phi^{k-1}(G_q)}. \tag{3.36}$$

*Proof.* First, observe that[3]

$$\overline{C \sim \Phi(C)} = \overline{\operatorname{int}(C \sim \Phi(C))}, \tag{3.37}$$

as follows. If $x \in \overline{C \sim \Phi(C)}$, then any open neighbourhood $U$ of $x$ must intersect $\operatorname{int}(C \sim \Phi(C))$, because $\overline{C \sim \Phi(C)}$ is the closure of its interior, by Theorem 3.5.11. Hence $x \in \overline{\operatorname{int}(C \sim \Phi(C))}$. The reverse inclusion is clear.

Using (3.37), we have

$$\bigcup_{q=1}^{Q} \overline{G_q} = \overline{\bigsqcup_{q=1}^{Q} G_q} = \overline{\operatorname{int}(C \sim \Phi(C))} = \overline{C \sim \Phi(C)} = T_1. \tag{3.38}$$

Now take $\Phi^{k-1}$ of both sides, using Lemma 3.5.7 on the left and Theorem 3.5.13 on the right, to obtain the conclusion:

$$\overline{\bigsqcup_{q=1}^{Q} \Phi^{k-1}\left(G_q\right)} = \Phi^{k-1}\left(\overline{\bigsqcup_{q=1}^{Q} G_q}\right) = \Phi^{k-1}(T_1) = T_k. \tag{3.39}$$

The union $\bigsqcup_{q=1}^{Q} \Phi^{k-1}(G_q)$ is disjoint because each $\Phi_j$ is injective, $G_q \subseteq \operatorname{int} C$, and the tileset condition (3.7) prohibits overlaps of interiors. □

**Theorem 3.5.15.** *The collection $\mathcal{T} = \{\Phi_w(G_q)\}$ is an open tiling of $C$, in the sense of Definition 3.2.10. In fact, $\mathcal{T}$ is an open tiling of $C \sim F$.*

*Proof.* (i) To see that $C = \bigcup \overline{R_n} = \bigcup \overline{\Phi_w(G_q)}$, it suffices to show $C = \bigcup T_k$, by Theorem 3.5.14. Pick $x \in C \sim F$. Since $F = \bigcap C_k$ by Cor. 3.5.5, this means we can find $k$ such that $x \in C_{k-1}$ but $x \notin C_k$. Then

$$x \in C_{k-1} \sim C_k \subseteq \overline{C_{k-1} \sim C_k} = T_k. \tag{3.40}$$

The reverse inclusion is obvious from Theorem 3.5.1 and the definition of the tiles as subsets of the $C_k$, in (3.14).

(ii) To see that the tiles are disjoint, note first that the generators are disjoint by definition. Suppose $R_n$ and $R_m$ are both in the same tileset $T_k$. Then (3.39) shows that they are disjoint. Now suppose $R_n \subseteq T_k$ and $R_m \subseteq T_\ell$, where $k < \ell$. Then

[3]The equality (3.37) is not trivial because the right side has $C \sim \Phi(C)$, not $\overline{C \sim \Phi(C)}$.

$R_n$ is disjoint from $C_k$ by definition of $T_k$, and it follows from Theorem 3.5.1 that $R_n$ is disjoint from $C_\ell$ for all $\ell \geq k$. (See, e.g., Figure 3.2.)

It is also clear that $R_n \cap C_k = \varnothing$ implies that $R_n \cap F = \varnothing$, so no tiles intersect the attractor $F$. Thus, $\mathcal{T}$ is an open tiling of $C \sim F$. □

**Corollary 3.5.16.** *The tiling $\mathcal{T}$ is subselfsimilar in that $\Phi(\mathcal{T}) = \mathcal{T} \sim \bigsqcup_q G_q$.*

In fact, somewhat more is true. It is clear from the preceding theorems that the containment $\Phi(\mathcal{T}) \subseteq \mathcal{T}$ has a special structure in that $\Phi$ sends tiles from one generation (that is from one stage of the construction) into tiles of the next. More precisely, if $R_n \subseteq T_k$ is a tile, then $\Phi_j(R_n)$ will be also be a tile, and it is contained in $T_{k+1}$.

Figure 3.1 illustrates Theorems 3.5.14–3.5.15 for the Koch tiling $\mathcal{K}$.

# 3.6 Concluding remarks on the tiling

## 3.6.1 Properties of the generators

What kinds of generators are possible? In general, this is a difficult question to answer; it will be explored in detail in [LaPe3]. The generators inherit many geometric properties from the convex hull $C = [F]$ and may therefore have a finite or infinite number of nonregular boundary points. In fact, by an observation of [StWa], it is possible (even generic) for the boundary of a 2-dimensional generator to be a piecewise $C^1$ curve; however, it is impossible for it to be a piecewise $C^2$ curve. In §3.4.5, the pentagasket provides an example of a tiling with multiple generators, and it is clear that these need not be similar. In §6.7, the Menger sponge provides an example of a tiling which has a nonconvex generator. Indeed, the generator of the Menger tiling does not even have positive reach. See also Remark 4.4.4.

## 3.6.2 Affine mappings

The construction presented in this paper remains true if the mappings are taken to be affine contractions, instead of similarities. Indeed, the key properties of similarity mappings that have been exploited to prove the theorems of §3.5 are as follows: similarity transformations are continuous, open, and closed mappings which preserve convexity.

However, I have not pursued the generalization to affine maps, as the tiling was developed as a tool for computing the tube formula associated with a system $\Phi$. The strategy of Chapter 5 is to use tube formulas for the generators to obtain tube formulas for all the tiles. Under affine transformations, however, such an idea does not seem to work.

### 3.6.3 The convex hull

One might ask why the convex hull plays such a unique role in the construction of the tiling. There may exist other sets which are suitable for initiating the construction; however, some properties seem to make the convex hull the natural choice:

1. Any convex set is the closure of its interior, and hence so is any polyconvex set (as shown in the proof of Cor. 3.5.9), like $\Phi^k(C)$.
2. The convex hull satisfies certain nesting properties with respect to the action of $\Phi$. By Theorem 3.5.1, we have $\Phi(C) \subseteq C$ and hence $\Phi^k(C) \subseteq \Phi^\ell(C)$ for any $k \geq \ell$.
3. The convex hull of $F$ obviously contains $F$.

### 3.6.4 The dynamics

The self-similar tiling gives a portrait of attraction for $\Phi$. If $x \in R_n$ and $R_n$ is a tile contained in $T_k$, then $\Phi_j(x)$ lies in a tile which is contained in $T_{k+1}$, etc. In this way, $\{T_k\}$ gives a kind of portrait of the trajectory

$$\Phi_{w_1}(x), \Phi_{w_1 w_2}(x), \Phi_{w_1 w_2 w_3}(x), \ldots$$

of $x$ under $\Phi_w$. Indeed, for $A \subseteq R_n$, one sees that $\Phi^\ell(A)$ is contained in the tiles of $T_{k+\ell}$. At a later date, it would be interesting to see if this can be pursued further.

# Chapter 4

# Measures and Zeta Functions

## 4.1 Introduction

The self-similar tiling was developed as a tool for extending the work of [La-vF4] to higher dimensions. The research monograph [La-vF4] studies fractal subsets of $\mathbb{R}$ via the theory of fractal strings. As described in §1.1, a *fractal string* is defined to be a bounded open subset of $\mathbb{R}$. The motivation for this definition is to have an open set whose boundary is some fractal subset of $\mathbb{R}$ that one wishes to study. Thus, the definition may alternatively rephrased as: a *fractal string* is the complement of a fractal subset of $\mathbb{R}$ within its convex hull. The two are immediately seen to be equivalent when $\partial\mathcal{L}$ is a fractal subset of $\mathbb{R}$. For $F \subseteq \mathbb{R}^d$, however, these may not be the same. The Sierpinski gasket tiling provides an example of when the boundary of $\mathcal{T}$ is exactly the original fractal subset of $\mathbb{R}^2$ (see Figure 4.1) and the Koch tiling provides an example of when the boundary of $\mathcal{T}$ strictly contains the original fractal subset (compare to Figure 3.1). Roughly, this corresponds to the difference between fractal domains, and domains with fractal boundary. Because of such technicalities, we have chosen to concentrate on $\mathcal{T}$ instead of $F$ in this dissertation.

As in §1.1, $\mathcal{L}$ may be represented by

$$\mathcal{L} := \{\ell_n\}_{n=1}^{\infty}, \quad \text{with} \sum_{n=1}^{\infty} \ell_n < \infty. \tag{4.1}$$

The fractal strings considered in [La-vF4] are more general objects than those

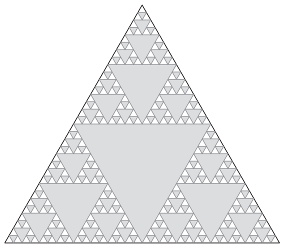

Figure 4.1: Tiling the complement of the Sierpinski gasket.

discussed in this dissertation. The self-similar tiling developed in Chapter 3 is the higher-dimensional analogue of the self-similar strings discussed in [La-vF4, Chap. 2–3]; a general theory of higher-dimensional fractal sets is still somewhat distant.

From [La-vF4], the *geometric zeta function* of the fractal string (4.1) is the meromorphic extension of the function

$$\zeta_{\mathcal{L}}(s) = \sum_{n=1}^{\infty} \ell_n^s. \tag{4.2}$$

This tool can be used to study the geometry of $\mathcal{L}$ and of its (presumably fractal) boundary $\partial\mathcal{L}$. In what follows, it will be important to think of the string as the measure

$$\eta_{\mathcal{L}} = \sum_{n=1}^{\infty} \delta_{1/\ell_n}, \tag{4.3}$$

where $\delta_x$ denotes the Dirac mass (or Dirac measure) at $x$. In view of (4.3), one sees that $\zeta_{\mathcal{L}}(s)$ is the Mellin transform of this measure:

$$\zeta_{\mathcal{L}}(s) = \int_0^\infty x^{-s}\, d\eta_{\mathcal{L}}(x). \tag{4.4}$$

This differs slightly from the definition of Mellin transform of a (test) function $\varphi$ used in Chapter 5 below:

$$\widetilde{\varphi}(s) := \int_0^\infty x^{s-1}\varphi(\varepsilon)\, d\varepsilon.$$

The authors of [La-vF4] are able to relate geometric and physical properties of fractal strings through the use of zeta functions which contain geometric and spectral information about the given string. This information includes the fractal dimension and measurability of the fractal under consideration. One of the main results of [La-vF4] is an explicit formula for the volume $V_{\mathcal{L}}(\varepsilon)$ of the $\varepsilon$-neighbourhood of a fractal subset $\partial\mathcal{L}$ of $\mathbb{R}$, obtained by applying certain distributional methods to the geometric zeta function. It is a long-term goal to obtain similar results for suitable fractal subsets of $\mathbb{R}^d$. In Chapter 5 of the present work, a first step is made by computing the tube formula $V_{\mathcal{T}}(\varepsilon)$ for self-similar tilings and fractal sprays. Fractal sprays are a more generalized higher-dimensional analogue of fractal strings which are discussed in §5.4. A self-similar tiling is a special case of a fractal spray where (among other things) the scaling measure is derived from a self-similar system. Fractal sprays were introduced in [La-vF4, §1.4].

In §4.5 of this chapter, we will obtain the geometric zeta function of a tiling $\zeta_{\mathcal{T}}$. Using the geometric zeta function, we will obtain the following key result, which is stated fully (and in more generality) in Theorem 5.4.5:

**Theorem 4.1.1.** *The $d$-dimensional volume of the inner tubular neighbourhood of $\mathcal{T}$ is given by the following distributional explicit formula:*

$$V_{\mathcal{T}}(\varepsilon) = \sum_{\omega \in \mathcal{D}_{\mathcal{T}}} \operatorname{res}\left(\zeta_{\mathcal{T}}(\varepsilon, s); \omega\right). \tag{4.5}$$

*where the set of complex dimensions $\mathcal{D}_{\mathcal{T}}$ of the tiling $\mathcal{T}$ consists of the poles of $\zeta_{\mathcal{T}}$.*

The first ingredient of $\zeta_{\mathcal{T}}$ is a *scaling zeta function* $\zeta_{\mathfrak{s}}(s)$, a generating function for the the scaling properties of the tiling. This Dirichlet series is the Mellin transform of a discrete *scaling measure* $\eta_{\mathfrak{s}}$ which encodes the combinatorics of the scaling ratios of a self-similar tiling. More precisely, the measure $\eta_{\mathfrak{s}}$ is a sum of Dirac masses, where each mass is located at a reciprocal scaling ratio of some composition of the similarity transformations $\{\Phi_j\}$. Such a mass is weighted by the multiplicity of the corresponding scaling ratio. Some examples of these measures are illustrated in §6.1; e.g., Figure 6.4, Figure 6.8 and Figure 6.11. The scaling zeta function $\zeta_{\mathfrak{s}}$ coincides with the zeta functions studied in [La-vF4]. The function $\zeta_{\mathfrak{s}}$ also allows us to define the scaling complex dimensions of a self-similar set in $\mathbb{R}^d$ (as the poles of $\zeta_{\mathfrak{s}}$), and we find these dimensions to have the same structure as in the 1-dimensional case. The definition and properties of the scaling measure $\eta_{\mathfrak{s}}$ and zeta function $\zeta_{\mathfrak{s}}$ are discussed in §4.3.

The next ingredient of $\zeta_{\mathcal{T}}$ is an *(adaptive) tile tube formula* $\gamma_G$. From Chapter 3, we know that certain tiles $G_1, \dots, G_Q$ of $\mathcal{T}$ are generators. More precisely, any tile $R_n$ of $\mathcal{T}$ is the image of a generator under some composition of the mappings $\Phi_j$:

$$R_n = \Phi_{w_k} \circ \dots \circ \Phi_{w_1}(G_q),$$

for some $G_q$ and some $w = w_1 \dots w_k \in \mathcal{W}$. In §4.4, we discuss the role of the generators and introduce the function $V_G(\varepsilon)$ which gives the inner tube formula for a generator. From this, we obtain the function $\gamma_G(x, \varepsilon)$, which is defined so that $\gamma_G(1, \varepsilon)$ gives the volume of the inner $\varepsilon$-neighbourhood of a generator $G$ scaled to have inradius 1, and $\gamma_G(x, \varepsilon)$ gives the volume of a tile which is similar to $G$, but has inradius $1/x > \varepsilon$. Therefore, by integrating $\gamma_G$ against $\eta_{\mathfrak{g}}$, one obtains the total contribution of $G_q$ (and its iterates under $\Phi$) to the final tube formula $V_{\mathcal{T}}$. This is elaborated upon in §5.2.1.

At last, in §4.5, the geometric zeta function of the tiling $\zeta_{\mathcal{T}}$ is assembled from the scaling zeta function, the inradii, and the function $\gamma_G$ (or the functions $\gamma_q := \gamma_{G_q}$ when there are multiple generators). In some precise sense, $\zeta_{\mathcal{T}}$ is a generating function for the geometry of the self-similar tiling.

In Chapter 5, we will use $\zeta_{\mathcal{T}}$, and follow the distributional techniques and explicit formulas of [La-vF4] to obtain an explicit distributional tube formula for self-similar tilings. This is accomplished by exploiting the self-similar nature of the tiling and the scaling properties of various components via the method alluded to above, and is described in greater detail in §5.1.

## 4.2 $\varepsilon$-neighbourhoods and the inradius

For higher-dimensional sets, we need to replace the notion of "lengths" that proved so useful for studying fractal strings in [La-vF4], with something that makes sense for any set $A \subseteq \mathbb{R}^d$. Since we are most concerned with inner tube volumes, the appropriate notion to use is the *inradius*.

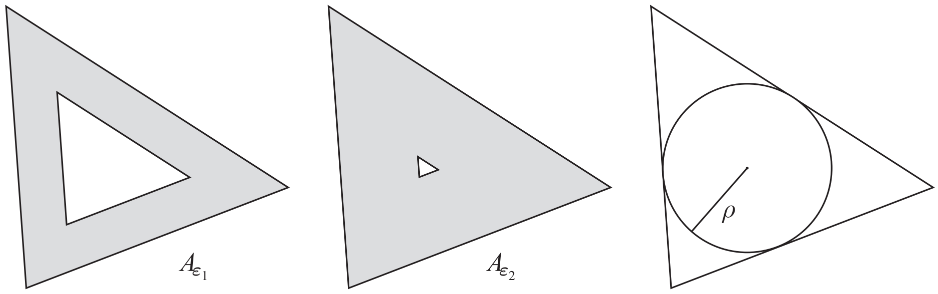


Figure 4.2: Here are two inner $\varepsilon$-neighbourhoods of a triangle $A \subseteq \mathbb{R}^2$. As $\varepsilon$ increases, $A_\varepsilon \to A$ (in the Hausdorff metric, for example). The inradius $\rho$ is depicted at the far right.

**Definition 4.2.1.** The *volume of the (inner) tubular neighbourhood* of $A$ is

$$V_A(\varepsilon) := \mathrm{vol}_d\{x \in A \,\vdots\, dist(x, \partial A) < \varepsilon\}, \qquad d \in \mathbb{N}, \tag{4.6}$$

that is, the $d$-dimensional Lebesgue measure of the set of points which lie within $A$, and within $\varepsilon$ of the boundary of $A$.

The tube formula $V_{\mathcal{T}}(\varepsilon)$ for a self-similar tiling should be useful for studying the dimension and spectral asymptotics of $\mathcal{T}$ and the original self-similar set; see [La-vF4] and [We], for example. To compute the tube formula for a tiling, note that the tiles $R_n$ have disjoint interior by Theorem 3.5.15, so the formula will simply be a sum taken over the tiles:

$$V_{\mathcal{T}}(\varepsilon) = \sum V_{R_n}(\varepsilon). \tag{4.7}$$

This sum naturally splits into two parts; one with smaller tiles which are entirely within $\varepsilon$ of their own boundary, and one with larger tiles:

$$V_{\mathcal{T}}(\varepsilon) = \sum_{\rho(R_n) \geq \varepsilon} V_{R_n}(\varepsilon) + \sum_{\rho(R_n) < \varepsilon} V_{R_n}(\varepsilon). \tag{4.8}$$

This is the natural higher-dimensional analogue of the split sum which first appeared in [LaPo1]; see also [LaPo2, Eqn. (3.2)] and [La-vF4].

The quantity which determines the split in (4.8) is called the inradius $\rho$, and is introduced in Definition 4.2.2 below. By Proposition 4.2.3 below, the terms of the second sum on the right-hand side of (4.8) satisfy $V_{R_n}(\varepsilon) = \mathrm{vol}_d(R_n)$.

**Definition 4.2.2.** The *inradius* (sometimes also called *inner radius*) of a set $A$ is

$$\rho = \rho(A) := \sup\{\varepsilon \vdots V_A(\varepsilon) < \mathrm{vol}_d(A)\}. \tag{4.9}$$

Note that the supremum is taken over $\varepsilon > 0$, because $A_0 = \overline{A}$. As mentioned just above, the inradii replace the lengths $\ell_n$ of the 1-dimensional theory.

**Proposition 4.2.3.** *In $\mathbb{R}^d$, the inradius is the furthest distance from a point of $A$ to $\partial A$, or equivalently, the radius of the largest ball contained in $A$.*

$$\rho(A) = \sup\{\varepsilon \vdots V_A(\varepsilon) < \mathrm{vol}_d(A)\} \tag{4.10a}$$

$$= \sup\{dist(x, \partial A) \vdots\ x \in A\} \tag{4.10b}$$

$$= \sup\{r \vdots \exists x \text{ with } B(x,r) \subseteq A\}. \tag{4.10c}$$

*Proof.* Observe that $V_A(\varepsilon) < \mathrm{vol}_d(A)$, if and only if there is a set $B$ such that

$$\mathrm{vol}_d(B) > 0, \quad B \subseteq A, \quad \text{and} \quad dist(x, \partial A) > \varepsilon,\ \forall x \in B.$$

Thus, taking supremums over those $\varepsilon$ for which the inequalities hold gives equivalence between (4.10a) and (4.10b).

Now let $r$ be the radius of the largest circle which can be inscribed in $A$. For a point $x \in A$, we have $dist(x, \partial A) \geq r$ if and only if a circle of radius $r$ can be inscribed in $A$ with center at $x$, i.e., if and only if $B(x,r) \subseteq A$. This suffices to show the equivalence of (4.10b) and (4.10c). □

**Definition 4.2.4.** The *generating inradii* are the inradii of the generators $G_q$ and denoted

$$g_q := \rho(G_q), \qquad \text{for } q = 1, \dots, Q. \tag{4.11}$$

Equations (3.1) and (3.18) shows that under iteration of the system (3.3), the images of the $G_q$ will be a sequence of tiles with inradii

$$\rho(\Phi_w(G_q)) = r_1^{e_1} \dots r_J^{e_J} g_q, \tag{4.12}$$

for some positive exponents $e_j$ and $q = 1, \dots, Q$. In fact, this is one of the main reasons why the inradii prove so useful: they behave well with respect to the similarity transformations $\Phi_j$ see (4.30).

Following [La-vF4], these inradii appear with multiplicity

$$m(\rho) := \sum_{q=1}^{Q} \sum \binom{\sum_{j=1}^{J} e_j}{e_1 \dots e_J}, \tag{4.13}$$

where there is a term in the second sum for every inradius of the form $\rho = r_1^{e_1} \dots r_J^{e_J} g_q$, and the multinomial coefficients are

$$\binom{\sum_{j=1}^{J} e_j}{e_1 \dots e_J} = \frac{\left(\sum_{j=1}^{J} e_j\right)!}{e_1! \dots e_J!}.$$

When discussing the indexed family of sets $\{R_n\}_{n \in \mathbb{N}}$, it is convenient to use the shorthand script

$$\rho_n := \rho(R_n). \tag{4.14}$$

As a general rule, the inradii are indexed so as to be in nonincreasing order of size, in other words, so that we have

$$\rho_1 \geq \rho_2 \geq \dots \geq \rho_n \geq \dots > 0,$$

where $\rho_n = \rho(R_n)$ is the inradius of the $n^{\text{th}}$ tile.

## 4.3 The scaling zeta function

In this section, we define a certain meromorphic function to encode the combinatorics of the scaling ratios of a self-similar tiling; the scaling zeta function.

**Definition 4.3.1.** The *scaling measure* encodes all products of scaling ratios as a sum of Dirac masses:

$$\eta_{\mathfrak{s}}(x) := \sum_{w \in \mathcal{W}} \delta_{1/r_w}(x). \tag{4.15}$$

Then the *geometric measure* is defined to be

$$\begin{aligned}\eta_{\mathfrak{g}}(x) &:= \left[\sum_{w\in\mathcal{W}} \delta_{1/g_1 r_w}(x), \dots, \sum_{w\in\mathcal{W}} \delta_{1/g_Q r_w}(x)\right] \\ &= \left[\eta_{\mathfrak{s}}(x/g_1), \dots, \eta_{\mathfrak{s}}(x/g_Q)\right], \end{aligned} \tag{4.16}$$

a $Q$-vector of horizontally dilated (or 'predilated') scaling measures which encodes the multiplicities and inradii of the tiles of $\mathcal{T}$. More precisely, the geometric measure is supported on the reciprocal inradii, and the weight associated to each Dirac mass corresponds to the multiplicity of tiles with that inradius. Both of the measures $\eta_{\mathfrak{s}}$, $\eta_{\mathfrak{g}}$ are defined on $(0, \infty)$.

The geometric measure is vector-valued for multiple generators (as opposed to being a sum over $q = 1$ to $Q$, for example) because there is a need to keep separate the inradii from different generators. Suppose that we have two tiles $R_n = \Phi_w(G_1)$ and $R_m = \Phi_{w'}(G_2)$. Then $V_{R_n}(\varepsilon) \neq V_{R_m}(\varepsilon)$ in general, even if $\rho(R_n) = \rho(R_m)$. Looking ahead to Chapter 5, these tiles will contribute different terms to the tube formula of $\mathcal{T}$. Thus the contributions stemming from generators of different types must be kept separate. To see how the contribution of $R_n$ to the net tube formula would be recovered from $G_1$, see Remark 4.4.3.

**Definition 4.3.2.** The decomposition (4.16) also shows the term corresponding to each $G_q$ for $q = 1, \dots, Q$; the $q^{th}$ *geometric measure*

$$\eta_{\mathfrak{g}q}(x) := \eta_{\mathfrak{s}}(x/g_q), \tag{4.17}$$

where $g_q$ is given by (4.11). This will be useful in the proof of Theorem 5.4.5; see also the lead-up to the proof given in §5.2.1.

*Remark* 4.3.3. The reader may wonder $\eta_{\mathfrak{s}}$ is defined in terms of the inverse scaling ratios, instead of just the scaling ratios themselves. Indeed, looking ahead to (4.29), (5.8), and the proof of Theorem 5.4.5 may lead one to believe that this is an unnecessary complication. However, there are many excellent reasons for adopting this convention.

The main reason is that in [La-vF4], the geometric formalism is developed in parallel with the spectral formalism. That is, on the geometric side, we have the measure $\eta$ associated to the string $\mathcal{L}$, we have the *geometric counting function* $N_\eta$ which counts the lengths of $\mathcal{L}$, and we have the geometric zeta function $\zeta_\eta$:

$$N_\eta := \#\{j \geq 1 \,\vdots\, l_j^{-1} \leq x\} = \int_0^x \eta(x), \text{ and}$$
$$\zeta_\eta(s) := \int_0^\infty x^{-s} d\eta(x).$$

Meanwhile, one also has the spectral measure[1] $\nu$ and the *spectral counting function* $N_\nu$ which counts the eigenvalues (normalized frequencies $f = \sqrt{\lambda}/\pi$) of $\mathcal{L}$ with respect to the Dirichlet Laplacian, and the spectral zeta function:

$$\nu(A) := \eta(A) + \eta\left(\frac{A}{2}\right) + \eta\left(\frac{A}{3}\right) + \dots, \text{ for any Borel set } A \subseteq \mathbb{R},$$
$$N_\nu(x) := \#\{x \,\vdots\, \text{frequency of } \mathcal{L}\text{, counted with multiplicity}\}, \text{ and}$$
$$\zeta_\nu(s) := \int_0^\infty x^{-s} d\nu(x).$$

Furthermore, one has the remarkable (and yet simple to prove) formula relating the two:

$$\zeta_\nu(s) = \zeta_\eta(s) \cdot \zeta(s),$$

where $\zeta(s)$ is the Riemann zeta function. Thus, adopting this convention allows one to see that the spectral properties of a string are related to the geometric properties via the dynamics, as provided by the Riemann zeta function. Indeed, the Riemann zeta function corresponds to the spectral zeta function of the unit interval $(0, 1)$.

**Definition 4.3.4.** Corresponding to the scaling measure (4.15), the *scaling zeta function* $\zeta_{\mathfrak{s}} : \mathbb{C} \to \mathbb{C}$ encodes the scaling factors of successively iterated maps and is given by

$$\zeta_{\mathfrak{s}}(s) := \sum_{w \in \mathcal{W}} r_w^s = \sum_{k=0}^{\infty} \sum_{w \in \mathcal{W}_k} r_w^s. \tag{4.18}$$

More precisely, "scaling zeta function" is understood to refer to the meromorphic

[1]The "spectral measure" mentioned here bears absolutely no relation to those which appear in the Spectral Theorem of functional analysis.

continuation of (4.18), here and henceforth. Note that $\zeta_{\mathfrak{s}}$ is the Mellin transform (as defined in (4.4)) of the scaling measure $\eta_{\mathfrak{s}}$; see Remark 4.3.1.

*Remark* 4.3.5. We also have the *geometric zeta function of the tiling* or *tiling zeta function* $\zeta_{\mathcal{T}}$, which encodes the density of geometric states of the tiling. However, further discussion of this object is postponed to Definition 5.4.3 because more tools are required before we can give the precise definition. While $\eta_{\mathfrak{g}}$ does not appear in $\zeta_{\mathfrak{s}}$, it is (implicitly) present in $\zeta_{\mathcal{T}}$. However, the usefulness of $\eta_{\mathfrak{g}}$ is primarily confined to the proof of Theorem 5.4.5.

The following theorem is the higher-dimensional counterpart of [La-vF4, Thm. 2.4] and can, in fact, be viewed as a corollary of it (see Remark 4.3.1).

**Theorem 4.3.6.** *The scaling zeta function of a self-similar system is*

$$\zeta_{\mathfrak{s}}(s) = \frac{1}{1 - \sum_{j=1}^{J} r_j^s}. \tag{4.19}$$

*This remains valid for the meromorphic extensions of $\zeta_{\mathfrak{s}}$ to all of $\mathbb{C}$.*

*Proof of* (4.19). As in [La-vF4, Thm. 2.4], the proof comes by applying the geometric series formula to $\sum_{j=1}^{J} r_j^{\operatorname{Re} s}$ to obtain the result for $s$ such that $1 - \sum_{j=1}^{J} r_j^{\operatorname{Re} s} > 0$ (i.e., for $\operatorname{Re} s > D$), then extending meromorphically to all of $\mathbb{C}$. □

**Definition 4.3.7.** We can now define the *(scaling) complex dimensions* of a tiling $\mathcal{T}$ (or the *complex dimensions of* $\Phi$) as the poles of the scaling zeta function:

$$\mathcal{D}_{\mathfrak{s}} := \{\omega \in \mathbb{C} \,\vdots\, \zeta_{\mathfrak{s}}(s) \text{ has a pole at } \omega\}. \tag{4.20}$$

**Proposition 4.3.8.** *$D$ is the only real pole of $\zeta_{\mathfrak{s}}$.*

*Proof.* (Following [La-vF4, Thm. 2.17].) Consider the continuous function

$$f(s) = \sum_{j=1}^{J} r_j^s \tag{4.21}$$

for *real* values of $s$. Since $0 < r_j < 1$, $f$ is strictly decreasing. Since $f(0) = J > 1$, there is a unique value $D > 0$ such that $f(D) = 1$. □

If, in addition, $\sum r_j < 1$, then one can show $0 < D < d$, as in [La-vF4, Thm. 2.17].

### 4.3.1 Comparison with the 1-dimensional case

Although the measures and zeta function defined in Definition 4.3.1 and Definition 4.3.4 above correspond to fractal subsets of $\mathbb{R}^d$, it is crucial to note that they are also formally identical to the objects $\eta, \zeta_\eta$ studied in [La-vF4]. To be precise, the scaling measure and the components of the geometric measure all meet the criteria for being a generalized fractal string in the sense of [La-vF4, Def. 4.1]; see Definition 5.3.1 below. Moreover, they are actually self-similar strings of the sort studied in [La-vF4, Chap. 2–3]. In the terminology of [La-vF4], $\zeta_\mathfrak{s}$ is just the geometric zeta function of a self-similar string with scaling ratios $\{r_j\}_{j=1}^J$ and a single *gap*, which has been normalized so as to have $\ell_1 = 1$, where $\ell_1$ is the first length of the string. (The term "gap" of [La-vF4] has been replaced by "generator" in the present paper.) Thus, all of the explicit formulas developed in [La-vF4] are applicable to the measures and zeta functions described in this paper. This will be useful in the proof of Theorem 5.4.5.

One can also check (as in [La-vF4, §5.1]) that $\zeta_\mathfrak{s}$ satisfies

$$\eta_\mathfrak{s}(x) = \frac{1}{2\pi\mathbb{i}} \int_{c-\mathbb{i}\infty}^{c+\mathbb{i}\infty} x^{s-1}\zeta_\mathfrak{s}(s)\,ds, \quad \text{and} \quad \zeta_\mathfrak{s}(s) = \int_0^\infty x^{-s}\,\eta_\mathfrak{s}(dx), \tag{4.22}$$

for some real constant $c > D$.

By (4.19), $\mathcal{D}_\mathfrak{s}$ consists of the set of complex solutions of the equation

$$\sum_{j=1}^J r_j^s = 1 \tag{4.23}$$

which is studied in detail in [La-vF3] and [La-vF4, Chap. 2–3]. One major consequence of the above observation is that the Structure Theorem for complex dimensions [La-vF4, Thm. 2.17] holds for the set defined in (4.20). This set consists of the solutions to (4.23), and is studied in greater generality in [La-vF4, Thm. 3.6]. Below, we recall some of these results.

*Remark* 4.3.9 (The Lattice/Nonlattice Dichotomy). One distinguishes two complementary cases: the lattice case and the nonlattice case. This is also referred to as the arithmetic/nonarithmetic dichotomy, especially in probabilistic renewal theory. Essentially, the dichotomy stems from the fact that every additive subgroup of $\mathbb{R}$ is either dense or discrete. See [La-vF4, §2.4] for further discussion of the lattice/nonlattice dichotomy. In either case, the complex dimensions appear in complex conjugate pairs and lie in a horizontally bounded strip of the form $D_l \leq \operatorname{Re} s \leq D$, where $D$ is the unique real solution of (4.23).

The positive number $D$ is called the *similarity dimension* of $F$ and coincides with the abscissa of convergence of $\zeta_{\mathfrak{s}}$ by [La-vF4, Thm. 1.10]. If the self-similar system defining $F$ satisfies the *open set condition*, or OSC, (see, Remark 3.2.8 and also, e.g., [Hut], as described in [Fal1] or [Kig]), then $D$ coincides with the Hausdorff and Minkowski dimensions of $F$. By Remark 3.5.4, any tiling satisfying the tileset condition (3.7) must also satisfy OSC. We will sometimes refer to $D$ as the (real) dimension of the tiling.

- In the *lattice case*, i.e., when the logarithms of the underlying scaling ratios are all rationally dependent, the complex dimensions $\mathcal{D}_{\mathfrak{s}}$ lie periodically on finitely many vertical lines (including the line $\operatorname{Re} s = D$). In this case, all scaling ratios are integral powers of some fixed base $r \in (0, 1)$, and the positive real constant $\mathbf{p} = 2\pi / \log r^{-1}$ is the *oscillatory period*. In the lattice case, there are infinitely many complex dimensions with real part $D$.

- In the *nonlattice case*, the complex dimensions $\mathcal{D}_{\mathfrak{s}}$ are quasiperiodically distributed and $s = D$ is the *only* complex dimension with real part $D$. Moreover, there exists an infinite sequence of complex dimensions approaching the line $\operatorname{Re} s = D$ from the left. Indeed, the complex dimensions lie in a horizontally bounded strip so that $D_l \leq \operatorname{Re} s \leq D$ for all $s \in \mathcal{D}_{\mathfrak{s}}$. Further, the complex dimensions appear to be arranged so that their real parts are dense in the interval $(D_l, D)$, although this has not yet been proven. The term "quasiperiodic" is meant to indicate that nonlattice complex dimensions can be approximated in a precise and explicit fashion, as a limit of a sequence of sets of lattice complex dimensions, each with successively larger oscillatory period. See [La-vF4, Chap. 2–3 and Chap. 8] for details, including a discussion of quasiperiodicity.

*Remark* 4.3.10. In [La-vF4, §8.3–8.4], it is shown that a self-similar fractal string (i.e., a 1-dimensional self-similar tiling) is Minkowski measurable if and only if it is nonlattice. Gatzouras showed in [Gat] that nonlattice self-similar subsets of $\mathbb{R}^d$ are Minkowski measurable, thereby extending to higher dimensions a result in [La3] and [Fal2] and partially proving the geometric part of [La3, Conj. 3.3]. The present paper shows that self-similar tilings in $\mathbb{R}^d$ are nonlattice if and only if they are Minkowski measurable (Cor. 5.5.2), in virtue of Theorem 5.4.5 and Remark 4.3.1. With the exception of Remark 6.3.3, each of the examples discussed in §6.1 below is lattice and hence not Minkowski measurable. Our results, however, apply to nonlattice tilings as well.

## 4.4 The tube formula for generators

The simplest tilings have just one generator, i.e., for each $n$, $R_n = \Phi_w(G)$ for some $w \in \mathcal{W}$. Let $\mu_i$ denote $i$-dimensional invariant measure (as discussed further in Remark 4.4.5 below), and let $xG$ be a homothetic image of $G$, scaled by $x > 0$. Then $V_G(\varepsilon)$ is the tube formula for a generator, and $V_{xG}(\varepsilon)$ is the tube formula for a scaled generator.

**Definition 4.4.1.** The (adaptive) tube formula for a tile is

$$\gamma_G(x,\varepsilon) := V_{(1/xg)G}(\varepsilon), \quad \text{for } 1/x > \varepsilon, \tag{4.24}$$

so that $\gamma_G(1,\varepsilon)$ denotes the volume of the inner $\varepsilon$-neighbourhood of $\frac{1}{g}G$, a homothetic of $G$ with inradius 1. Then $\gamma_G(x,\varepsilon)$ is the volume of a tile which is similar to $G$ by some $\Phi_w$, but has inradius $1/x > \varepsilon$.

The reason for defining $\gamma_G$ to correspond to a tile with inradius $1/x$ (rather than $x$) will become clear in (5.8); see also Remark 4.3.3. The general motivation for Definition 4.4.1 becomes apparent in (4.30) and (6.1). In the case of multiple generators, $\gamma_q$ will be used to indicate the tube formula of the $q^{\text{th}}$ generator. In general, the computation of $\gamma_G(x,\varepsilon)$ may be nontrivial. However, it is possible to obtain or approximate such a formula (depending on the specific system involved). This is the subject of [LaPe3], as it is beyond the scope of the present discussion. For now, we make the following assumptions.

(i) For $\varepsilon < g$, we can write $V_G$ as

$$V_G(\varepsilon) = \gamma_G(\tfrac{1}{g}, \varepsilon) = \sum_{i=0}^{d-1} \kappa_i(G)\varepsilon^{d-i}, \tag{4.25}$$

for some real coefficients $\kappa_i(G) = \kappa_i(G;\varepsilon)$ defined for $i = 0, \ldots, d-1$.

(ii) Each $\kappa_i(G)$ is homogeneous of degree $i$, so that for $x > 0$,

$$\kappa_i\,(xG) = \kappa_i(G)\, x^i. \tag{4.26}$$

(iii) Each $\kappa_i(G)$ is rigid motion invariant, so that

$$\kappa_i\,(T(G)) = \kappa_i(G), \tag{4.27}$$

for any (affine) isometry $T$ of $\mathbb{R}^d$.

(iv) If the functions $\kappa_i(G) = \kappa_i(G;\varepsilon)$ depend on $\varepsilon$, they are measurable and bounded for $\varepsilon \in (0, g)$.

Up to this point, $\kappa_i$ has only been defined for $i = 0, 1, \ldots, d-1$, and for $\varepsilon < g$. To rectify this, put $\kappa_i(G;\varepsilon) = 0$ for $\varepsilon \geq g$, and define

$$\kappa_d(G;\varepsilon) := \begin{cases} 0, & \varepsilon < g, \\ -\mu_d(G), & \varepsilon \geq g. \end{cases} \tag{4.28}$$

where $\mu_d$ is Lebesgue measure on $\mathbb{R}^d$, so that $\kappa_i(G;\varepsilon)$ is bounded on all of $(0,\infty)$ for $i = 1, \ldots, d$. Now when (i)–(iv) are satisfied, (4.24) may be expressed as

$$\gamma_G(x,\varepsilon) = \begin{cases} \sum_{i=0}^{d-1} \kappa_i(G)x^{-i}\varepsilon^{d-i}, & \varepsilon < 1/x, \\ -\kappa_d(G)x^{-d}, & \varepsilon \geq 1/x. \end{cases} \tag{4.29}$$

Recall that the function $\gamma_G(x,\varepsilon)$ gives the volume of the $\varepsilon$-neighbourhood of a tile with inradius $1/x$. Although it may not be immediately obvious from (4.29) that

$\gamma_G$ is continuous at $x = \frac{1}{\varepsilon}$, it becomes clear after consideration of (4.24) and (4.25) and the fact that $\gamma_G(\frac{1}{g}, \varepsilon) = \mu_d(G)$, where $g = \rho(G)$, in virtue of their geometric interpretations. That is, the value $x = \frac{1}{\varepsilon}$ just corresponds to the point where the volume of a set is equal to the volume of its inner $\varepsilon$-neighbourhood, i.e., where the set becomes contained in its inner $\varepsilon$-neighbourhood. Note, however, that $\gamma_G$ is generally not differentiable at $x = \frac{1}{\varepsilon}$.

**Definition 4.4.2.** We refer to a formula like (4.25) which satisfies (i)–(iv) above as a *Steiner-like formula*, and we describe sets (especially generators) whose inner tube formula satisfies these conditions as being *Steiner-like*.

*Remark* 4.4.3. By Theorem 3.5.14, any tile $R_n$ is the image of a generator $G_q$ under some composition of mappings, i.e., $R_n = \Phi_w(G_q)$. Properties (4.26)–(4.27) above allow us to use the equality

$$V_{R_n}(\varepsilon) = V_{\Phi_w(G_q)}(\varepsilon) = V_{r_1^{e_1} \dots r_J^{e_J} G_q}(\varepsilon) = V_{(\rho_n/g)G_q}(\varepsilon) = \gamma_q(1/\rho_n, \varepsilon), \tag{4.30}$$

where $\rho_n = \rho(R_n)$ is the inradius of $R_n$, as given by (4.12). Thus, the usefulness of having Steiner-like generators is that it suffices to know $V_G(\varepsilon)$ in order to find any $V_{R_n}(\varepsilon)$. That is, it allows one to reduce questions about the geometry of $\mathcal{T}$ (and hence also $F$) to questions about $\zeta_{\mathfrak{s}}$ and the generators, i.e., the geometry of $\mathcal{T}$ can be reconstituted from these ingredients. This is the strategy of §5.2.

*Remark* 4.4.4. The final provision (iv) is for the most general case. For the examples discussed in §6, $\boldsymbol{\kappa}$ is piecewise constant with respect to $\varepsilon$, with a single jump at $\varepsilon = g$. For more complicated generators, the relationship may be more subtle. In fact, it is a notion akin to Federer's *reach* (see [Fed]) which will be important here. For such cases, the inner tube formula will be obtained in [LaPe3] via the more general formulas of [Sta] and [HLW]. In this case, additivity may be lost or subject to conditions on $\varepsilon$. Note that (i)–(iv) are automatically satisfied if $\kappa_i$ is independent of $\varepsilon$ or, if $\kappa_i$ is piecewise constant. Since all examples of the functions $\kappa_i$ discussed in the sequel are constant for $\varepsilon < g$, we write (depending on whether or not there are multiple generators)

$$\kappa_i := \kappa_i(G), \quad \text{or} \quad \kappa_{qi} := \kappa_i(G_q). \tag{4.31}$$

The hypotheses (i)–(iv) will be useful in §5.2.1, as well as in the proof of Theorem 5.4.5. The extent to which they hold will be studied further in [LaPe3]. However, they are definitely what one might expect from geometric measure theory, especially Federer's generalizations in [Fed] of the tube formulas of Weyl [We] and Steiner [Schn2, Chap. 4]. Although Weyl's formula is for smooth submanifolds of $\mathbb{R}^d$, and both Weyl's and Steiner's formulas are for exterior $\varepsilon$-neighbourhoods, this does not obscure obvious similarities to the present results.

*Remark* 4.4.5. Caution: the description of $\kappa_i(G)$ given in conditions (i)–(iv) above is intended to suggest that $\kappa_i(G)$ bears a remarkable resemblance to the $i^{\text{th}}$ curvature measure of $G$ (as in [Schn2]); however, $\kappa_i(G)$ may be signed (even when $G$ is convex and $i = d-1, d$) and is in general a more complicated object. By way of comparison, recall that the Steiner formula gives the $d$-dimensional volume of the outer $\varepsilon$-neighbourhood of a compact convex subset of $\mathbb{R}^d$ (i.e., the measure of all points within $\varepsilon$ of the set, which lie outside the set itself, a set quite different from the inner $\varepsilon$-neighbourhood) as discussed in §5.1:

$$V_A(\varepsilon) = \sum_{i=0}^{d-1} \mu_i(A)\mu_{d-i}(B^{d-i})\varepsilon^{d-i}, \tag{4.32}$$

where for $i = 0, \dots, d-1$, $\mu_i$ is the $i$-dimensional invariant (or *intrinsic*) measure and $B^i$ is the $i$-dimensional unit ball. When $A$ is a convex body, the relation between the invariant measures $\mu_i$, the curvature measures $C_i$ and the curvatures $\kappa_i$ is given by

$$\kappa_i(A) = d \cdot \mu_i(A)\mu_{d-i}(B^d) = \binom{d}{i} C_i(A). \tag{4.33}$$

In this case, the homogeneity and invariance of $\kappa_i$ (as expressed in (4.26)–(4.27)) follow directly from the corresponding properties of the $\mu_i$. More precisely, the $\mu_i$ satisfy the following properties.

1. Each $\mu_i$ is homogeneous of degree $i$, so that for $x > 0$,

$$\mu_i(xA) = \mu_i(A)\, x^i. \tag{4.34}$$

2. Each $\mu_i$ is rigid motion invariant, so that for any (affine) isometry $T$ of $\mathbb{R}^d$,

$$\mu_i\left(T(A)\right) = \mu_i(A). \tag{4.35}$$

The second equality of (4.33) is always true; the first may not be true if $A$ is not convex. The quantity $C_i(A)$ is sometimes called the *total curvature of* $A$ and is a special case of the generalized curvature measure

$$C_i(A) := C_i(A, \mathbb{R}^d) = \Theta_i(A, \mathbb{R}^d \times S^{d-1}).$$

Here, $\Theta_i$ is defined on $U(\mathbb{K}_c^d) \times \mathcal{B}(\Sigma)$, where $U(\mathbb{K}_c^d)$ is the ring of polyconvex sets[2] of dimension not exceeding $d$, and $\mathcal{B}(\Sigma)$ is the $\sigma$-algebra of Borel sets of $\Sigma = \mathbb{R}^d \times S^{d-1}$, the normal bundle of $d$-dimensional Euclidean space, as in [Schn2, §4.2]. Recent results of [Wi] and [HLW] have shed light on methods for directly extending the notion of curvature to fractal and more general spaces, respectively. We hope to establish tighter connections with these results in [LaPe4].

*Remark* 4.4.6. The Steiner–Weyl–Federer tube formula has been extended in various directions by a number of researchers in integral geometry and geometric measure theory, including [Schn1–2], [Zä1–2], [Fu1–2], [Sta], and most recently (and most generally) in [HLW]. The books [Gr] and [Schn2] contain extensive endnotes with further information and many other references.

## 4.5 The geometric zeta function of a tiling

In this section, we develop the geometric zeta function $\zeta_{\mathcal{T}}(s)$ of a self-similar tiling $\mathcal{T}$. The meromorphic distribution-valued function $\zeta_{\mathcal{T}}$ is a generating function for the geometry of a self-similar tiling: it encodes the density of geometric states of a tiling, including curvature and scaling properties.

Just below, Definition 4.5.1 through Definition 4.5.3 describe the components of the geometric zeta function of a fractal spray, a generalized self-similar tiling which will be useful in Chapter 5. These notions are the ingredients of the geometric zeta function as presented in Definition 4.5.4. Throughout, we work with

[2] A *polyconvex set* is a finite union of nonempty convex compact subsets of $\mathbb{R}^d$.

the tiling

$$\mathcal{T} := \left( \{\Phi_j\}_{j=1}^J, \{G_q\}_{q=1}^Q \right). \tag{4.36}$$

**Definition 4.5.1.** The $Q$-dimensional vector of generating inradii $g_q := \rho(G_q)$ is

$$\vec{g}(s) := \left[ g_1^s, g_2^s, \ldots, g_Q^s \right]. \tag{4.37}$$

**Definition 4.5.2.** The *curvature matrix* $\boldsymbol{\kappa}$ is a $Q \times (d+1)$ matrix with entries

$$\boldsymbol{\kappa} := [\kappa_{qi}(\varepsilon)] = \begin{bmatrix} \kappa_{10} & \kappa_{11} & \ldots & \kappa_{1d} \\ \kappa_{20} & \kappa_{21} & \ldots & \kappa_{2d} \\ \vdots & \vdots & & \vdots \\ \kappa_{Q0} & \kappa_{Q1} & \ldots & \kappa_{Qd} \end{bmatrix}, \tag{4.38}$$

Recall from §4.4 that $\kappa_{qd} := -\mu_d(G_q)$ for $\varepsilon \geq g$, and that for $i = 1, \ldots, d-1$ and $\varepsilon < g$, we define $\kappa_{qi} = \kappa_i(G_q)$ as the $i^{\text{th}}$ coefficient of the Steiner-like formula

$$V_{G_q}(\varepsilon) = \sum_{i=0}^{d-1} \kappa_{qi} \varepsilon^{d-i}.$$

For other values of $\varepsilon$, we set $\kappa_{qi}(\varepsilon) = 0$ for $i = 1, \ldots, d$.

**Definition 4.5.3.** The $(d+1)$-vector $\mathcal{E}(\varepsilon, s)$ of 'boundary terms' is given by

$$\mathcal{E}(\varepsilon, s) := \left[ \frac{\varepsilon^{i-s}}{s-i} \right]_{i=0}^d = \left[ \frac{1}{s}, \frac{1}{s-1}, \ldots, \frac{1}{s-d} \right] \varepsilon^{d-s}. \tag{4.39}$$

We are now ready to define the geometric zeta function of a self-similar tiling.

**Definition 4.5.4.** Define the *geometric zeta function of a self-similar tiling* by the matrix product (or bilinear form)

$$\zeta_{\mathcal{T}}(\varepsilon, s) := \zeta_{\mathfrak{s}}(s) \langle \vec{g}(s), \mathcal{E}(\varepsilon, s) \rangle_{\boldsymbol{\kappa}(\varepsilon)} = \zeta_{\mathfrak{s}} \cdot \left( \vec{g}^\top \boldsymbol{\kappa} \mathcal{E} \right), \tag{4.40}$$

where $\vec{g}^\top$ is the transpose of $\vec{g}$. The action of $\zeta_{\mathcal{T}}$ on a test function $\varphi$ is given by

$$\langle \zeta_{\mathcal{T}}(\varepsilon, s), \varphi(\varepsilon) \rangle = \int_0^\infty \zeta_{\mathcal{T}}(\varepsilon, s) \varphi(\varepsilon) \, d\varepsilon. \tag{4.41}$$

Thus $\zeta_{\mathcal{T}}(\varepsilon, s_0)$ is a distribution for any fixed $s_0 \in \mathbb{C}$; see Appendix C for details. The zeta function given by the product (4.40) can also be written as

$$\begin{bmatrix} g_1^s \ g_2^s \ \dots \ g_Q^s \end{bmatrix} \begin{bmatrix} \kappa_{10} & \kappa_{11} & \dots & \kappa_{1d} \\ \kappa_{20} & \kappa_{21} & \dots & \kappa_{2d} \\ \vdots & \vdots & & \vdots \\ \kappa_{Q0} & \kappa_{Q1} & \dots & \kappa_{Qd} \end{bmatrix} \begin{bmatrix} \frac{1}{s} \\ \frac{1}{s-1} \\ \vdots \\ \frac{1}{s-d} \end{bmatrix} \varepsilon^{d-s}\zeta_{\mathfrak{s}}(s). \tag{4.42}$$

or even more concretely as

$$\zeta_{\mathcal{T}}(\varepsilon, s) = \sum_{i=0}^{d} \sum_{q=1}^{Q} g_q^s \frac{\varepsilon^{d-s}}{s-i} \kappa_{qi}(\varepsilon) \zeta_{\mathfrak{s}}(s), \tag{4.43}$$

as appears in (5.52) or, more precisely, in (C.11) of App. C. It turns out that $\zeta_{\mathcal{T}}$ is a meromorphic distribution-valued function. This definition and verification is given in Appendix C; see Definition C.1.10 and Theorem C.1.12 for further explanation and justification.

**Definition 4.5.5.** The set of *complex dimensions of the self-similar tiling $\mathcal{T}$* is set of poles of $\zeta_{\mathcal{T}}$ and is denoted

$$\mathcal{D}_{\mathcal{T}} := \mathcal{D}_{\mathfrak{s}} \cup \{0, 1, \dots, d-1\}.$$

Thus, the complex dimensions of the tiling consist of the scaling dimensions (the complex dimensions of the associated fractal string) together with the same integer dimensions $i = 0, 1, \dots, d-1$ that appear in the theory of convex bodies.

*Remark* 4.5.6. The geometric zeta function defined in Definition 4.5.4 differs from the presentation given in [La-vF4], wherein there is no real distinction between scaling and geometric zeta functions. For several reasons, it behooves one to think of $\zeta_{\mathcal{T}}$ as the geometric zeta function most naturally associated with the spray (or tiling), especially as pertains to the tube formula:

(i) The function $\zeta_{\mathcal{T}}$ encodes all the geometric information of $\mathcal{T}$.

(ii) Using $\zeta_{\mathcal{T}}$ leads to the natural unification of expressions which previously appeared unrelated. This will be seen by comparing (5.53) to (5.55) of Cor. 5.5.3. Also, it is interesting to compare (5.19) to (5.65).

(iii) The function $\zeta_{\mathcal{T}}$ arises naturally in the expression of the tube formula for the tiling as will be seen in Theorem 5.4.5 and Theorem 5.5.1.

(iv) It is the poles of $\zeta_{\mathcal{T}}(\varepsilon, s)$ that naturally index the sum appearing in $V_{\mathcal{T}}$, and the residues of $\zeta_{\mathcal{T}}$ that give the actual volume.

It is especially interesting that the unification mentioned in (ii) leads to a geometric interpretation of the term $\{2\varepsilon\zeta_{\eta}(0)\}$ in (5.19); see §5.6. Some other interesting facts about the special case $d = 1$ are also discussed in §5.6. For example, the geometric zeta function of a string, considered as a spray in the present context, is given by the formula occurring in (5.19)–(5.20) below:

$$\zeta_{\mathcal{T}}(\varepsilon, s) = \zeta_{\mathfrak{s}}(s)\frac{(2\varepsilon)^{1-s}}{s(1-s)}.$$

# Chapter 5

# The Tube Formula of a Self-Similar Tiling

## 5.1 Introduction

In Chapter 3, we have shown that a self-similar tiling $\mathcal{T}$ is canonically associated with any self-similar system satisfying the tileset condition. Such a tiling $\mathcal{T}$ is essentially a decomposition of the complement of the unique self-similar set associated with $\Phi$, as described in detail in §3.2.

In Chapter 4, we constructed a geometric zeta function for the tiling, that is, a generating function which encodes the scaling data of $\Phi$, along with geometric data coming from the generators. The goal of this chapter is the following theorem, stated fully (and in more generality) in Theorem 5.4.5:

**Theorem 5.1.1.** *The $d$-dimensional volume of the inner tubular neighbourhood of $\mathcal{T}$ is given by the following distributional explicit formula:*

$$V_{\mathcal{T}}(\varepsilon) = \sum_{\omega \in \mathcal{D}_{\mathcal{T}}} \operatorname{res}\left(\zeta_{\mathcal{T}}(\varepsilon, s); \omega\right). \tag{5.1}$$

In fact, this theorem will be proved for the more general case of fractal sprays. These objects are defined in §5.4, and it is readily apparent that self-similar tilings are a special case of fractal sprays.

It will also be apparent from this chapter, that the self-similar tiling constructed in Chapter 3 is the appropriate higher-dimensional analogue of the self-similar fractal strings studied in [La-vF4]. Recall that a *fractal string* is just a countable collection $L = \{L_n\}_{n=1}^{\infty}$ of disjoint open intervals which form a bounded open subset of $\mathbb{R}$. Due to the exceedingly simple geometry of such intervals, this reduces to studying the lengths of these intervals $\mathcal{L} = \{\ell_n\}_{n=1}^{\infty}$, and the sequence $\mathcal{L}$ is also referred to as a fractal string.

The tube formula for a fractal string $\mathcal{L}$ (and in particular, for a self-similar tiling in $\mathbb{R}^1$) is defined to be $V_{\mathcal{L}}(\varepsilon) := V_L(\varepsilon)$ and is shown to be essentially given by a sum of the form

$$V_{\mathcal{L}}(\varepsilon) = \sum_{\omega \in \mathcal{D}_{\mathcal{L}} \cup \{0\}} c_\omega \varepsilon^{1-\omega} \tag{5.2}$$

in [La-vF4, Thm. 8.1]. Here, the sum is taken over the set of complex dimensions $\mathcal{D}_{\mathcal{L}} = \{\text{poles of } \zeta_{\mathcal{L}}\}$, where the coefficients $c_\omega$ are given in terms of the residues of $\zeta_{\mathcal{L}}(s)$, the geometric zeta function of $\mathcal{L}$.

Moreover, the tube formula for tilings not only extends the 1-dimensional tube formula for fractal strings (5.2), but is also a fractal extension of the renowned Steiner formula

$$V_A(\varepsilon) = \sum_{i=0}^{d-1} \mu_{d-i}(B^{d-i}) \mu_i(A) \varepsilon^{d-i} = \sum_{i \in \{0,1,\ldots,d-1\}} c_i \varepsilon^{d-i}. \tag{5.3}$$

Here, for $i = 0, 1, \ldots, d$, the $\mu_i$ are the invariant/intrinsic measures of dimension $i$ (i.e., which are homogeneous of degree $i$). Also, $A$ is a $d$-dimensional convex body (that is, a nonempty convex compact set), and $B^i$ is the $i$-dimensional unit ball.

The $\varepsilon$-neighbourhood considered in the Steiner formula includes all points exterior to the set, but within $\varepsilon$ of the set; see Remark 4.4.5. We consider the inner $\varepsilon$-neighbourhood, which consists of those points inside the set and within $\varepsilon$ of its boundary. This is quite different from Steiner's neighbourhood, but the obvious similarities between the tube formulas are striking. In fact, we show in Theorem 5.5.1 that for a self-similar tiling $\mathcal{T}$, we have the following tube formula (see Remark 5.5.4):

$$V_{\mathcal{T}}(\varepsilon) = \sum_{\omega \in \mathcal{D}_{\mathfrak{s}} \cup \{0,1,\ldots,d-1\}} c_\omega(\varepsilon) \varepsilon^{d-\omega}. \tag{5.4}$$

Our tube formula is a power series in $\varepsilon$, rather than just a polynomial in $\varepsilon$ (as in Steiner's formula). Moreover, our series is summed not just over the 'integer dimensions' $\{0, 1, \ldots, d-1\}$, but also over the countable set $\mathcal{D}_{\mathfrak{s}}$ of scaling complex dimensions. The coefficients $c_\omega(\varepsilon)$ of the tube formula are expressed in terms of the 'curvatures' and the inradii of the generators of the tiling. They can also be written as in Theorem 5.5.1 (and in its extension Theorem 5.4.5) as the residues of the geometric zeta function of the tiling $\zeta_\mathcal{T}$ defined in §4.5.

The rest of this chapter is organized as follows. §5.3 reviews the explicit formulas for fractal strings from [La-vF4] which will be used in the proof of the main results. §5.5 defines the geometric zeta function of a fractal spray (a generalization of a tiling), and states and proves the tube formula for fractal sprays given in Theorem 5.4.5, from which the tube formula for self-similar tilings follows readily. In §5.6, we recover Theorem 5.3.7 (the 1-dimensional tube formula for fractal strings, [La-vF4, Thm. 8.1]) from the higher-dimensional framework.

It may be helpful to look ahead at §6.1, which discusses several examples illustrating the theory, and at the appendices. Additionally, Appendix B contains the technical definition of *languid* from [La-vF4], which is used in the proof of Theorem 5.4.5 and in Appendices C–D. Appendix C verifies the validity of the definition of the geometric zeta function $\zeta_\mathcal{T}$. Appendix D verifies the distributional error term and its estimate from Theorem 5.4.5.

## 5.2 The basic strategy

Motivation for this section comes from the tube formula given in [La-vF4, Thm. 8.1], and the relationships outlined in [La-vF4, Chap. 5.1.1] between the measure $\eta$ and the geometric zeta function $\zeta_\eta$. We will see that the tube formula for a self-similar tiling is given by a distributional expression of the form

$$V_\mathcal{T}(\varepsilon) = \langle \eta, \gamma_G \rangle, \tag{5.5}$$

where $V_\mathcal{T}(\varepsilon)$ is the volume of the region within $\varepsilon$ of the boundary of the tiling, as discussed in Definition 4.2.1.

In (5.5), $\eta$ is a local positive measure with support bounded away from 0 (i.e., a *fractal string* in language of [La-vF4, Chap. 4.1]), which defines the density of geometric states of the system. In other words, $\eta$ encodes the distribution of the scaled copies of the generators. For example, a point mass of weight 2 above $x = 3$ indicates that the inradius $\rho = 1/3$ occurs twice; this is discussed further in Definition 4.16 below. The polynomial $\gamma_G$ appearing in (5.5) encodes geometric measure data for the $i$-skeletons ($i = 0, 1, \ldots, d$) of each generator $G_q$. Thus, $\gamma_G(x, \varepsilon)$ gives the volume contribution of state $x$ to the total inner tube volume $V_{\mathcal{T}}(\varepsilon)$.

In light of this interpretation of $\eta$ and $\gamma_G$, (5.5) is just a distributional version of the basic notion

$$\text{Total value} = \sum (\text{value of an } x) \times (\text{number of } x\text{'s}) \tag{5.6}$$

where the sum is taken over all different types of items $x$; compare to (5.10). Throughout the sequel, it will be helpful to keep the idea behind (5.6) in mind. This chapter uses the measures and associated zeta functions developed in Chapter 4 to compute an explicit formula for (5.6), and obtain an explicit formula for $V_{\mathcal{T}}(\varepsilon)$ analogous to [La-vF4, Thm. 8.1].

### 5.2.1 Tilings with one generator

Suppose we have a tiling $\mathcal{T}$ with just one generator $G$. Recall from (4.8) that the inner tube formula of $\mathcal{T}$ is given by

$$\begin{aligned} V_{\mathcal{T}}(\varepsilon) &= \sum_{n=1}^{\infty} V_{R_n}(\varepsilon) \\ &= \sum_{\rho_n \geq \varepsilon} V_{R_n}(\varepsilon) + \sum_{\rho_n < \varepsilon} V_{R_n}(\varepsilon). \end{aligned} \tag{5.7}$$

Here again, $\rho_n$ is the inradius of the tile $R_n$. For $R_n = \Phi_w(G_q)$, invariance under rigid motions allows us to use the equality (4.30) to rewrite the sums in (5.7) as integrals with respect to $\eta_{\mathfrak{g}}$:

$$V_{\mathcal{T}}(\varepsilon) = \sum_{\rho_n^{-1} \leq 1/\varepsilon} V_{R_n}(\varepsilon) + \sum_{\rho_n^{-1} > 1/\varepsilon} V_{R_n}(\varepsilon)$$

$$= \int_0^{1/\varepsilon} V_{(1/xg)G}(\varepsilon)\, d\eta_{\mathfrak{g}}(x) + \mu_d(G) \int_{1/\varepsilon}^{\infty} x^{-d}\, d\eta_{\mathfrak{g}}(x) \tag{5.8}$$

$$= \int_0^{\infty} \gamma_G(x,\varepsilon)\, d\eta_{\mathfrak{g}}(x)$$

$$= \langle \eta_{\mathfrak{g}}, \gamma_G \rangle, \tag{5.9}$$

where $\gamma_G$ is the 'test function' defined by (4.24) and given explicitly by (4.29). Recall that $\gamma_G(x,\varepsilon)$ gives the volume of a tile which is similar to $G$, but has inradius $1/x$, and that $\eta_{\mathfrak{g}}$ is given in Definition 4.3.1.

Further recall that $\gamma_G$ is a continuous function of $\varepsilon$, but may not be differentiable. Although it may not be immediately obvious from (4.29) that $\gamma_G$ is continuous at $x = \frac{1}{\varepsilon}$, it becomes clear after consideration of (4.24) and (4.25) and the fact that, in virtue of their geometric interpretations, $\gamma_G(\frac{1}{g},\varepsilon) = \mu_d(G)$ for $g = \rho(G)$, as noted in the discussion following (4.29). The value $x = \frac{1}{\varepsilon}$ just corresponds to the point where the volume of a set is equal to the volume of its inner $\varepsilon$-neighbourhood, i.e., where the set becomes contained in its inner $\varepsilon$-neighbourhood. Note, however, that $\gamma_G$ is generally not differentiable at $x = \frac{1}{\varepsilon}$.

### 5.2.2 Tilings with multiple generators

Upon replacing $G$ by $G_q$, we use the notation $V_q, \gamma_q, \kappa_{qi}$, etc., to refer to the corresponding quantity for the $q^{\text{th}}$ generator. For example, $\gamma_G(x,\varepsilon)$ is replaced by the $q^{\text{th}}$ component $\gamma_q(x,\varepsilon) = \gamma_{G_q}(x,\varepsilon)$, i.e., the volume of the $\varepsilon$-neighbourhood of a tile which is similar to $G_q$ and has inradius $1/x$.

Again using the notation $\langle\cdot,\cdot\rangle$ as defined in (5.9) above, the key concept lies in the formula

$$V_{\mathcal{T}}(\varepsilon) = \langle \eta_{\mathfrak{g}}, \gamma_G \rangle = \sum_{q=1}^{Q} \langle \eta_{\mathfrak{g}q}, \gamma_q \rangle, \tag{5.10}$$

where we consider $\eta_{\mathfrak{g}}$ to be the density of geometric states as in [La-vF4, §5.1.1 and §6.3.1]. Compare (5.10) to (5.6). Note that the contribution to $V_{\mathcal{T}}(\varepsilon)$ resulting from one generator $G_q$ and its successive images is

$$V_q(\varepsilon) := \langle \eta_{\mathfrak{g}q}, \gamma_q \rangle. \tag{5.11}$$

## 5.3 Distributional explicit formulas for fractal strings

We now recall some key results from [La-vF4] which will be needed for the proof of Theorem 5.4.5.

**Definition 5.3.1.** Following [La-vF4], a *generalized fractal string* is defined to be a local positive measure on $(0, \infty)$ and is denoted by $\eta$. Here, *local* means locally bounded with support bounded away from 0.

*Remark* 5.3.2. It is clear that the scaling and geometric measures $\eta_{\mathfrak{s}}$ and $\eta_{\mathfrak{g}}$ introduced in Definition 4.3.1 are special cases of generalized fractal strings. As in (4.15)–(4.16), each corresponds to a sum of Dirac masses:

$$\eta_{\mathfrak{s}} = \sum_{w \in \mathcal{W}} \delta_{1/r_w}, \qquad \eta_{\mathfrak{g}} = \sum_{\rho} \delta_{1/\rho}.$$

See also §4.3.1.

**Definition 5.3.3.** The string $\eta$ is said to be *languid* if its associated geometric zeta function $\zeta_\eta$ (defined more precisely in (5.22) below) satisfies certain mild polynomial growth conditions on horizontal lines and a vertical contour in $\mathbb{C}$. The vertical contour is called the *screen* and denoted $S$; the region to the right of it is called the window $W$. Also, we define $\sup S := \sup\{\operatorname{Re} s \,\vdots\, s \in S\}$ and $\inf S := \inf\{\operatorname{Re} s \,\vdots\, s \in S\}$, and require that both of these be finite. These notions are precisely defined in Appendix B.

The function $\zeta_\eta$ is assumed to have a meromorphic continuation to a neighbourhood of $W$; see Definition 5.4.1. The poles lying in the window are called the *visible complex dimensions* and the set of such poles is denoted $\mathcal{D}_\eta = \mathcal{D}_\eta(W)$. See [La-vF4, §5.3] for a full discussion.

Taking [La-vF4, Thm. 5.26 and Thm. 5.30] at level $k = 0$ gives the following distributional explicit formula for the action of a fractal string $\eta$ on a test function $\varphi \in C^\infty(0, \infty)$. While $\varphi$ may not have compact support, it must satisfy decay properties as described in (5.12)–(5.13).

**Theorem 5.3.4** (Extended distributional explicit formula)**.** [La-vF4, Thm. 5.26] *Let $\eta$ be a generalized fractal string which is languid of order $M$.*[1] *Let $\varphi \in C^\infty(0,\infty)$ with $n^{th}$ derivative satisfying, for some $\delta > 0$, and every $0 \le n \le N = [M]+2$,*

$$\varphi^{(n)}(x) = O\left(x^{-n-D-\delta}\right) \quad \text{as } x \to \infty, \quad \text{and} \tag{5.12}$$

$$\varphi^{(n)}(x) = \sum_{\alpha} a_\alpha^{(n)} x^{-\alpha-n} + O\left(x^{-n-\inf S+\delta}\right) \quad \text{as } x \to 0^+. \tag{5.13}$$

*Then we have the following distributional explicit formula with error term for $\eta$:*[2]

$$\langle \eta, \varphi \rangle = \sum_{\omega \in \mathcal{D}_\eta} \operatorname{res}\left(\zeta_\eta(s)\widetilde{\varphi}(s);\omega\right) + \sum_{\alpha \in W \setminus \mathcal{D}_\eta} a_\alpha \zeta_\eta(\alpha) + \langle \mathcal{R}, \varphi \rangle, \tag{5.14}$$

*where the error term $\mathcal{R}(x)$ is the distribution given by*

$$\langle \mathcal{R}, \varphi \rangle = \tfrac{1}{2\pi \mathbb{i}} \int_S \zeta_\eta(s)\widetilde{\varphi}(s)\, ds \tag{5.15}$$

*and estimated by*

$$\mathcal{R}(x) = O\left(x^{\sup S - 1}\right), \quad \text{as } x \to \infty. \tag{5.16}$$

Here, $\widetilde{\varphi}$ is the Mellin transform of the function $\varphi$, defined by

$$\widetilde{\varphi}(s) := \int_0^\infty x^{s-1}\varphi(x)\, dx. \tag{5.17}$$

Note that the sum in (5.13) is taken over finitely many complex exponents $\alpha$ with $\operatorname{Re}\alpha > -\sigma_l + \delta$. This condition is described by saying that $\varphi$ has an asymptotic expansion of order $-\sigma_l + \delta$ at 0. Further, the order of the distributional error term, as in (5.16), is defined in Definition D.1.22 of Appendix D.

---

[1] "Languid of order $M$" *refers to the fact that $M$ is the exponent appearing in conditions* **L1** *and* **L2** *of Definition B.1.2. Also, $[M]$ is the integer part of $M$.*

[2] *Here, $\mathcal{D}_\eta := \mathcal{D}_\eta(W)$ and $W \setminus \mathcal{D}_\eta$ is the complement of $\mathcal{D}_\eta$ in the window $W$. Further,* $\operatorname{res}(g(s);\omega)$ *denotes the residue at $\omega$ of the meromorphic function $g$.*

*Remark* 5.3.5. One also has the more suggestive way of writing (5.14):

$$\eta = \sum_{\omega \in \mathcal{D}_\eta} \operatorname{res}\left(x^{s-1}\zeta_\eta(s); \omega\right) + \sum_{\alpha \in W \setminus \mathcal{D}_\eta} \tau_\alpha(x)\zeta_\eta(\alpha) + \mathcal{R}(x), \tag{5.18}$$

where the distribution $\tau_\alpha$ is defined by $\langle \tau_\alpha, \varphi \rangle := a_\alpha$ (as in (5.13)).

*Remark* 5.3.6. If $\eta$ is *strongly languid* (which implies that $W = \mathbb{C}$, in particular), then it follows from the explicit formula [La-vF4, Thm. 5.26] that formula (5.14) has an analogue without error term. I.e., (5.14) holds with $\mathcal{R} \equiv 0$ for the appropriate test functions. As stated in the conclusion of Theorem 5.3.7, the same comment applies to formula (5.19) below; see also Remark 5.4.8. The precise definition of strongly languid is given in Definition B.1.3 of Appendix B. A full discussion of the strongly languid case may be found in [La-vF4, Def. 5.3].

**Theorem 5.3.7** (Tube formula for fractal strings)**.** [La-vF4, Thm. 8.1] *Let $\eta = \eta_{\mathcal{L}}$ be a languid fractal string with geometric zeta function $\zeta_\eta$. The volume of the (one-sided) tubular neighbourhood of radius $\varepsilon$ of the boundary of $\eta$* [3] *is given by the following distributional explicit formula for test functions $\varphi \in C_c^\infty(0,\infty)$, the space of $C^\infty$ functions with compact support contained in $(0,\infty)$:*

$$V_\eta(\varepsilon) = \sum_{\omega \in \mathcal{D}_\eta(W)} \operatorname{res}\left(\frac{\zeta_\eta(s)(2\varepsilon)^{1-s}}{s(1-s)}; \omega\right) + \{2\varepsilon\zeta_\eta(0)\} + \mathcal{R}(\varepsilon). \tag{5.19}$$

*Here the term in braces is only included if $0 \in W \setminus \mathcal{D}_\eta(W)$, and $\mathcal{R}(\varepsilon)$ is the error term, given by*

$$\mathcal{R}(\varepsilon) = \frac{1}{2\pi\mathbb{i}} \int_S \frac{\zeta_\eta(s)(2\varepsilon)^{1-s}}{s(1-s)}\, ds \tag{5.20}$$

*and estimated by*

$$\mathcal{R}(\varepsilon) = O(\varepsilon^{1-\sup S}), \qquad \textit{as } \varepsilon \to 0^+. \tag{5.21}$$

*If $\eta$ is strongly languid, then $W = \mathbb{C}$ and the error term vanishes, i.e., $\mathcal{R}(\varepsilon) \equiv 0$.*

[3] *When $\eta = \eta_{\mathcal{L}}$ corresponds to an ordinary fractal string $\mathcal{L}$, as in* (4.1) *above, then $V_\eta(\varepsilon) = V_L(\varepsilon)$ as in Definition 4.2.1, where $L$ is the bounded open set defining $\mathcal{L}$. See also §1.1.*

The order of the distributional error term, as in (5.21), is defined in Definition D.1.22 of Appendix D.

## 5.4 The tube formula for fractal sprays

In this section, we prove the main result of the chapter, a higher-dimensional analogue of Theorem 5.3.7. While the proof parallels that of [La-vF4, Thm. 8.1], it is significantly more involved; especially if Appendices C and D are taken into account. The current work provides new insight, particularly with regard to the geometric interpretation of the terms of the formula. Indeed, it will be apparent from Theorem 5.4.5 that the origin of the term $\{2\varepsilon\zeta_{\mathcal{L}}(0)\}$ in (5.19) is now understood to come from a Steiner-like formula (akin to (4.25)) for the unit interval; see §5.6. In fact, all terms coming from the third sum in [La-vF4, Thm. 5.26] are now understood to be related to a Steiner-type formula, and are naturally included in the first sum. In the proof of Theorem 5.4.5, the calculation (5.49) shows how this unification may be accomplished.

Although our primary goal of this chapter is to obtain a tube formula for self-similar tilings, we first prove this result for the more general class of fractal sprays, as we expect it to be useful in the study of other fractal structures and tilings. We hope to investigate this further in forthcoming work. The important special case of self-similar tilings will be stated in Theorem 5.5.1 of the next section.

In [La-vF4, §1.4] (following [LaPo2]), a *fractal spray* is defined to be a nonempty bounded open set $B \subseteq \mathbb{R}^d$ (called the *basic shape* or *generator*), scaled by a fractal string $\eta$. That is, a fractal spray is a bounded open subset of $\mathbb{R}^d$ which is the disjoint union of open sets $\Omega_n$ for $n = 1, 2, \dots$, where $\Omega_n$ is congruent to $\ell_n B$ (the homothetic of $\Omega$ by $\ell_n$) for each $\ell_n$. Thus, a fractal string is a fractal spray on the basic shape $B = (0, 1)$, the unit interval.

In the context of the current section, a *self-similar tiling* is a special type of fractal spray with one or more generators. More precisely, a self-similar tiling is a union of fractal sprays on each of the basic shapes $G_1, \dots, G_Q$, all scaled by the same *self-similar* string. In this dissertation, a general fractal spray may have multiple generators, but they are all scaled by the same measure $\eta$. Throughout this section, we continue to assume that each $G_q$ is Steiner-like, and that $Q < \infty$.

**Definition 5.4.1.** Define the *scaling zeta function of a fractal spray* by

$$\zeta_\eta(s) = \int_0^\infty x^s \, d\eta(x), \tag{5.22}$$

and the *visible scaling dimensions of a fractal spray* by

$$\mathcal{D}_\eta(W) := \{\omega \in W \,\vdots\, \omega \text{ is a pole of } \zeta_\eta\}. \tag{5.23}$$

Note that $\mathcal{D}_\eta(W)$ is a discrete subset of $W \subseteq \mathbb{C}$, and hence is at most countable.

*Remark* 5.4.2. A fractal spray, unlike a self-similar tiling, is not automatically strongly languid (see Appendix B). Thus, there is a need for a screen and the notion of *visible* scaling dimensions; see Appendices C–D to see how the screen is used to obtain rigourous proofs via the descent method, and so forth. The proof of Theorem 5.5.1 shows how all of the scaling complex dimensions are visible in the case of a self-similar tiling. Essentially, extra technicalities (like visibility) arise in the study of the more general fractal sprays because the Structure Theorem for complex dimensions (see §4.3.1) only holds for the self-similar case.

**Definition 5.4.3.** We extend Definition 4.5.4 by defining the *geometric zeta function of a fractal spray* as the matrix product (or bilinear form)

$$\zeta_{\mathcal{T}}(\varepsilon, s) := \zeta_\eta(s) \langle \vec{g}(s), \mathcal{E}(\varepsilon, s) \rangle_{\boldsymbol{\kappa}(\varepsilon)} = \zeta_\eta \cdot \left( \vec{g}^\top \boldsymbol{\kappa} \mathcal{E} \right), \tag{5.24}$$

where $\vec{g}$, $\mathcal{E}$, and $\boldsymbol{\kappa}$ are exactly as in Definition 4.5.1–Definition 4.5.3. The only difference from the geometric zeta function of a self-similar tiling given in Definition 4.5.4 is the more general scalar-valued zeta function $\zeta_\eta$ which replaces $\zeta_{\mathfrak{s}}$. As before, the action of $\zeta_{\mathcal{T}}$ on a test function $\varphi$ is given by

$$\langle \zeta_{\mathcal{T}}(\varepsilon, s), \varphi(\varepsilon) \rangle = \int_0^\infty \zeta_{\mathcal{T}}(\varepsilon, s) \varphi(\varepsilon) \, d\varepsilon. \tag{5.25}$$

The geometric zeta function of a fractal spray may also be given as a matrix product, as in (5.24), or more concretely as a double sum, as in (4.43) or as in (C.11) of App. C.

Just as for the geometric zeta function of a self-similar tiling, it turns out that $\zeta_{\mathcal{T}}$ is a meromorphic distribution-valued function. This verification is given in

Appendix C; see Definition C.1.10 and Theorem C.1.12.

**Definition 5.4.4.** We also extend Definition 4.5.5 by defining the *visible complex dimensions of a fractal spray* to be

$$\mathcal{D}_{\mathcal{T}}(W) := \mathcal{D}_{\eta}(W) \cup \{0, 1, \ldots, d-1\}, \tag{5.26}$$

where $\mathcal{D}_{\eta}(W)$ is as in Definition 5.4.1. Thus, $\mathcal{D}_{\mathcal{T}}(W)$ consists of the visible scaling complex dimensions and the integer dimensions of the spray. Note that $\mathcal{D}_{\eta}(W)$ and $\mathcal{D}_{\mathcal{T}}(W)$ are discrete subsets of $W \subseteq \mathbb{C}$, and hence are at most countable. Also, it is clear from (4.42) that the poles of $\zeta_{\mathcal{T}}$ are contained in $\mathcal{D}_{\mathcal{T}}$.

We are now ready to present and prove the main result of this dissertation.

**Theorem 5.4.5** (Tube formula for fractal sprays)**.** *Let $\eta$ be a fractal spray on generators $\{G_q\}_{q=1}^Q$, with generating inradii $g_q = \rho(G_q) > 0$. Assume that $\zeta_\eta$ is languid on a screen $S$ which avoids the dimensions $\mathcal{D}_{\mathcal{T}}(W)$, and that each generator is Steiner-like (as in Definition 4.4.2). Then for test functions in $C_c^\infty(0,\infty)$, the $d$-dimensional volume of the inner tubular neighbourhood of the spray is given by the following distributional explicit formula:*

$$V_{\mathcal{T}}(\varepsilon) = \sum_{\omega \in \mathcal{D}_{\mathcal{T}}(W)} \operatorname{res}\left(\zeta_{\mathcal{T}}(\varepsilon, s); \omega\right) + \mathcal{R}(\varepsilon), \tag{5.27}$$

*where the sum ranges over the set* (5.26) *of integral and visible complex dimensions dimensions of the spray. Here, the error term $\mathcal{R}(\varepsilon)$ is given by*

$$\mathcal{R}(\varepsilon) = \frac{1}{2\pi \mathbb{i}} \int_S \zeta_{\mathcal{T}}(\varepsilon, s)\, ds, \tag{5.28}$$

*and estimated by*

$$\mathcal{R}(\varepsilon) = O(\varepsilon^{d - \sup S}), \qquad \text{as } \varepsilon \to 0^+. \tag{5.29}$$

The order of the distributional error term is defined in Definition D.1.22. Due to their technical and specialized nature, we leave the proofs of (5.28) and (5.29) to Appendix D. The concrete form of (5.27) can be found in (5.52) or, more precisely, in (C.11) of App. C.

*Proof of Theorem 5.4.5.* as in §5.2.2, fix $q \in \{1, \dots, Q\}$, put $\eta_{\mathfrak{g}q}(x) := \eta(x/g_q)$ and let $\gamma_q = \gamma_{G_q}(x, \varepsilon)$. This will allow us to calculate an explicit formula $V_q(\varepsilon)$ for the contribution of the fractal spray on one generator $G_q$, scaled by $\eta$. At the very end of the proof, in (5.52), we will sum over $q = 1, \dots, Q$ to obtain the volume formula for the entire spray.

Recall that we understand $V_{\mathcal{T}}(\varepsilon)$ as a distribution,[4] so we understand $V_q(\varepsilon) = \langle \eta_{\mathfrak{g}q}, \gamma_q \rangle$ by computing $\big\langle \langle \eta_{\mathfrak{g}q}, \gamma_q \rangle, \varphi \big\rangle$, the action of $V_q(\varepsilon)$ on a test function $\varphi = \varphi(\varepsilon) \in C_c^\infty(0, \infty)$, i.e., a smooth function with compact support contained in $(0, \infty)$:

$$\begin{aligned} \langle V_q(\varepsilon), \varphi \rangle = \langle \langle \eta_{\mathfrak{g}q}, \gamma_q \rangle, \varphi \rangle &= \int_0^\infty \left( \int_0^\infty \gamma_q(x, \varepsilon) \eta_{\mathfrak{g}q}(dx) \right) \varphi(\varepsilon) \, d\varepsilon \\ &= \int_0^\infty \int_0^\infty \gamma_q(x, \varepsilon) \varphi(\varepsilon) \, d\varepsilon \, d\eta_{\mathfrak{g}q}(x) \\ &= \langle \eta_{\mathfrak{g}q}, \langle \gamma_q, \varphi \rangle \rangle . \end{aligned} \tag{5.30}$$

Now, we use (4.29) to compute $\langle \gamma_q, \varphi \rangle$ as follows:

$$\begin{aligned} \int_0^\infty \gamma_q \varphi(\varepsilon) \, d\varepsilon &= \sum_{i=0}^{d-1} \int_0^{1/x} \kappa_{qi}(\varepsilon) x^{-i} \varepsilon^{d-i} \varphi(\varepsilon) \, d\varepsilon - \int_{1/x}^\infty \kappa_{qd}(\varepsilon) x^{-d} \varphi(\varepsilon) \, d\varepsilon \\ &= \sum_{i=0}^{d} \varphi_{qi}(x) \end{aligned} \tag{5.31}$$

where, for $x > 0$, we have introduced

$$\varphi_{qi}(x) := \begin{cases} x^{-i} \int_0^{1/x} \kappa_{qi}(\varepsilon) \varepsilon^{d-i} \varphi(\varepsilon) \, d\varepsilon, & 0 \le i \le d-1, \\ x^{-i} \int_\infty^{1/x} \kappa_{qi}(\varepsilon) \varphi(\varepsilon) \, d\varepsilon, & i = d, \end{cases} \tag{5.32}$$

in the last line. Caution: $\varphi_{qi}$ is a function of $x$, whereas $\varphi$ is a function of $\varepsilon$. Putting (5.31) into (5.30), we obtain

$$\langle V_q(\varepsilon), \varphi \rangle = \left\langle \eta_{\mathfrak{g}q}, \sum_{i=0}^{d} \varphi_{qi} \right\rangle = \sum_{i=0}^{d} \langle \eta_{\mathfrak{g}q}, \varphi_{qi} \rangle . \tag{5.33}$$

[4] Indeed, $V_{\mathcal{T}}(\varepsilon)$ is clearly continuous and bounded (by the total volume of the spray), hence it defines a locally integrable function on $(0, \infty)$.

To apply Theorem 5.3.4, we must first check that the functions $\varphi_{qi}$ satisfy the hypotheses (5.12)–(5.13). Recall that $\varphi \in C_c^\infty(0,\infty)$.

For $i < d$, (5.12) is satisfied because for large $x$, the integral is taken over a set outside the (compact) support of $\varphi$. This gives $\varphi_{qi}(x) = 0$ for sufficiently large $x$, and it is clear that, *a fortiori*,

$$\varphi_{qi}^{(n)}(x) = O(x^{-n-D-\delta}) \quad \text{for } x \to \infty,\ \forall n \geq 0. \tag{5.34}$$

To see that (5.13) is satisfied, note that $\varphi$ vanishes for $x$ sufficiently large and thus we have

$$\varphi_{qi}(x) = x^{-i} \int_0^\infty \kappa_{qi}(\varepsilon)\varepsilon^{d-i}\varphi(\varepsilon)\, d\varepsilon \quad \text{for } x \approx 0,$$

i.e., $\varphi_{qi}(x) = a_{qi}x^{-i}$ for small enough $x > 0$, where $a_{qi}$ is the constant

$$a_{qi} := \int_0^\infty \kappa_{qi}(\varepsilon)\varepsilon^{d-i}\varphi(\varepsilon)\, d\varepsilon = \lim_{x\to 0} x^i \varphi_{qi}(x). \tag{5.35}$$

Thus, the expansion (5.13) for the test function $\varphi_{qi}$ consists of only one term, and for each $n = 0, 1, \ldots, N$,[5]

$$\varphi_{qi}^{(n)}(x) = \tfrac{d^n}{dx^n}\left[a_{qi}x^{-i}\right] = O(x^{-n-i}) \quad \text{for } x \to 0^+,\ \forall n \geq 0. \tag{5.36}$$

A key point is that since $\varphi$ is smooth, (5.34) and (5.36) will hold for each $n = 0, 1, \ldots, N$, as required by Theorem 5.3.4. Since the expansion of $\varphi_{qi}$ has only one term, the only $\alpha$ in the sum is $\alpha = i$. Thus $a_{qi}$ is the constant corresponding to $a_\alpha$ in (5.13).

Applying Theorem 5.3.4 in the case when $i < d$, (5.14) becomes

$$\begin{aligned}\langle \eta_{\mathfrak{g}q}, \varphi_{qi}\rangle = \sum_{\omega\in\mathcal{D}_\eta(W)} \operatorname{res}\left(g_q^s\zeta_\eta(s)\widetilde{\varphi}_{qi}(s);\omega\right) \;+\; \{a_{qi}g_q^s\zeta_\eta(i)\}_{i\in W\setminus\mathcal{D}_\eta} \\ +\; \tfrac{1}{2\pi\mathbb{i}} \int_S g_q^s\zeta_\eta(s)\widetilde{\varphi}_{qi}(s)\, ds,\end{aligned} \tag{5.37}$$

[5] Recall from Theorem 5.3.4 that $N = [M] + 2$ and that $\eta$ is languid of order $M$.

where the term in braces is to be included iff $i \in W \setminus \mathcal{D}_\eta$.

The case when $i = d$ is similar (or antisimilar). The compact support of $\varphi$ again gives

$$\kappa_{qd}(x) = -x^{-d} \int_0^\infty \kappa_{qd}(\varepsilon)\varphi(\varepsilon)\,d\varepsilon, \quad \text{for } x \to \infty, \tag{5.38}$$

so that for some positive constant $c$, and for all sufficiently large $x$, we have $\kappa_{qd}(x) = cx^{-d}$. Hence

$$\varphi_{qd}^{(n)}(x) = O(x^{-n-d}) \quad \text{for } x \to \infty,\ \forall n \geq 0, \tag{5.39}$$

and (5.12) is satisfied. For very small $x$, the integral in the definition of $\kappa_{qd}(x)$ is taken over an interval outside the support of $\varphi$, and hence $\kappa_{qd}(x) = 0$ for $x \approx 0$. Then clearly (5.13) is satisfied:

$$\varphi_{qd}^{(n)}(x) = 0 \quad \text{for } x \to 0^+,\ \forall n \geq 0. \tag{5.40}$$

An immediate consequence of (5.40) is that for $i = d$ in (5.35), the constant term is

$$a_{qd} = \lim_{x \to 0} x^d \varphi_{qd}(x) = 0, \tag{5.41}$$

and compared with (5.37) we have one term less in

$$\langle \eta_{\mathfrak{g}q}, \kappa_{qd} \rangle = \sum_{\omega \in \mathcal{D}_\eta(W)} \operatorname{res}\left(g_q^s \zeta_\eta(s) \widetilde{\varphi}_{dq}(s); \omega\right) + \tfrac{1}{2\pi\mathrm{i}} \int_S g_q^s \zeta_\eta(s) \widetilde{\varphi}_{qd}(s)\,ds. \tag{5.42}$$

As in (5.17), denote the Mellin transform of $\psi$ by $\widetilde{\psi}$ and compute

$$\begin{aligned}
\widetilde{\varphi}_{qi}(s) = \int_0^\infty x^{s-1} \varphi_{qi}(x)\,dx &= \int_0^\infty x^{s-i-1} \int_0^{1/x} \kappa_{qi}(\varepsilon)\varepsilon^{d-i}\varphi(\varepsilon)\,d\varepsilon\,dx \\
&= \int_0^\infty \left( \int_0^{1/\varepsilon} x^{s-i-1}\,dx \right) \kappa_{qi}(\varepsilon)\varepsilon^{d-i}\varphi(\varepsilon)\,d\varepsilon \\
&= \frac{1}{s-i} \int_0^\infty \varepsilon^{i-s} \kappa_{qi}(\varepsilon)\varepsilon^{d-i}\varphi(\varepsilon)\,d\varepsilon \\
&= \frac{1}{s-i} (\widetilde{\kappa_{qi}\varphi})(d-s+1)
\end{aligned} \tag{5.43}$$

and

$$\begin{aligned}\widetilde{\varphi}_{qd}(s) = \int_0^\infty x^{s-1}\varphi_{qd}(x)\,dx &= \int_0^\infty x^{s-d-1}\int_\infty^{1/x}\kappa_{qd}(\varepsilon)\varphi(\varepsilon)\,d\varepsilon\,dx \\ &= \int_0^\infty\left(\int_\infty^{1/\varepsilon} x^{s-d-1}\,dx\right)\kappa_{qd}(\varepsilon)\varphi(\varepsilon)\,d\varepsilon \\ &= \frac{1}{s-d}\int_0^\infty \varepsilon^{d-s}\kappa_{qd}(\varepsilon)\varphi(\varepsilon)\,d\varepsilon \\ &= \frac{1}{s-d}(\widetilde{\kappa_{qd}\varphi})(d-s+1), \end{aligned} \tag{5.44}$$

where in both (5.43) and (5.44),

$$(\widetilde{\kappa_{qi}\varphi})(s) = \int_0^\infty \varepsilon^{s-1}\kappa_{qi}(\varepsilon)\varphi(\varepsilon)\,d\varepsilon. \tag{5.45}$$

Note that for $0 \le i < d-1$, (5.43) is valid for $\operatorname{Re} s > i$, and for $i = d$, (5.44) is valid for $\operatorname{Re} s < i$. Thus both are valid in the strip $d-1 < \operatorname{Re} s < d$, and hence by analytic (meromorphic) continuation, they are valid everywhere in $\mathbb{C}$. Indeed, by Cor. C.1.9, $(\widetilde{\kappa_{qi}\varphi})$ is entire for each $q$ and $i = 0, \ldots, d$.

We return to the evaluation of (5.33), applying Theorem 5.3.4 to find the action of $\eta_{\mathfrak{g}q}$ on the test function $\varphi_{qi}$, for $i = 0\ldots, d$. Substituting (5.43) and (5.44) into (5.37) gives

$$\begin{aligned}\langle \eta_{\mathfrak{g}q}, \varphi_{qi}\rangle = \sum_{\omega\in\mathcal{D}_\eta(W)} &\operatorname{res}\left(g_q^s\zeta_\eta(s)\tfrac{1}{s-i}(\widetilde{\kappa_{qi}\varphi})(d-s+1);\omega\right) \\ &+\ \{a_{qi}g_q^s\zeta_\eta(i)\}_{i\in W\setminus\mathcal{D}_\eta}\ +\ \langle\mathcal{R}_{qi},\varphi\rangle,\end{aligned} \tag{5.46}$$

where $\mathcal{R}_{qi}$ is defined by

$$\langle\mathcal{R}_{qi},\varphi\rangle := \tfrac{1}{2\pi\mathbb{i}}\int_S g_q^s\zeta_\eta(s)(\widetilde{\kappa_{qi}\varphi})(s)\,ds. \tag{5.47}$$

Substituting (5.46) into (5.33), we obtain

$$\langle V_q(\varepsilon),\varphi\rangle = \sum_{i=0}^d\left(\sum_{\omega\in\mathcal{D}_\eta(W)}\operatorname{res}\left(g_q^s\zeta_\eta(s)\tfrac{1}{s-i}(\widetilde{\kappa_{qi}\varphi})(d-s+1);\omega\right)\right.$$

$$+ \{a_{qi} g_q^s \zeta_\eta(i)\}_{i \in W \setminus \mathcal{D}_\eta} + \langle \mathcal{R}_{qi}(\varepsilon), \varphi(\varepsilon) \rangle \Bigg) ,$$

which, by Remark 5.3.5, may also be written as the distribution

$$V_q(\varepsilon) = \sum_{\omega \in \mathcal{D}_\eta(W)} \operatorname{res} \left( \sum_{i=0}^{d} g_q^s \zeta_\eta(s) \tfrac{\varepsilon^{d-s}}{s-i} \kappa_{qi}(\varepsilon); \omega \right) + \sum_{i=0}^{d-1} \left\{ g_q^s \zeta_\eta(i) \kappa_{qi}(\varepsilon) \varepsilon^{d-i} \right\} + \mathcal{R}_q(\varepsilon), \tag{5.48}$$

where $\mathcal{R}_q(\varepsilon) := \sum_{i=0}^{d} \mathcal{R}_{qi}(\varepsilon)$ and the braces indicate that the terms of the second sum are only included for $i \in W \setminus \mathcal{D}_\eta(W)$.

Recall from (5.41) that the $d^{\text{th}}$ term is $a_{qd} = 0$, so it is left out of the second sum. Since the terms of the second sum are only included for $i \in W \setminus \mathcal{D}_\eta(W)$, at each such $i$ we have a residue

$$\begin{aligned} \operatorname{res} \left( g_q^s \zeta_\eta(s) \kappa_{qi}(\varepsilon) \frac{\varepsilon^{d-s}}{s-i}; i \right) &= \lim_{s \to i} g_q^s \zeta_\eta(s) \kappa_{qi}(\varepsilon) \varepsilon^{d-s} \\ &= g_q^s \zeta_\eta(i) \kappa_{qi}(\varepsilon) \varepsilon^{d-i}. \end{aligned} \tag{5.49}$$

Thus we can put

$$\mathcal{D}_{\mathcal{T}}(W) := \mathcal{D}_\eta(W) \cup \{0, 1, \dots, d-1\} \tag{5.50}$$

and combine the two sums of (5.48) without losing or duplicating terms:

$$V_q(\varepsilon) = \sum_{\omega \in \mathcal{D}_{\mathcal{T}}(W)} \operatorname{res} \left( \sum_{i=0}^{d} g_q^s \zeta_\eta(s) \frac{\varepsilon^{d-s}}{s-i} \kappa_{qi}(\varepsilon); \omega \right) + \mathcal{R}_q(x). \tag{5.51}$$

Now sum (5.51) over $q = 1, \dots, Q$ and then interchange the resulting sums over $\omega$ and $q$, using the linearity of the residue and the notation of (5.24) and the identity (4.42). Since $V_{\mathcal{T}}(\varepsilon) = \sum_{q=1}^{Q} V_q(\varepsilon)$, as indicated at the start of the proof, we obtain

$$V_{\mathcal{T}}(\varepsilon) = \sum_{\omega \in \mathcal{D}_{\mathcal{T}}(W)} \operatorname{res} \left( \sum_{i=0}^{d} \sum_{q=1}^{Q} g_q^s \zeta_\eta(s) \frac{\varepsilon^{d-s}}{s-i} \kappa_{qi}(\varepsilon); \omega \right) + \mathcal{R}(\varepsilon) \tag{5.52}$$

$$= \sum_{\omega \in \mathcal{D}_{\mathcal{T}}(W)} \operatorname{res}\left(\zeta_{\mathcal{T}}(\varepsilon, s); \omega\right) + \mathcal{R}(\varepsilon),$$

where $\mathcal{R}(\varepsilon) := \sum_{q=1}^{Q} \mathcal{R}_q(\varepsilon)$.

This completes the proof of (5.27). All that remains is the verification of (5.28) for the error term, and the error estimate (5.29). As these issues are of a more technical and somewhat different nature, we postpone them to Appendix D. □

*Remark* 5.4.6 (To $d$ or not to $d$). The reader may wonder why some sums include a $d^{\text{th}}$ summand and others do not. The explanation is as follows: the residue of $\zeta_{\mathcal{T}}$ at $d$ does not appear in the formula, for the reasons given in (5.41) and near (5.49). The essential reason for the absence of the $d^{\text{th}}$ residue in (5.50) is that $a_{qd} = 0$, as in (5.41). However, the $d^{\text{th}}$ term is necessary in the definition of $\zeta_{\mathcal{T}}$ itself, as evinced by (5.52). When the residue of $\zeta_{\mathcal{T}}$ is taken at any complex dimension (including $\{0, 1, \ldots, d-1\}$), all terms of $\zeta_{\mathcal{T}}$ must be included in the evaluation of the residue. Intuitively, if this sum over the terms $\kappa_i$ neglected the $d^{\text{th}}$ term, the volumes of all the small tiles with $g < \varepsilon$ would be missing from $V_{\mathcal{T}}(\varepsilon)$.

*Remark* 5.4.7 (Comparison with the Steiner formula). In the 'trivial' case when the spray consists only of finitely many scaled copies of the generators (i.e., when the scaling measure $\eta$ is supported on a finite set), and the generators are convex, the geometric zeta function will have no poles in $\mathbb{C}$. Therefore, the tube formula becomes a sum over only the numbers $0, 1, \ldots, d-1$ (recall from (5.41) that $a_{qd} = 0$, so the $d^{\text{th}}$ summand vanishes), for which the residues simplify greatly as in (5.49). In this case, The zeta function is $\zeta_\eta(i) = \rho_1^i + \cdots + \rho_N^i$, so each residue from (5.49) becomes a finite sum

$$\begin{aligned} g_q^s \zeta_\eta(i) \kappa_{qi}(\varepsilon) &= \rho_1^i \kappa_{qi} \varepsilon^{d-i} + \cdots + \rho_N^i \kappa_{qi} \varepsilon^{d-i} \\ &= \kappa_{qi}(r_{w_1} G_q) \varepsilon^{d-i} + \cdots + \kappa_{qi}(r_{w_N} G_q) \varepsilon^{d-i} \end{aligned}$$

where $N$ is the number of scaled copies of the generator $G_q$, and $r_{w_n}$, $n = 1, \ldots, N$ is the corresponding scaling factor. Thus, for each $q$ and each $n$, we obtain a Steiner-like polynomial for the volume of the inner $\varepsilon$-neighbourhood of the scaled basic shape $r_{w_n} G_q$. Recall that for a self-similar tiling, every tile $R_m$ is congruent to $r_w G_q$ for some $q$ and some $w \in \mathcal{W}$.

*Remark* 5.4.8. In the case when $\zeta_\eta$ is not only languid but also strongly languid (see Appendix B), then by Remark 5.3.6, we may choose $W = \mathbb{C}$ and the error term vanishes, i.e. $\mathcal{R}(\varepsilon) \equiv 0$. Indeed, each individual error term obtained in the proof of Theorem 5.4.5 vanishes identically in that case. This is just as in [La-vF4, Thm. 8.1].

In particular, a self-similar tiling will always be strongly languid. This is explained in detail in [La-vF4, §6.4] and follows from the fact that a (normalized) self-similar fractal string $\eta$ is formally indistinguishable from the scaling measure of a self-similar tiling, as described in Remark 4.3.1. Hence Theorem 5.4.5 above may be strengthened for self-similar tilings to yield Theorem 5.5.1 just below. (See also Remark 4.3.1 above.) See Appendix B for the definitions of languid and strongly languid.

*Remark* 5.4.9 (Reality principle). The nonreal complex dimensions appear in complex conjugate pairs and produce terms with coefficients which are also complex conjugates, in the general tube formula for fractal sprays. This ensures that formulas (5.27) and (5.53) are real-valued. Compare with Remark 2.5.5

## 5.5 The tube formula for self-similar tilings

The following corollary of Theorem 5.4.5 provides a higher-dimensional counterpart of the tube formula obtained for self-similar strings in [La-vF4, §8.4]. It should be noted that Theorem 5.5.1 applies to a slightly smaller class of test functions than Theorem 5.4.5. Indeed, the support of the test functions must be bounded away from 0 by $\mu_d(C)g_Q/r_J$, where $C = [F]$ is the hull of the attractor (as in §3.3), $g_Q$ is the smallest generating inradius (as in §4.2), and $r_J$ is the smallest scaling ratio of $\Phi$ (as in (3.2)). This technicality is discussed further in [La-vF4, Def. 5.3 and Thm. 5.27, §6.4, and Thm. 8.1].

**Theorem 5.5.1** (Tube formula for self-similar tilings)**.** *Suppose a self-similar tiling $\mathcal{T} = (\{\Phi_j\}_{j=1}^J, \{G_q\}_{q=1}^Q)$, has generating inradii $g_q = \rho(G_q)$ and zeta function $\zeta_{\mathcal{T}}$. Also suppose that each generator is Steiner-like, as in Definition 4.4.2. Then the $d$-dimensional volume of the inner tubular neighbourhood of $\mathcal{T}$ is given* *by the following distributional explicit formula:*

$$V_{\mathcal{T}}(\varepsilon) = \sum_{\omega \in \mathcal{D}_{\mathcal{T}}} \operatorname{res}\left(\zeta_{\mathcal{T}}(\varepsilon, s); \omega\right), \tag{5.53}$$

*where* $\mathcal{D}_{\mathcal{T}} = \mathcal{D}_{\mathfrak{s}} \cup \{0, 1, \ldots, d-1\}$.

*Proof.* Note that in this (self-similar) case, one has $\zeta_\eta(s) = \zeta_{\mathfrak{s}}(s)$ and $\mathcal{D}_\eta(\mathbb{C}) = \mathcal{D}_{\mathfrak{s}}$, with $\eta = \eta_{\mathfrak{s}}$ as in (4.15); see also Remark 5.4.2. The proof follows [La-vF4, §8.4]. According to Theorem 4.3.6, the scaling zeta function of a self-similar tiling has the form

$$\zeta_{\mathfrak{s}}(s) = \frac{1}{1 - \sum_{j=1}^{J} r_j^s}.$$

Let $r_J$ be the smallest scaling ratio. Then from

$$|\zeta_{\mathfrak{s}}(s)| \ll \left(\frac{1}{r_J}\right)^{-|\sigma|} \quad \text{as } \sigma = \operatorname{Re}(s) \to -\infty,$$

we deduce that $\zeta_{\mathcal{T}}$ is strongly languid, in the sense of Definition B.1.3. Hence, we can apply the extension of Theorem 5.4.5 mentioned in Remark 5.4.8. This argument follows from the analogous ideas regarding fractal strings, which may be found in [La-vF4, Ch. 2–3]. The relevance of this reference is discussed in §4.3.1. □

**Corollary 5.5.2** (Measurability and the lattice/nonlattice dichotomy)**.** *A self-similar tiling is Minkowski measurable if and only if it is nonlattice.*

*Proof.* We define a self-similar tiling $\mathcal{T}$ to be Minkowski measurable iff

$$0 < \lim_{\varepsilon \to 0^+} V_{\mathcal{T}}(\varepsilon)\varepsilon^{-(d-D)} < \infty, \tag{5.54}$$

i.e., if the limit in (5.54) exists *and* takes a value in $(0, \infty)$. A tiling has infinitely many complex dimensions with real part $D$ iff it is lattice type, as mentioned in Remark 4.3.1. Furthermore, all the poles with real part $D$ are simple in that case. A glance at (5.56) then shows that $V_{\mathcal{T}}(\varepsilon)\varepsilon^{-(d-D)}$ is a sum containing infinitely many purely oscillatory terms $c_\omega \varepsilon^{\mathbb{i}n\mathbf{p}}$, $n \in \mathbb{Z}$, where $\mathbf{p}$ is some fixed period. Thus, the limit (5.54) cannot exist; see also [La-vF4, §8.4.2]. Conversely, the tiling is nonlattice iff $D$ is the only complex dimension with real part $D$. In this case, $D$ is simple and no term in the sum $V_{\mathcal{T}}(\varepsilon)\varepsilon^{-(d-D)}$ is purely oscillatory; thus the tiling $\mathcal{T}$ is measurable. See also [La-vF4, §8.4.4].

$\square$

The following corollary of Theorem 5.5.1 will be used in §6.1. Since this corollary pertains to tilings with a single generator $G$, we suppress dependence on $q$ for convenience. From (5.51)–(5.52), it is clear that an analogous result holds in the case of multiple generators.

**Corollary 5.5.3.** *If, in addition to the hypotheses of Theorem 5.5.1, $\mathcal{T}$ is a self-similar tiling with one generator and $\zeta_{\mathcal{T}}(s)$ has only simple poles, then*

$$V_{\mathcal{T}}(\varepsilon) = \sum_{\omega \in \mathcal{D}_{\mathfrak{s}}} \sum_{i=0}^{d} \operatorname{res}\left(\zeta_{\mathfrak{s}}(s); \omega\right) g^{\omega} \kappa_i(\varepsilon) \tfrac{\varepsilon^{d-\omega}}{\omega - i} + \sum_{i=0}^{d-1} g^i \kappa_i(\varepsilon) \zeta_{\mathfrak{s}}(i) \varepsilon^{d-i}. \tag{5.55}$$

It is not an error that the first sum extends to $d$ in (5.55), while the second stops at $d-1$; see Remark 5.4.6. Note that in Cor. 5.5.3, $\mathcal{D}_{\mathfrak{s}}$ does not contain any integer $i = 0, 1, \ldots, d-1$, because this would imply that $\zeta_{\mathcal{T}}$ has a pole of multiplicity at least 2. In general, at most one integer can possibly be a pole of $\zeta_{\mathfrak{s}}$; see §4.3.1.

*Remark* 5.5.4. For self-similar tilings satisfying the hypotheses of Cor. 5.5.3, it is clear that the general form of the tube formula is

$$V_{\mathcal{T}}(\varepsilon) = \sum_{\omega \in \mathcal{D}_{\mathcal{T}}} c_\omega(\varepsilon) \varepsilon^{d-\omega}, \tag{5.56}$$

where for each fixed $\omega \in \mathcal{D}_{\mathfrak{s}}$,

$$c_\omega(\varepsilon) := \operatorname{res}\left(\zeta_{\mathfrak{s}}; \omega\right) \sum_{i=0}^{d} \frac{g^{\omega} \kappa_i(\varepsilon)}{\omega - i}, \tag{5.57}$$

and for each fixed $\omega \in \{0, 1, \ldots, d-1\}$,

$$c_\omega(\varepsilon) := \zeta_{\mathfrak{s}}(\omega) g^{\omega} \kappa_i(\varepsilon). \tag{5.58}$$

If the curvature matrix $\boldsymbol{\kappa}$ is constant on $(0, g)$, as is the case for the examples of Chapter 6, then each $c_\omega$ will also be independent of $\varepsilon$, for $\varepsilon < g$. The analogous statement to (5.56) will also hold in the case of multiple generators, as long as all complex dimensions are simple poles of $\zeta_{\mathfrak{s}}$ (in this case, the analogue of (5.57) would also contain a sum over $q = 1, \ldots, Q$). In fact, this remark holds more generally, as alluded to in the Introduction. By (5.51), the tube formula for fractal sprays has essentially the same form as (5.56).

*Remark* 5.5.5. The oscillatory nature of the geometry of $\mathcal{T}$ is apparent in (5.56). In particular, the existence of the limit in (5.54) can be determined by examining (5.56) and $\mathcal{D}_{\mathcal{T}}$.

*Remark* 5.5.6. In the literature regarding the 1-dimensional case, the terms "gaps" and "multiple gaps" have been used where we have used "generators". See [La-vF4] and [Fra].

## 5.6 Recovering the tube formula for fractal strings

In this section, we discuss a result which is true for general (i.e., not necessarily self-similar) fractal strings and which can be recovered from Theorem 5.4.5. Suppose that $\mathcal{L} = \{\ell_n\}_{n=1}^\infty$ is a fractal string with associated measure $\eta = \sum_{n=1}^\infty \delta_{1/\ell_n}$, as in (4.3), and geometric zeta function $\zeta_{\mathcal{L}}$, as in (4.2). However, write $\mathcal{L}$ as $L = \{L_n\}_{n=1}^\infty$ to emphasize the fact that we are thinking of it as a spray instead of as a string. The spray $L$ has a single 1-dimensional generator $G = (0,1)$.[6] In keeping with the tiling context, we use inradii $\rho_n = \frac{1}{2}\ell_n$ instead of lengths. Thus

$$\zeta_{\mathcal{L}}(s) = g^s \zeta_{\mathfrak{s}}(s) = \left(\tfrac{1}{2}\right)^s \sum_{n=1}^\infty \rho_n^s. \tag{5.59}$$

By inspection, we find the generator tube formula (for $d = 1$)

$$\gamma_G(x, \varepsilon) = \sum_{i=0}^{d-1} \kappa_i(\varepsilon)(x)^i \varepsilon^{d-i} = \kappa_0(x)^0 = 2\varepsilon. \tag{5.60}$$

[6] Even a self-similar string with multiple generators can be thought of as a fractal spray on one generator (albeit with a different scaling measure) in this fashion, as all open intervals are homothetic to each other. See also Example 6.2 and Remark 6.6.1 of Example 6.6.

and

$$\mu_d(xG) = -\kappa_1(\varepsilon)x^1 = 2x, \tag{5.61}$$

so that we have

$$\boldsymbol{\kappa} = [2,\ -2] \tag{5.62}$$

$$\mathcal{E}(\varepsilon, s) = \left[\tfrac{\varepsilon^{1-s}}{s}, \tfrac{\varepsilon^{1-s}}{s-1}\right] = \left[\tfrac{1}{s}, \tfrac{1}{s-1}\right]\varepsilon^{1-s}. \tag{5.63}$$

Since the generator of a string is always just an open interval, the terms $\kappa_i = \kappa_i(\varepsilon)$ will be constants (in particular, independent of $\varepsilon$ for $\varepsilon < g$).

Using (5.59), one obtains[7]

$$\zeta_L(\varepsilon, s) = \left(\tfrac{1}{2}\right)^s \zeta_{\mathfrak{s}}(s)\left(\frac{2}{s} + \frac{-2}{s-1}\right)\varepsilon^{1-s} = \zeta_{\mathfrak{s}}(s)\frac{(2\varepsilon)^{1-s}}{s(1-s)} \tag{5.64}$$

so the volume (5.27) becomes

$$V_{\mathcal{L}}(\varepsilon) = \sum_{\omega \in \mathcal{D}_{\mathfrak{s}}(W)\cup\{0\}} \operatorname{res}\left(\zeta_{\mathfrak{s}}(s)\frac{(2\varepsilon)^{1-s}}{s(1-s)}; \omega\right) + \mathcal{R}(\varepsilon) \tag{5.65}$$

and we have exactly recovered (5.19), the tube formula for fractal strings discussed in Theorem 5.3.7. Indeed, from (5.64), (5.29) and (5.28) we even see the error term $\mathcal{R}(\varepsilon)$ is the same (and satisfies the same estimate) as in (5.20)–(5.21).

In addition, we gain a geometric interpretation of the terms appearing in (5.65), in view of (5.60)–(5.64). In particular, the mysterious linear term in braces in (5.19) is actually the inner Steiner formula for an interval, and can be dissected as

$$2\varepsilon\zeta_{\mathfrak{s}}(0) = \kappa_0(G)\varepsilon^{1-0}\zeta_{\mathfrak{s}}(0) = (-2)\mu_\omega(G)\varepsilon^{d-\omega}\zeta_{\mathfrak{s}}(\omega), \tag{5.66}$$

where $\omega = 0$ and $d = 1$. Note that $\mu_0(G) = -1$ is the Euler characteristic of an open interval. This will be discussed further in [LaPe3].

[7] In (5.64), we use the symbol $\zeta_L$ to denote the tiling zeta function of the string, as in Definition 5.4.3, in contrast to $\zeta_{\mathcal{L}}$, the geometric zeta function of a string defined in (4.2). See also §1.1.

# Chapter 6

# A Gallery of Examples

## 6.1 Introductory remarks

Each of the examples chosen in this section is a *lattice* self-similar tiling, in the sense of Remark 4.3.9: the scaling ratios $r_j$ are all integral powers of some number $r \in (0,1)$. As will be verified, they all have Steiner-like generators in the sense of Definition 4.4.2. This allows us to find the tube formula for each tile from the tube formula for the generators $\gamma_G(x,\varepsilon) = V_{(1/xg)G}(\varepsilon)$, as defined in (4.24). Recall that $\gamma_G(x,\varepsilon)$ gives the tube formula for a generator which is congruent to $G$, but has inradius $1/x$. In each example, $\gamma_G(1,\varepsilon)$ or $\gamma_G(1/g,\varepsilon) = V_G(\varepsilon)$ is computed 'by hand' so that the homogeneity property (4.26) can be used to obtain $\gamma_G(x,\varepsilon)$. Then, when $\gamma_G(x,\varepsilon)$ is integrated with respect to $d\eta_{\mathfrak{g}}(x)$, each point $x = 1/\rho$ in the support of $\eta_{\mathfrak{g}}$ will contribute

$$\gamma_G(x,\varepsilon) = V_{(\rho/g)G}(\varepsilon) = V_{r_1^{e_1}\dots r_J^{e_J}G}(\varepsilon) = V_{\Phi_w(G)}(\varepsilon) = V_{R_n}(\varepsilon) \tag{6.1}$$

to the integral, corresponding to the tile $R_n = \Phi_w(G_q)$.

Moreover, the scaling zeta function $\zeta_{\mathfrak{s}}$ of each example has only simple poles, with a single line of complex dimensions distributed periodically on the line $\operatorname{Re} s = D$. Thus, the tube formula may be substantially simplified via Cor. 5.5.3.

*Remark* 6.1.1. Much as in the case of fractal strings where $d = 1$ (see [La-vF4, §8.4.2]), it follows from Theorem 5.5.1 that for a lattice self-similar tiling $\mathcal{T}$,[1]

[1]Here, $\mathcal{T}$ is assumed to have generators which all have piecewise constant curvature coeffi-

each line of complex dimensions $\beta + i n\mathbf{p}$ (where $\beta \in \mathbb{R}$ and $\mathbf{p} = 2\pi/\log r^{-1}$ is the oscillatory period of $\mathcal{T}$) gives rise to a function which consists of a multiplicatively periodic function times $\varepsilon^{d-\beta}$. Recall that for lattice fractals, the scaling ratios are all integral powers of some number $r \in (0,1)$. Since all the examples considered in this section are of this type, and also have a single line of simple complex dimensions of the form $D + i n\mathbf{p}$, we have

$$V_{\mathcal{T}}(\varepsilon) = h\left(\log_{r^{-1}}(\varepsilon^{-1})\right)\varepsilon^{d-\beta} + P(\varepsilon), \tag{6.2}$$

where $h$ is an additively periodic function of period 1, and $P$ is a polynomial in $\varepsilon$. For example, the periodic function appearing in the tube formula (6.15) for the Koch tiling $\mathcal{K}$ has the following Fourier expansion:

$$h(u) = \tfrac{g}{\log 3}\sum_{n\in\mathbb{Z}} g^{i n\mathbf{p}}\left(-\tfrac{1}{D+i n\mathbf{p}} + \tfrac{2}{D-1+i n\mathbf{p}} - \tfrac{1}{D-2+i n\mathbf{p}}\right)e^{2\pi i n u}, \tag{6.3}$$

where $g = \sqrt{3}/18$, $D = \log_3 4$, $r = 1/\sqrt{3}$, and $\mathbf{p} = 4\pi/\log 3$.

For some purposes, it might also be helpful to truncate the tube formula by using a suitable screen (and restricting to the visible complex dimensions) and applying a special case of the tube formula with error term (5.27). This is needed, for example, to give a detailed proof of Cor. 5.5.2. The interested reader may wish to consult [La-vF4, §8.4], but this will not be discussed further here.

The examples chosen have only simple poles, so that the volume formulas can be substantially simplified. We begin by revisiting the classic 1-dimensional example of [La-vF4].

## 6.2 The Cantor tiling

First, we compute the tube formula for the Cantor Tiling $\mathcal{C}$ (called the Cantor String in [La-vF4, §1.1.2, §1.2.2 and §2.3.1]) using these techniques. The Cantor Tiling $\mathcal{C}$ is constructed via the self-similar system

$$\Phi_1(x) = \tfrac{x}{3}, \qquad \Phi_2(x) = \tfrac{x+2}{3}.$$

cients $\kappa_{qi}$, as in Remark 5.5.4.

Thus $d = 1$ and we have one scaling ratio $r = \frac{1}{3}$, and one generator $G = \left(\frac{1}{3}, \frac{2}{3}\right)$ which has generating inradius $g = \frac{1}{6}$. The string has inradii $\rho_k = gr^k$ with multiplicity $2^k$ for $k = 0, 1, 2, \ldots$, so the scaling zeta function is

$$\zeta_{\mathfrak{s}}(s) = \frac{1}{1 - 2 \cdot 3^{-s}}, \tag{6.4}$$

with scaling complex dimensions

$$\mathcal{D}_{\mathfrak{s}} = \{D + \mathbb{i}n\mathbf{p} \,\vdots\, n \in \mathbb{Z}\} \qquad \text{for } D = \log_3 2,\ \mathbf{p} = \tfrac{2\pi}{\log 3}. \tag{6.5}$$

Now an application of (5.65) from the previous section gives the following tube formula for $\mathcal{C}$:

$$\begin{aligned} V_{\mathcal{C}}(\varepsilon) &= \sum_{n \in \mathbb{Z}} \operatorname{res}\left(\tfrac{3^{-s}}{1-2\cdot 3^{-s}}; D + \mathbb{i}n\mathbf{p}\right)\left(\tfrac{(2\varepsilon)^{1-s}}{(D+\mathbb{i}n\mathbf{p})(1-D-\mathbb{i}n\mathbf{p})}\right) + 2\varepsilon\zeta_{\mathfrak{s}}(0) \\ &= \frac{1}{2\log 3}\sum_{n \in \mathbb{Z}} \frac{(2\varepsilon)^{1-D-\mathbb{i}n\mathbf{p}}}{(D + \mathbb{i}n\mathbf{p})(1 - D - \mathbb{i}n\mathbf{p})} - 2\varepsilon, \end{aligned} \tag{6.6}$$

exactly as obtained for the Cantor string in [La-vF4, §1.1.2].

Alternatively, this may be written as a series in $\left(\frac{\varepsilon}{g}\right)$ as

$$V_{\mathcal{C}}(\varepsilon) = \frac{1}{3\log 3}\sum_{n \in \mathbb{Z}}\left(\frac{1}{D + \mathbb{i}n\mathbf{p}} - \frac{1}{D - 1 + \mathbb{i}n\mathbf{p}}\right)\left(\frac{\varepsilon}{g}\right)^{1-D-\mathbb{i}n\mathbf{p}} - 2\varepsilon, \tag{6.7}$$

with $g = \frac{1}{6}$, $D = \log_3 2$, and $\mathbf{p} = 2\pi/\log 3$. It is this form of the tube formula which is closer in appearance to the following examples.

## 6.3 The Koch tiling

The standard Koch tiling $\mathcal{K}$ (see Fig. 6.1) is constructed via the self-similar system

$$\Phi_1(z) := \xi\overline{z} \quad \text{and} \quad \Phi_2(z) := (1 - \xi)(\overline{z} - 1) + 1. \tag{6.8}$$

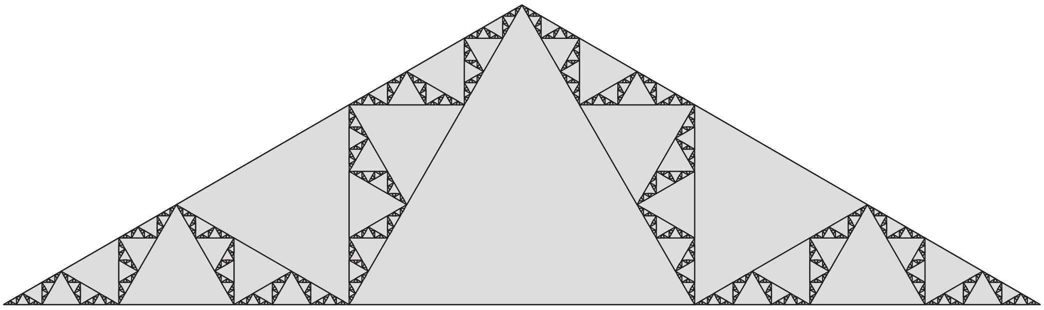

Figure 6.1: The Koch tiling $\mathcal{K}$.

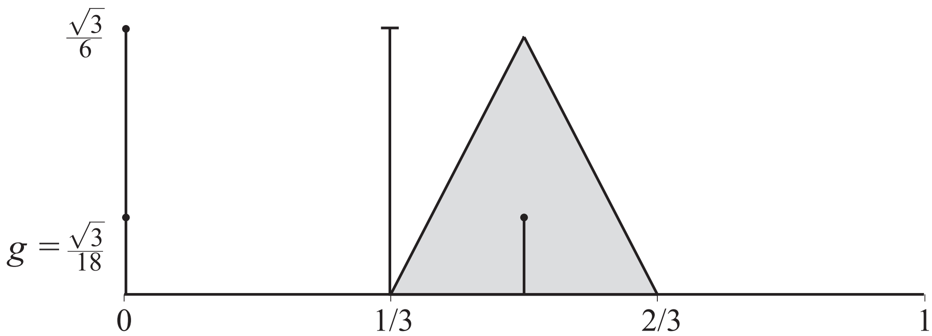


Figure 6.2: The generator for the Koch tiling.

with $\xi = \frac{1}{2} + \frac{1}{2\sqrt{3}}\mathbb{i}$. Thus we have one scaling ratio $r = |\xi| = 1/\sqrt{3}$, and one generator $G$ which is an equilateral triangle of side length $\frac{1}{3}$. Then the height of $G$ is $\frac{\sqrt{3}}{6}$ and the generating inradius is $g = \frac{\sqrt{3}}{18}$; see Fig. 6.2.

This tiling has inradii $\rho_k = gr^k$ with multiplicity $2^k$ for $k = 0, 1, 2, \ldots$, so the scaling zeta function is

$$\zeta_{\mathfrak{s}}(s) = \frac{1}{1 - 2 \cdot 3^{-s/2}}, \tag{6.9}$$

with scaling complex dimensions

$$\mathcal{D}_{\mathfrak{s}} = \{D + \mathbb{i}n\mathbf{p} \,\vdots\, n \in \mathbb{Z}\} \qquad \text{for } D = \log_3 4,\ \mathbf{p} = \tfrac{4\pi}{\log 3}. \tag{6.10}$$

Now to find the tube formula for the generator. By inspection of Fig. 6.2 and

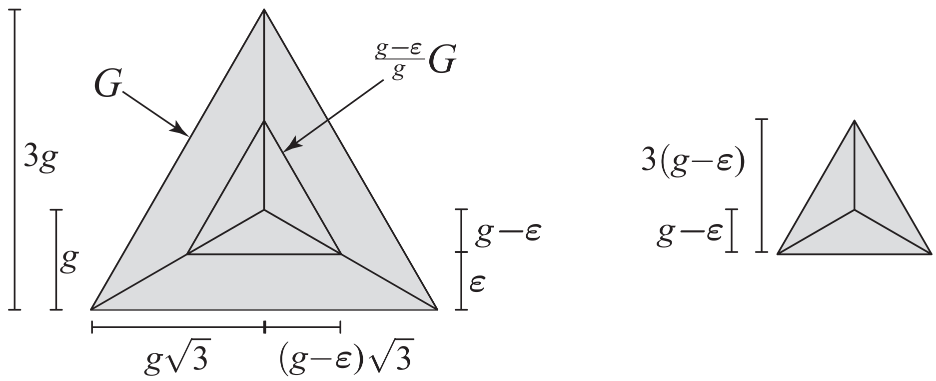


Figure 6.3: The volume $V_G(\varepsilon)$ of the generator of the Koch tiling.

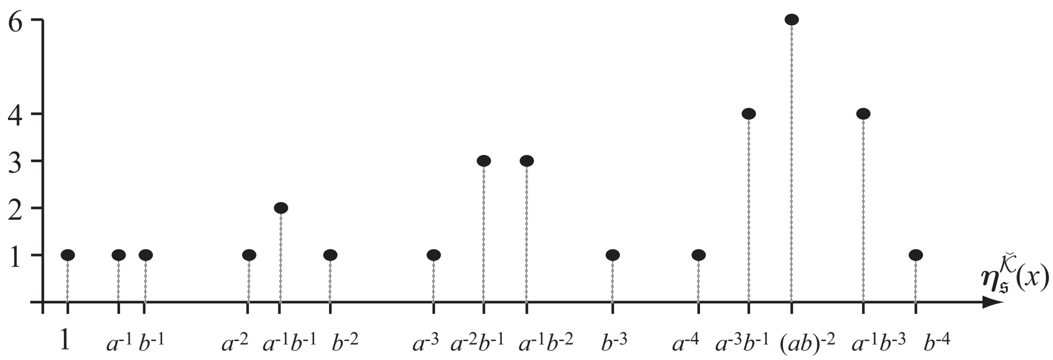


Figure 6.4: The scaling and geometric measures of a nonstandard Koch tiling (see Figures 3.4–3.5). Here, $a$ is the generating inradius of the larger isosceles triangles, and $b$ is the generating inradius of the smaller. This graph is not to scale, but note the binomial multiplicities with which the inverse scaling ratios appear.

Fig. 6.3, we would like to find $\gamma_{\mathcal{K}}(x, \varepsilon)$ so that $\gamma_{\mathcal{K}}(1/g, \varepsilon)$ gives

$$V_G(\varepsilon) = \mathrm{vol}_2(G) - \mathrm{vol}_2\left(\tfrac{g-\varepsilon}{g}G\right) = 3^{3/2}\left(2g - \varepsilon\right)\varepsilon \quad \text{for } \varepsilon < g. \tag{6.11}$$

The reasoning for (6.11) is as follows: $G$ has inradius $g$, so subtract the volume of a smaller, scaled copy which has inradius $g - \varepsilon$, as in Fig. 6.3. Then the tube formula for a scaled copy of $G$ with $\rho(G) = x$ is simply obtained by replacing $g$ with $x$:

$$\gamma_{\mathcal{K}}(x, \varepsilon) = \sum_{i=0}^{1} \kappa_i(\varepsilon)x^i = \kappa_0(\varepsilon)x^0 + \kappa_1(\varepsilon)x^1 = 3^{3/2}\left(-\varepsilon^2 + 2\varepsilon x\right), \tag{6.12}$$

$$\mu_2(xG) = \kappa_2(\varepsilon)x^2 = 3^{3/2}x^2. \tag{6.13}$$

For a given tile, $x$ is fixed as $\varepsilon \to 0^+$ (since $x$ represents the inradius of the tile) and it is clear that the expressions (6.12) and (6.13) coincide when $\varepsilon = x$. Thus we have

$$\begin{aligned} \zeta_{\mathcal{K}}(s) &= g^s \zeta_{\mathfrak{s}}(s) = \frac{g^s}{1 - 2 \cdot 3^{-s/2}} \\ \boldsymbol{\kappa}(\varepsilon) &= [\kappa_0 \quad \kappa_1 \quad \kappa_2] = 3^{3/2}\,[-1 \quad 2 \quad -1], \\ \mathcal{E}(\varepsilon, s) &= \left[\frac{1}{s}, \frac{1}{s-1}, \frac{1}{s-2}\right]\varepsilon^{2-s}. \end{aligned}$$

Now applying (5.55), the tube formula for the Koch tiling $\mathcal{K}$ is

$$\begin{aligned} V_{\mathcal{K}}(\varepsilon) = 3^{3/2}g^2 \sum_{\omega \in \mathcal{D}_{\mathfrak{s}}} &\operatorname{res}\left(\frac{1}{1 - 2 \cdot 3^{-s/2}}; \omega\right)\left(-\tfrac{1}{\omega} + \tfrac{2}{\omega-1} - \tfrac{1}{\omega-2}\right)\left(\tfrac{\varepsilon}{g}\right)^{2-\omega} \\ &+ \tfrac{g}{2}\zeta_{\mathfrak{s}}(0)\operatorname{res}\left(-\tfrac{1}{s}; 0\right)\left(\tfrac{\varepsilon}{g}\right)^{2-0} + \tfrac{g}{2}\zeta_{\mathfrak{s}}(1)\operatorname{res}\left(\tfrac{2}{s-1}; 1\right)\left(\tfrac{\varepsilon}{g}\right)^{2-1} \end{aligned} \tag{6.14}$$

$$\begin{aligned} = \frac{g}{\log 3}\sum_{n \in \mathbb{Z}} &\left(-\tfrac{1}{D + \mathbb{i}n\mathbf{p}} + \tfrac{2}{D-1+\mathbb{i}n\mathbf{p}} - \tfrac{1}{D-2+\mathbb{i}n\mathbf{p}}\right)\left(\tfrac{\varepsilon}{g}\right)^{2-D-\mathbb{i}n\mathbf{p}} \\ &+ 3^{3/2}\varepsilon^2 + \tfrac{1}{1-2\cdot 3^{-1/2}}\varepsilon, \end{aligned} \tag{6.15}$$

where $D = \log_3 4$ and $\mathbf{p} = \frac{4\pi}{\log 3}$ as before. The previous line (6.15) comes by observing that $g = \frac{\sqrt{3}}{18} = \frac{3^{1/2}}{2\cdot 3^2} = \frac{1}{2}3^{-3/2}$, so we have $3^{3/2}g^2 = \frac{g}{2}$, and then

$\varepsilon^2/2g = 3^{3/2}\varepsilon^2$.

*Remark* 6.3.1. In [LaPe1], a tube formula was obtained for the inner $\varepsilon$-neighbourhood of the Koch snowflake curve (rather than of the tiling associated with it) and the possible complex dimensions of this curve were inferred to be

$$\mathcal{D}_{\mathcal{K}\star} = \{D + \mathbb{i}n\mathbf{p} \,\vdots\, n \in \mathbb{Z}\} \cup \{0 + \mathbb{i}n\mathbf{p} \,\vdots\, n \in \mathbb{Z}\},$$

where $D = \log_3 4$ and $\mathbf{p} = \frac{2\pi}{\log 3}$. It is pleasing to see that $\mathcal{D}_{\mathcal{K}}$ is a subset of this. Note that the zeta function for the Koch curve was not defined prior to the present paper. In both [La-vF1] and [LaPe1], one reasoned by analogy with the tube formula (5.19) to deduce the possible complex dimensions. In the present work, however, the complex dimensions are defined directly as the poles of the scaling zeta function given in Chapter 4.

*Remark* 6.3.2. One may also compute the $\varepsilon$-neighbourhood of the Koch tiling from scratch, with a certain amount of effort. We begin with a tile $R_k$ which has inradius $\rho_k = gr^k$. For $\varepsilon < \rho$, we have $\text{vol}_2(G) = 3^{3/2}\rho^2$ and $V_G(\varepsilon) = 3^{3/2}(2\varepsilon g - \varepsilon^2)$ as in (6.11). Replacing $x$ by $gr^k$, in (6.13) and (6.12), one finds the volume formula for a tile of the $k^{\text{th}}$ generation to be

$$V_{R_k}(\varepsilon) = \begin{cases} \gamma_{\mathcal{K}}(gr^k, \varepsilon) = 3^{3/2}\left(-\varepsilon^2 + 2\varepsilon gr^k\right), & \varepsilon < \rho_k \\ \mu_2(gr^k G) = 3^{3/2}g^2r^{2k}, & \varepsilon \geq \rho_k. \end{cases} \tag{6.16}$$

Note that $V_{R_k}(\varepsilon) = V_{r^kG}(\varepsilon)$, as in (6.1). Since the components of the $k^{\text{th}}$ generation $T^k$ of tiles have inradius $\rho_k = gr^k$, with multiplicity $w_k = 2^k$, for $k = 0, 1, 2, \dots$, we have

$$\begin{aligned} V_{\mathcal{K}}(\varepsilon) &= \sum_{n \,\vdots\, \rho_n \geq \varepsilon} V_{R_n}(\varepsilon) + \sum_{n \,\vdots\, \rho_n < \varepsilon} V_{R_n}(\rho_n) \\ &= \sum_{k=0}^{N-1} w_k V_{r^kG}(\varepsilon) + \sum_{k=N}^{\infty} w_k V_{r^kG}(\rho_k). \end{aligned} \tag{6.17}$$

Here the sums split for $gr^N < \varepsilon \leq gr^{N-1}$, so $N = [\log_r \frac{\varepsilon r}{g}]$. Continuing,

$$V_{\mathcal{K}}(\varepsilon) = \sum_{k=0}^{N-1} 2^k 3^{3/2}\left(2\varepsilon gr^k - \varepsilon^2\right) + \sum_{k=N}^{\infty} 2^k 3^{3/2} g^2 r^{2k}$$

$$= 3^{3/2}\left[(-\varepsilon^2)\sum_{k=0}^{N-1}2^k + 2\varepsilon g\sum_{k=0}^{N-1}2^k r^k + g^2\sum_{k=N}^{\infty}2^k(r^2)^k\right]$$
$$= 3^{3/2}\left[-\varepsilon^2\left(\frac{1-2^N}{1-2}\right) + 2\varepsilon g\left(\frac{1-(2r)^N}{1-2r}\right) + g^2\frac{(2r^2)^N}{1-2r^2}\right]$$
$$= 3^{3/2}\left[\tfrac{\varepsilon^2}{1-2}2^N - \tfrac{2\varepsilon g}{1-2r}(2r)^N + \tfrac{g^2}{1-2r^2}(2r^2)^N\right] + 3^{3/2}\varepsilon^2 + \tfrac{2\cdot 3^{3/2}}{1-2r}\varepsilon g. \quad (6.18)$$

Now we use the fact that with $x = \log_r(\varepsilon r/g) = \log_r(\varepsilon/g) + 1$,

$$b^N = b^{[x]} = b^x b^{-\{x\}} = \left(\tfrac{\varepsilon}{g}\right)^{\log_r b} b^{1-\{\log_r \varepsilon/g\}}. \quad (6.19)$$

Recall $x = [x] + \{x\}$, where $[x]$ denotes the integer part and $\{x\}$ denotes the fractional part. Then for $r = \frac{1}{3}$ and $g = \frac{1}{6}$, (6.19) becomes

$$b^N = (2\varepsilon)^{-\log_3 b} b^{-\{-\log_3 6\varepsilon\}} = (2\varepsilon)^{-\log_3 b} b^{-\{-\log_3 2\varepsilon\}}.$$

Recall that

$$D = \log_3 4 = \log_{\sqrt{3}} 2 = \log_{1/r} 2 = -\log_r 2.$$

With $b = 2, 2r, 2r^2$, some terms from (6.18) are

$$\varepsilon^2 2^N = \varepsilon^2\left(\tfrac{\varepsilon}{g}\right)^{-D} 2^{1-\{\log_r \varepsilon/g\}} = g^2\left(\frac{\varepsilon}{g}\right)^{2-D} 2^{1-\{\log_r \varepsilon/g\}},$$
$$g\varepsilon\,(2r)^N = g\varepsilon\left(\tfrac{\varepsilon}{g}\right)^{-D+1}(2r)^{1-\{\log_r \varepsilon/g\}} = g^2\left(\frac{\varepsilon}{g}\right)^{2-D}(2r)^{1-\{\log_r \varepsilon/g\}},$$
$$g^2\left(2r^2\right)^N = g^2\left(\tfrac{\varepsilon}{g}\right)^{-D+2}\left(2r^2\right)^{1-\{\log_r \varepsilon/g\}} = g^2\left(\frac{\varepsilon}{g}\right)^{2-D}\left(2r^2\right)^{1-\{\log_r \varepsilon/g\}}.$$

Now we rewrite (6.18), replacing the discrete variable $N$ with a function of the continuous variable $\varepsilon$ and using $u = \log_r \varepsilon/g$.

$$V_{\mathcal{K}}(\varepsilon) = 3^{3/2}g^2\left[\varepsilon^2\tfrac{2}{1-2}2^{-\{u\}} - 2\varepsilon g\tfrac{2r}{1-2r}(2r)^{-\{u\}} + g^2\tfrac{2r^2}{1-2r^2}(2r^2)^{-\{u\}}\right]\left(\frac{\varepsilon}{g}\right)^{2-D}$$
$$- 3^{3/2}\left(\frac{\varepsilon^2}{1-2} - \frac{2\varepsilon g}{1-2r}\right). \quad (6.20)$$

Again noting that $g = \frac{\sqrt{3}}{18} = \frac{3^{1/2}}{2\cdot 3^2} = \frac{1}{2}3^{-3/2}$, the coefficient at far left of the above is $3^{3/2}g^2 = \frac{g}{2}$. Using $\log_r \frac{\varepsilon}{g} = -2\log_{r^{-2}}\frac{\varepsilon}{g}$ and with the oscillatory period

$\mathbf{p} = \frac{4\pi}{\log 3}$, we have

$$e^{2\pi \mathbb{i} n u} = e^{2\pi \mathbb{i} n(-2\log_3 \varepsilon/g)} = e^{-4\pi i n \log_3 \varepsilon/g} = \left(\tfrac{\varepsilon}{g}\right)^{-\mathbb{i} n \mathbf{p}}.$$

We use the following Fourier series from Appendix A:

$$b^{-\{u\}} = \frac{b-1}{b} \sum_{n\in\mathbb{Z}} \frac{e^{2\pi \mathbb{i} n u}}{\log b + 2\pi \mathbb{i} n} = \frac{b-1}{b} \frac{2}{\log 3} \sum_{n\in\mathbb{Z}} \frac{(\varepsilon/g)^{-\mathbb{i} n \mathbf{p}}}{\log_3 b^2 + \mathbb{i} n \mathbf{p}}, \tag{6.21}$$

to compute the following:

$$2^{-\{2\log_3 g/\varepsilon\}} = \frac{2}{\log 3} \frac{2-1}{2} \sum_{n\in\mathbb{Z}} \frac{(\varepsilon/g)^{-\mathbb{i} n \mathbf{p}}}{D + \mathbb{i} n \mathbf{p}}, \tag{6.22a}$$

$$(2r)^{-\{2\log_3 g/\varepsilon\}} = \frac{2}{\log 3} \frac{2r-1}{2r} \sum_{n\in\mathbb{Z}} \frac{(\varepsilon/g)^{-\mathbb{i} n \mathbf{p}}}{D - 1 + \mathbb{i} n \mathbf{p}}, \tag{6.22b}$$

$$\left(2r^2\right)^{-\{2\log_3 g/\varepsilon\}} = \frac{2}{\log 3} \frac{2r^2-1}{2r^2} \sum_{n\in\mathbb{Z}} \frac{(\varepsilon/g)^{-\mathbb{i} n \mathbf{p}}}{D - 2 + \mathbb{i} n \mathbf{p}}. \tag{6.22c}$$

Now using $3^{3/2}g^2 = \frac{g}{2}$ and (6.22a–c), the cancellations $\frac{b}{1-b} \cdot \frac{b-1}{b} = -1$ transform (6.20) into

$$\begin{aligned} V_{\mathcal{K}}(\varepsilon) &= \frac{g}{2} \left[ -\frac{2}{\log 3} \sum_{n\in\mathbb{Z}} \frac{(\varepsilon/g)^{-\mathbb{i} n \mathbf{p}}}{D + \mathbb{i} n \mathbf{p}} + \frac{4}{\log 3} \sum_{n\in\mathbb{Z}} \frac{(\varepsilon/g)^{-\mathbb{i} n \mathbf{p}}}{D - 1 + \mathbb{i} n \mathbf{p}} \right. \\ &\qquad \left. - \frac{2}{\log 3} \sum_{n\in\mathbb{Z}} \frac{(\varepsilon/g)^{-\mathbb{i} n \mathbf{p}}}{D - 2 + \mathbb{i} n \mathbf{p}} \right] \left(\frac{\varepsilon}{g}\right)^{2-D} + 3^{2/2}\varepsilon^2 + \tfrac{2\cdot 3^{3/2}}{1-2r}\varepsilon g \\ &= \frac{g}{\log 3} \sum_{n\in\mathbb{Z}} \left[ -\frac{1}{D + \mathbb{i} n \mathbf{p}} + \frac{2}{D - 1 + \mathbb{i} n \mathbf{p}} - \frac{1}{D - 2 + \mathbb{i} n \mathbf{p}} \right] \left(\frac{\varepsilon}{g}\right)^{2-D-\mathbb{i} n \mathbf{p}} \\ &\qquad + 3^{3/2}\varepsilon^2 + \tfrac{\varepsilon}{1-2\cdot 3^{-1/2}}. \end{aligned}$$

The point of this remark is to confirm Theorem 5.4.5 by alternative methods and to demonstrate the efficiency of the tube formula. Additionally, however, the development of $V_{\mathcal{K}}$ in this tortuous fashion allows one to see some of the roots of the tube formula. In particular, it is apparent that the components of the vector $\mathcal{E}(\varepsilon, s)$ in (4.39) are the fourier coefficients of $b^{-\{u\}}$ as in (6.21). In the simplification of terms of (6.18), one sees how the exponents of $\varepsilon$ always add

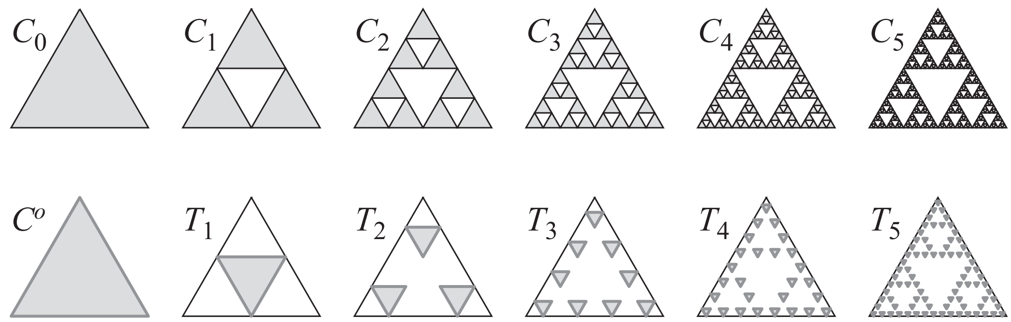


Figure 6.5: The Sierpinski gasket tiling.

to $d - s$, as in the general theorem. Furthermore, one can already see here the matrix $\boldsymbol{\kappa}$ in the coefficients of the term in square brackets, and the appearance of the $\zeta_{\mathfrak{s}}(0)$, $\zeta_{\mathfrak{s}}(1)$ terms coming from the 1 in the numerator of the finite geometric series formula.

*Remark* 6.3.3 (Nonlattice Koch tilings). By replacing $\xi = \frac{1}{2} + \frac{1}{2\sqrt{3}}\mathbb{i}$ in (6.8) with any other complex number $\xi \in \mathbb{C}$ satisfying

$$|\xi|^2 + |1 - \xi|^2 < 1,$$

we can easily construct family of examples of nonlattice self-similar tilings. The computation of the tube formula parallels that of the lattice case, almost identically. The lattice Koch tilings correspond to those $\xi \in B(\frac{1}{2}, \frac{1}{2})$ (the ball of radius $\frac{1}{2}$ centered at $\frac{1}{2} \in \mathbb{C}$) for which $\log_r |\xi|$ and $\log_r |1 - \xi|$ are both positive integers, for some fixed $0 < r < 1$. Any other choice of $\xi \in B(\frac{1}{2}, \frac{1}{2})$ will produce a nonlattice tiling. See [Pe] for further discussion (and illustrations) of nonlattice Koch tilings.

## 6.4 The Sierpinski gasket tiling

The Sierpinski gasket tiling $\mathcal{SG}$ (see Fig. 6.5) is constructed via the self-similar system

$$\Phi_1(z) := \tfrac{1}{2}z, \quad \Phi_2(z) := \tfrac{1}{2}z + \tfrac{1}{2}, \quad \Phi_3(z) := \tfrac{1}{2}z + \tfrac{1+\mathbb{i}\sqrt{3}}{4}.$$

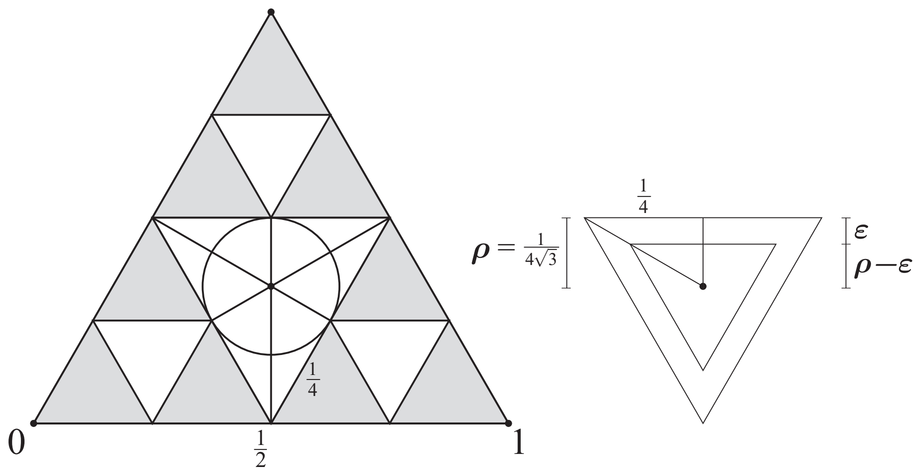


Figure 6.6: The generator for the Sierpinski gasket tiling $\mathcal{SG}$.

Thus we have one scaling ratio $r = 1/2$, and one generator $G$ which is an equilateral triangle with generating inradius $g = \frac{1}{4\sqrt{3}}$.

This tiling has inradii $\rho_k = gr^k$ with multiplicity $3^k$ for $k = 0, 1, 2, \ldots$, so the scaling zeta function is

$$\zeta_{\mathfrak{s}}(s) = \frac{1}{1 - 3 \cdot 2^{-s}}, \tag{6.23}$$

with scaling complex dimensions

$$\mathcal{D}_{\mathfrak{s}} = \{D + \mathbb{i}n\mathbf{p} \vdots n \in \mathbb{Z}\} \qquad \text{for } D = \log_2 3,\ \mathbf{p} = \tfrac{2\pi}{\log 2}. \tag{6.24}$$

Exactly as in the Koch curve example,

$$\gamma_{\mathcal{SG}}(x,\varepsilon) = \sum_{i=0}^{1} \kappa_i(\varepsilon)x^i = \kappa_0(\varepsilon)x^0 + \kappa_1(\varepsilon)x^1 = 3^{3/2}\left(-\varepsilon^2 + 2\varepsilon x\right), \tag{6.25}$$

$$\mu_2(xG) = \kappa_2(\varepsilon)x^2 = 3^{3/2}x^2. \tag{6.26}$$

Thus we have the matrices

$$\zeta_{\mathcal{SG}}(s) = g^s\zeta_{\mathfrak{s}}(s) = \frac{g^s}{1 - 3 \cdot 2^{-s}}$$
$$\boldsymbol{\kappa}(\varepsilon) = \begin{bmatrix}\kappa_0 & \kappa_1 & \kappa_2\end{bmatrix} = 3^{3/2}\begin{bmatrix}-\varepsilon^2 & 2\varepsilon & -1\end{bmatrix},$$

$$\mathcal{E}(\varepsilon, s) = \left[\frac{\varepsilon^{-s}}{s}, \frac{\varepsilon^{1-s}}{s-1}, \frac{\varepsilon^{2-s}}{s-2}\right]$$

The summand product is

$$\begin{aligned}\langle \zeta_{\mathcal{SG}}, \mathcal{E} \rangle_{\boldsymbol{\kappa}} &= 3^{3/2} \frac{g^s}{1 - 3 \cdot 2^{-s}} \begin{bmatrix} -\varepsilon^2 & 2\varepsilon & -1 \end{bmatrix} \begin{bmatrix} \frac{\varepsilon^{-s}}{s} \\ \frac{\varepsilon^{1-s}}{s-1} \\ \frac{\varepsilon^{2-s}}{s-2} \end{bmatrix} \\ &= 3^{3/2} \frac{g^s}{1 - 3 \cdot 2^{-s}} \left(-\tfrac{1}{s} + \tfrac{2}{s-1} - \tfrac{1}{s-2}\right) \varepsilon^{2-s}\end{aligned}$$

This tiling has inradii $\rho_k = gr^k$ with multiplicity $3^k$ for $k = 0, 1, 2, \ldots$, so the scaling zeta function is

$$\zeta_{\mathfrak{s}}(s) = \frac{1}{1 - 3 \cdot 2^{-s}}, \tag{6.27}$$

with complex dimensions

$$\mathcal{D}_{\mathfrak{s}} = \{D + \mathbb{i}n\mathbf{p} \,\vdots\, n \in \mathbb{Z}\} \qquad \text{for } D = \log_2 3,\ \mathbf{p} = \tfrac{2\pi}{\log 2}. \tag{6.28}$$

Except for $\zeta_{\mathfrak{s}}(s)$, the calculation for the tube formula for the Sierpinski tiling $\mathcal{SG}$ is just like that for the Koch tiling, so we omit the details and give the result:

$$\begin{aligned}V_{\mathcal{SG}}(\varepsilon) &= 3^{3/2} \sum_{\omega \in \mathcal{D}_{\mathcal{S}}} \operatorname{res}\left(\frac{g^s}{1 - 3 \cdot 2^{-s}} \left(-\tfrac{1}{s} + \tfrac{2}{s-1} - \tfrac{1}{s-2}\right) \varepsilon^{2-s}; \omega\right) \\ &= \tfrac{\sqrt{3}}{16 \log 2} \sum_{n \in \mathbb{Z}} \left(-\tfrac{1}{D + \mathbb{i}n\mathbf{p}} + \tfrac{2}{D - 1 + \mathbb{i}n\mathbf{p}} - \tfrac{1}{D - 2 + \mathbb{i}n\mathbf{p}}\right) \left(\tfrac{\varepsilon}{g}\right)^{2 - D - \mathbb{i}n\mathbf{p}} \\ &\qquad + \tfrac{3^{3/2}}{2}\varepsilon^2 - 3\varepsilon. \end{aligned} \tag{6.29}$$

In fact, a similar formula can be obtained for higher-dimensional analogues of the Sierpinski gasket, where the generator is a simplex instead of a triangle. The computations for the Sierpinski carpet, and its higher-dimensional analogue (the Menger sponge) are also extremely similar. In each case, the primary complication is to obtain the tube formula for the generator.

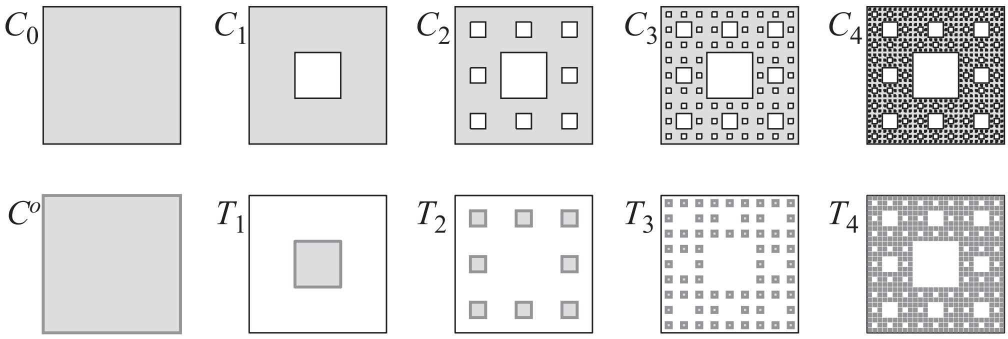


Figure 6.7: The Sierpinski carpet tiling $\mathcal{SC}$.

## 6.5 The Sierpinski carpet tiling

The Sierpinski carpet is constructed via the self-similar system

$$\Phi_k(x) = \tfrac{x}{3} + p_k,$$

where $p_k = (a_k, b_k)$ for $a_k, b_k \in \{0, \frac{1}{3}, \frac{2}{3}\}$, excluding the single case $(1/3, 1/3)$.

The maps $\Phi_k$ all have scaling ratio $r = 1/3$, so the Sierpinski carpet system has scales $3^{-k}$, each occurring with multiplicity $8^k$. The Sierpinski carpet scaling measure $\eta_{\mathfrak{s}}^{\mathcal{SC}}$ is thus the sum of the Dirac masses of weight $8^k$ at $x = 3^k$, and the Sierpinski carpet scaling zeta function is

$$\zeta_{\mathfrak{s}}(s) = \sum_{k=0}^{\infty} 8^k (3^{-k})^s = \frac{1}{1 - 8 \cdot 3^{-s}}, \tag{6.30}$$

with scaling complex dimensions

$$\mathcal{D}_{\mathfrak{s}} = \{D + \mathbb{i}n\mathbf{p} \,\vdots\, n \in \mathbb{Z}\} \qquad \text{for } D = \log_3 8,\ \mathbf{p} = \tfrac{2\pi}{\log 3}. \tag{6.31}$$

The Sierpinski carpet system is the first example with an infinitely ramified attractor. The single generator is a square with inradius $g = 1/6$. Similarly to prior examples, the volume of a tile is computed as the difference of two scaled tiles, one with inradius $x$ and the other with inradius $x - \varepsilon$. The resulting tube

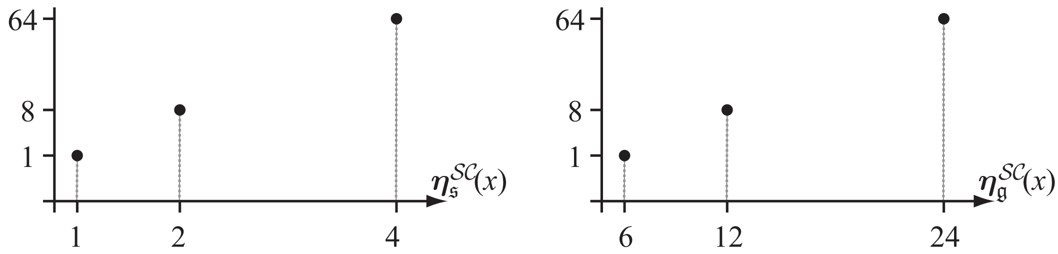


Figure 6.8: The Sierpinski carpet scaling measure (left) and geometric measure (right).

formula for a tile is

$$\begin{aligned}\gamma_{SC}(x,\varepsilon) &= \sum_{i=0}^{1} \kappa_i(\varepsilon)x^i = \kappa_0(\varepsilon)x^0 + \kappa_1(\varepsilon)x^1 = 4\left(-\varepsilon^2 + 2\varepsilon x\right) \\ \mu_2(G) &= \kappa_2(\varepsilon)x^2 = 4x^2.\end{aligned}$$

Thus we have the matrices

$$\begin{aligned}\zeta_{SC}(s) &= g^s\zeta_{\mathfrak{s}}(s) = \frac{6^{-s}}{1-8\cdot 3^{-s}} \\ \boldsymbol{\kappa}(\varepsilon) &= [\kappa_0 \quad \kappa_1 \quad \kappa_2] = 4\,[-1,2,-1]\,, \\ \mathcal{E}(\varepsilon,s) &= \left[\frac{1}{s}, \frac{1}{s-1}, \frac{1}{s-2}\right]\varepsilon^{2-s}\end{aligned}$$

The summand product is

$$\begin{aligned}\langle \zeta_{SC}, \mathcal{E}\rangle_{\boldsymbol{\kappa}} &= 4\frac{6^{-s}}{1-8\cdot 3^{-s}}\left[-\varepsilon^2 \quad 2\varepsilon \quad -1\right]\begin{bmatrix}\frac{\varepsilon^{-s}}{s} \\ \frac{\varepsilon^{1-s}}{s-1} \\ \frac{\varepsilon^{2-s}}{s-2}\end{bmatrix} \\ &= 4\frac{6^{-s}}{1-8\cdot 3^{-s}}\left(-\tfrac{1}{s} + \tfrac{2}{s-1} - \tfrac{1}{s-2}\right)\varepsilon^{2-s}\end{aligned}$$

The tube formula is then

$$V_{SC}(\varepsilon) = \sum_{\omega\in\mathcal{D}_{\mathcal{S}}} \operatorname{res}\left(\frac{g^2}{1-8\cdot 3^{-s}}\left(-\tfrac{1}{s} + \tfrac{2}{s-1} - \tfrac{1}{s-2}\right)\left(\tfrac{\varepsilon}{g}\right)^{2-s};\omega\right)$$

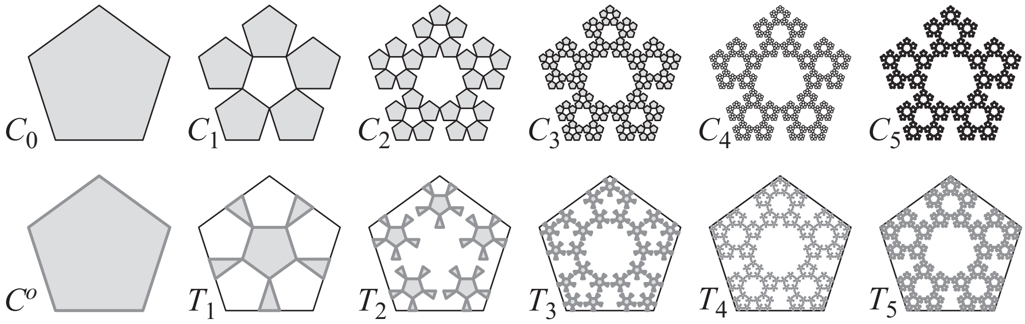


Figure 6.9: The pentagasket tiling.

$$= \frac{1}{36\log 3}\sum_{n\in\mathbb{Z}}\left(-\tfrac{1}{D+\mathbb{i}n\mathbf{p}}+\tfrac{2}{D-1+\mathbb{i}n\mathbf{p}}-\tfrac{1}{D-2+\mathbb{i}n\mathbf{p}}\right)\left(\tfrac{\varepsilon}{g}\right)^{2-D-\mathbb{i}n\mathbf{p}}+\tfrac{4}{7}\varepsilon^2-\tfrac{24}{5}\varepsilon \tag{6.32}$$

## 6.6 The pentagasket tiling

The pentagasket tiling $\mathcal{P}$ (see Fig. 6.9) is constructed via the self-similar system defined by the five maps

$$\Phi_j(x) = \tfrac{3-\sqrt{5}}{2}x + p_j, \qquad j = 1,\ldots,5,$$

with common scaling ratio $\phi^{-2}$, where $\phi = (1+\sqrt{5})/2$ is the golden ratio:

$$r = \tfrac{3-\sqrt{5}}{2} = \left(\tfrac{\sqrt{5}-1}{2}\right)^2 = \phi^{-2},$$

and the points $\frac{p_j}{1-r} = c_j$ form the vertices of a regular pentagon of side length 1. See Fig. 6.10 and Fig. 6.12. Then $\Phi_j(c_j) = rc_j + c_j(1-r) = c_j$ shows that $c_j$ is the fixed point of $\Phi_j$, for $j = 1,\ldots,5$.

The pentagasket is the first example of multiple generators $G_q$. In fact, the generators are $\operatorname{int} T_1 = G_1 \sqcup \cdots \sqcup G_6$ where $G_1$ is a regular pentagon and $G_2,\ldots,G_6$ are isosceles triangles (see Fig. 6.13). There are two distinct generating inradii:

$$g_1 = \tfrac{\phi^2}{2}\tan\tfrac{3}{10}\pi$$

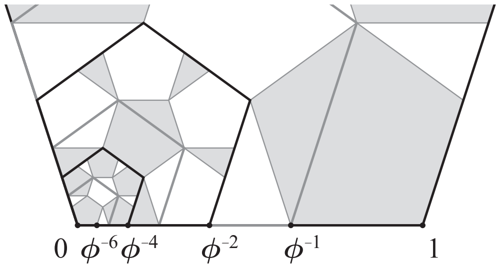


Figure 6.10: The pentagasket and the golden ratio $\phi$. The odd powers of $\phi^{-1}$ correspond to the pentagons with grey outlines.

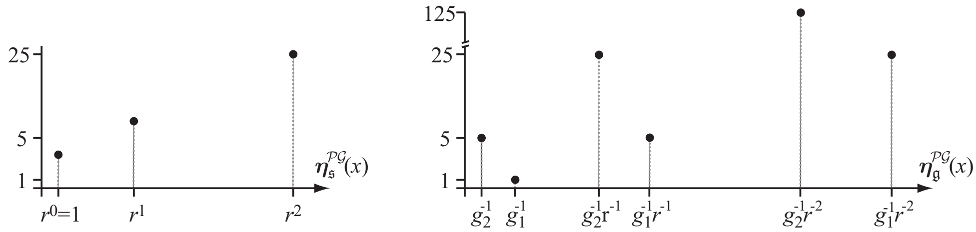


Figure 6.11: The pentagasket scaling measure (left) and geometric measure (right). Note that the presence of five congruent generators leads to quintuple multiplicities for $g_2$.

$$g_2 = \cdots = g_6 = \tfrac{\phi^3}{2} \tan \tfrac{\pi}{5}. \tag{6.33}$$

This leads to more interesting scaling and geometric measures; see Figure 6.11.

We omit the exercise of finding volumes for the pentagonal and triangular generators and simply give the results:

$$V_p(\rho) = 5 \cot \tfrac{3}{10}\pi\rho^2 = \alpha_1\rho^2, \tag{6.34}$$

for $\alpha_1 := 5 \cot \frac{3}{10}\pi$, and

$$V_t(\rho) = \frac{\cot \frac{\pi}{5}}{\left(1 - \tan^2 \frac{\pi}{5}\right)}\rho^2 = \alpha_2\rho^2 \tag{6.35}$$

for $\alpha_2 := (\cot \frac{\pi}{5}) / \left(1 - \tan^2 \frac{\pi}{5}\right)$.

The pentagasket tiling has inradii $\rho_k = g_q r^k$, $q = 1, 2$ with multiplicity $5^k$ for $k = 0, 1, 2, \ldots$, so the scaling zeta function is

$$\zeta_{\mathfrak{s}}(s) = \frac{1}{1 - 5 \cdot r^{-s}}, \tag{6.36}$$

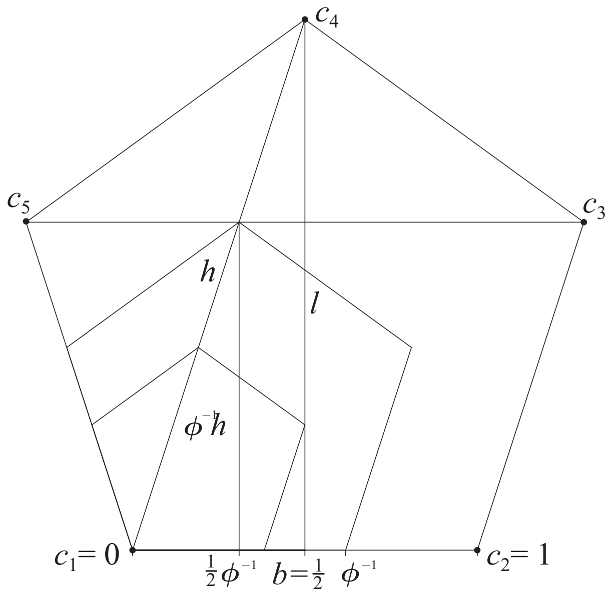


Figure 6.12: The vertices of the pentagasket.

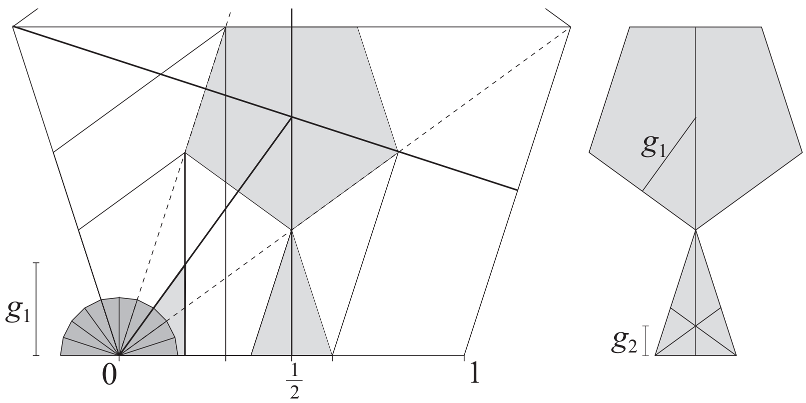


Figure 6.13: The generator of the pentagasket tiling.

with scaling complex dimensions

$$\mathcal{D}_{\mathfrak{s}} = \{D + \mathbb{i}n\mathbf{p} \,\vdots\, n \in \mathbb{Z}\} \qquad \text{for } D = \log_{1/r} 5,\ \mathbf{p} = \tfrac{2\pi}{\log r^{-1}}. \tag{6.37}$$

As in previous examples, for $\varepsilon < g$ we have

$$V_{G_q}(\varepsilon) = \mu_2(G_q) - \mu_2((1-\varepsilon)G_q) = \alpha_q(2\varepsilon - \varepsilon^2). \tag{6.38}$$

We find the generator tube formulas

$$\begin{aligned} \gamma_{\mathcal{P}q}(x,\varepsilon) &= \kappa_{q0}(\varepsilon)x^0 + \kappa_{q1}(\varepsilon)x^1 = \alpha_q\left(-\varepsilon^2 + 2\varepsilon x\right), \\ \mu_{q2}(G) &= \kappa_{q2}(\varepsilon)x^2 = \alpha_q x^2. \end{aligned}$$

*Remark* 6.6.1. Since $G_2, \ldots, G_6$ are similar (in fact, congruent), we can avoid writing a $6 \times 3$ matrix, and instead write a $2 \times 3$ matrix, by multiplying the contribution from one triangle by 5. This is the same shortcut discussed in the beginning of §5.6: collect several generators which are all similar, and alter the geometric measure $\eta_{\mathfrak{g}}$ appropriately to account for all appearing inradii, with multiplicity.

Thus we have the matrices

$$\begin{aligned} \zeta_{\mathcal{P}}(s) &= [g_1^s \ \ 5g_2^s]\zeta_{\mathfrak{s}}(s) \\ \boldsymbol{\kappa}(\varepsilon) &= [\kappa_{q0} \quad \kappa_{q1} \quad \kappa_{q2}] = \begin{bmatrix} -\alpha_1 & 2\alpha_1 & -\alpha_1 \\ -\alpha_2 & 2\alpha_2 & -\alpha_2 \end{bmatrix}, \\ \mathcal{E}(\varepsilon, s) &= \left[\frac{1}{s}, \frac{1}{s-1}, \frac{1}{s-2}\right] \varepsilon^{2-s}. \end{aligned}$$

The summand product is

$$\langle \zeta_{\mathcal{P}}, \mathcal{E} \rangle_{\boldsymbol{\kappa}} = \sum_{q=1}^{6} \frac{\alpha_q g_q^s}{1 - 5 \cdot r^{-s}} \left(-\tfrac{1}{s} + \tfrac{2}{s-1} - \tfrac{1}{s-2}\right) \varepsilon^{2-s}.$$

Hence the tube formula for the pentagasket tiling $\mathcal{P}$ is

$$V_{\mathcal{P}}(\varepsilon) = \sum_{q=1}^{6} \sum_{\omega \in \mathcal{D}_{\mathfrak{s}}} \operatorname{res}\left(\frac{\alpha_q g_q^2}{1 - 5 \cdot r^{-s}}; \omega\right) \left(-\tfrac{1}{\omega} + \tfrac{2}{\omega-1} - \tfrac{1}{\omega-2}\right) \left(\tfrac{\varepsilon}{g_q}\right)^{2-\omega}$$

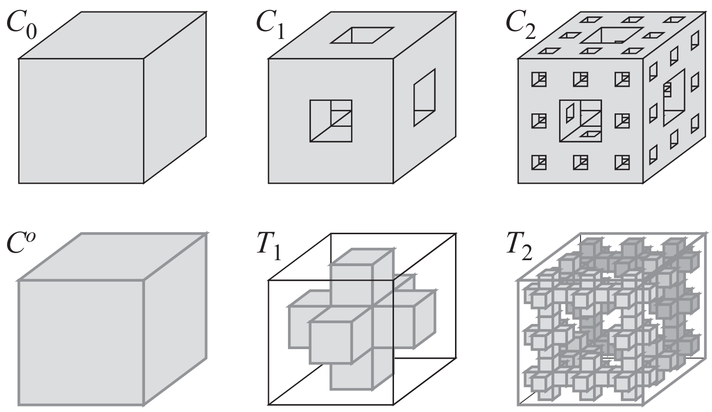


Figure 6.14: Successive approximations in the IFS construction of the Menger sponge.

$$
\begin{aligned}
&+\sum_{q=1}^{6}\alpha_q g_q^2\left[\zeta_{\mathfrak{s}}(0)\operatorname{res}\left(-\tfrac{1}{s};0\right)\left(\tfrac{\varepsilon}{g_q}\right)^2+\zeta_{\mathfrak{s}}(1)\operatorname{res}\left(\tfrac{2}{s-1};1\right)\left(\tfrac{\varepsilon}{g_q}\right)\right]\\
=&\frac{\alpha_1 g_1^2}{\log r^{-1}}\sum_{n\in\mathbb{Z}}\left(-\tfrac{1}{D+\mathbb{i}n\mathbf{p}}+\tfrac{2}{D-1+\mathbb{i}n\mathbf{p}}-\tfrac{1}{D-2+\mathbb{i}n\mathbf{p}}\right)\left(\tfrac{\varepsilon}{g_1}\right)^{2-D-\mathbb{i}n\mathbf{p}}\\
&+\frac{5\alpha_2 g_2^2}{\log r^{-1}}\sum_{n\in\mathbb{Z}}\left(-\tfrac{1}{D+\mathbb{i}n\mathbf{p}}+\tfrac{2}{D-1+\mathbb{i}n\mathbf{p}}-\tfrac{1}{D-2+\mathbb{i}n\mathbf{p}}\right)\left(\tfrac{\varepsilon}{g_2}\right)^{2-D-\mathbb{i}n\mathbf{p}}\\
&+\left[\left(\tfrac{\alpha_1}{4}+\tfrac{5\alpha_2}{4}\right)\varepsilon^2+\tfrac{(2\alpha_1 g_q+10\alpha_1 g_q r)r}{r-5}\varepsilon\right]. \qquad (6.39)
\end{aligned}
$$

with $r=\phi^{-2}$, $\alpha_1=5\cot\frac{3}{10}\pi$, $\alpha_2=(\cot\frac{\pi}{5})/\left(1-\tan^2\frac{\pi}{5}\right)$, $g_q$ as in (6.33), $D=\log_{1/r}5$ and $\mathbf{p}=\frac{2\pi}{\log r^{-1}}$ as before.

## 6.7 The Menger sponge

The Menger sponge is constructed via the self-similar system

$$\Phi_k(x)=\tfrac{x}{3}+p_k,$$

where $p_k=(a_k,b_k,c_k)$ for $a_k,b_k,c_k\in\{0,\frac{1}{3},\frac{2}{3}\}$, except for the six cases when exactly two coordinate are $1/3$, and the single case when all three coordinates are $1/3$.

The maps $\Phi_k$ all have scaling ratio $r=1/3$, so the Menger sponge system

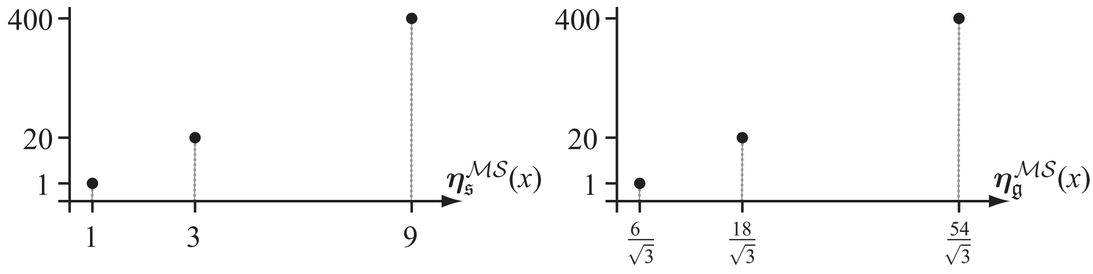


Figure 6.15: The Menger sponge scaling measure (left) and geometric measure (right).

has scales $3^{-k}$, each occurring with multiplicity $20^k$. The Menger sponge scaling measure $\eta_{\mathfrak{s}}^{\mathcal{MS}}$ is thus the sum of the Dirac masses of weight $20^k$ at $x = 3^k$, and the Menger sponge scaling zeta function is

$$\zeta_{\mathfrak{s}}^{\mathcal{MS}}(s) = \sum_{k=0}^{\infty} 20^k (3^{-k})^s = \frac{1}{1 - 20/3^s},$$

with scaling complex dimensions

$$\mathcal{D}_{\mathfrak{s}} = \left\{ \tfrac{\log 20}{\log 3} + in\mathbf{p} \,\vdots\, n \in \mathbb{Z}, \mathbf{p} = 2\pi/\log 3 \right\}.$$

The Menger sponge system is the first example with an attractor of dimension greater than 2, also the first example with a nonconvex generator. The inradius of the single generator is $g = \sqrt{3}/6$. The generator tube formula $V_G(\varepsilon)$ is quite complicated for this example, so discussion of it is postponed to [LaPe3].

The example of the Menger sponge also suggests another question which bears investigation: is there anything useful to be gained by subdividing the generators? It would clearly be much easier to work with this example if it were interpreted as having 7 cubical generators, instead of one nonconvex generator. This approach would also yield an open tiling (in the sense of Definition 3.2.10) of the complement of the Menger sponger, and it would have the advantage of a relatively simple tile formula $\gamma_G$. However, it is not as canonical as the construction given in Chapter 3. In general, it would be interesting to discover if anything useful remains when the generators are subdivided in such a fashion; especially if one can formalize an explicit relationship between the zeta function (and tube formula) obtained from such a subdivision, with the the original zeta function (and tube formula) obtained though the construction of Chapter 3. This idea will be investigated further in [LaPe4].

# Chapter 7

# Concluding Remarks

### 7.1.1 Fractality

In [La-vF4], a new definition of fractality is proposed; it states that the presence of complex dimensions characterize an object as being fractal. More specifically, [La-vF4] states that a fractal is an object with nonreal complex dimensions that have a positive real part. In this sense, this paper confirms the fractal nature of all the examples discussed.

### 7.1.2 Comparison with Chapter 2

Theorem 5.4.5 and its corollaries for self-similar tilings provide a fractal analogue of the classical Steiner formula and a higher-dimensional analogue of the tube formula for fractal strings (5.19) obtained in [La-vF4]. The present work can be considered as a further step towards a higher-dimensional theory of fractals, especially in the self-similar case. A first step was taken in [La-vF1, §10.2 and §10.3]. A second step (in the same spirit, but with significantly more precise results) was taken in Chapter 2 as discussed in Remark 6.3.1.

In Chapter 2, the emphasis was on obtaining an inner tube formula for the self-similar set itself (in that case, the Koch curve), rather than for the associated self-similar tiling. Moreover, because the geometry of the $\varepsilon$-neighbourhoods and hence the resulting computations were very complicated, the coefficients of the tube formula could not be explicitly calculated. More precisely, they could only be expressed in terms of the Fourier coefficients of a certain periodic function.

Here, in contrast to Remark 2.5.3, the scaling and tiling zeta functions are defined and used to obtain the explicit tube formula for a self-similar tiling. Then one may obtain the complex dimensions directly from these zeta functions; compare to (1.11).

### 7.1.3 Tilings vs. sets

Despite the fact that our tube formulas are obtained for the $\varepsilon$-neighbourhoods of self-similar tilings rather than of self-similar sets, they give us valuable information about self-similar geometries (and their associated dynamical systems). Indeed, given a self-similar set in $\mathbb{R}^d$, we can define its complex dimensions as those of the self-similar tiling canonically associated to it as in [Pe]. This is accomplished by turning to the IFS which defines the given self-similar set, and focusing on the dynamical system induced by the IFS. For example, §6.3 shows how the complex dimensions of the Koch curve really depend on the self-similar system $\Phi$.

### 7.1.4 Motivation for *inner* neighbourhoods

By using the inner $\varepsilon$-neighbourhoods of the generators, we believe the curvature coefficients $c_\omega$ appearing in the tube formula

$$V_{\mathcal{T}}(\varepsilon) = \sum_{\omega \in \mathcal{D}_{\mathcal{T}}} c_\omega \varepsilon^{d-\omega} \tag{7.1}$$

are intrinsic to the self-similar tiling. This should be the case, provided the curvature matrix $\boldsymbol{\kappa}$ is also intrinsic (i.e., does not depend on the embedding of $\mathcal{T}$ in the ambient space $\mathbb{R}^d$). Hermann Weyl also gave a tube formula for smooth submanifolds of $\mathbb{R}^d$ in [We], expressed as a polynomial in $\varepsilon$ with coefficients defined in terms of curvatures that are intrinsic to the submanifold. See [BeGo, §6.6–6.9] and [Gr].

### 7.1.5 Invariants of self-similar systems

Many classical fractal curves are attractors of more than one self-similar system. For example, the Koch curve discussed in §6.3 is also the attractor of a system of 4 mappings, each with scaling ratio $r = \frac{1}{3}$. In this particular example, changes in the scaling zeta function produce a different set of complex dimensions. In fact, we obtain a subset of the original complex dimensions: $\{\log_3 4 + \mathbb{i}n\mathbf{p} \,\vdots\, n \in \mathbb{Z}, \mathbf{p} = 4\pi/\log 3\}$. This has a natural geometric interpretation which is to be discussed in later work. In particular, it would be desirable to determine precisely which characteristics remain invariant between different tilings which are so related.

# Appendix A

# A Certain Useful Fourier Series

The Fourier Series for $f(u) = b^{-\{u\}}$ is used several times in this dissertation (e.g., (2.14) and (6.21)), so we provide the computation justifying this formula.

If $f(u) = b^{-\{u\}}$, then $\{u\} = u - [u]$ implies $f(u+1) = f(u)$. Therefore,

$$
\begin{aligned}
\int_0^1 f(u)\, e^{-2\pi i n u} du &= \int_0^1 b^{-\{u\}} e^{-2\pi i n u} du \\
&= \int_0^1 b^{-u} e^{-2\pi i n u} du \qquad \text{(A.1)} \\
&= \int_0^1 e^{-u \log b} e^{-2\pi i n u} du \\
&= \int_0^1 e^{-u(2\pi i n + \log b)} du \\
&= -\tfrac{1}{2\pi i n + \log b} \left(e^{-(2\pi i n + \log b)} - e^0\right) \\
&= \tfrac{1}{2\pi i n + \log b} \left(1 - e^{-2\pi i n} e^{\log \frac{1}{b}}\right) \\
&= \tfrac{1}{2\pi i n + \log b} \left(1 - \tfrac{1}{b}\right) \\
&= \tfrac{b-1}{b} \cdot \tfrac{1}{2\pi i n + \log b}.
\end{aligned}
$$

Collecting the coefficients into a series, we obtain

$$
b^{-\{u\}} = \tfrac{b-1}{b} \sum_{n \in \mathbb{Z}} \tfrac{e^{2\pi i n u}}{2\pi i n + \log b}.
$$

Note that equality (A.1) holds because $0 \leqslant u \leqslant 1 \implies b^{[u]} = b^0 = 1$.

# Appendix B

# Languid and Strongly Languid

The following definitions are excerpted from [La-vF4, §5.3]. The technical details described here are used in the proof of Theorem 5.4.5, especially in Appendix C and Appendix D.

**Definition B.1.1.** Let $f : \mathbb{R} \to \mathbb{R}$ be a bounded Lipschitz continuous function. Then the *screen* is $S = \{f(t) + \mathbb{i}t \vdots t \in \mathbb{R}\}$, the graph of a function with the axes interchanged. We let

$$\inf S := \inf_t f(t) = \inf\{\operatorname{Re} s \vdots s \in S\}, \text{ and} \tag{B.1}$$

$$\sup S := \sup_t f(t) = \sup\{\operatorname{Re} s \vdots s \in S\}. \tag{B.2}$$

The screen is thus a vertical contour in $\mathbb{C}$. The region to the right of the screen is the set $W$, called the *window*:

$$W := \{z \in \mathbb{C} \vdots \operatorname{Re} z \geq f(\operatorname{Im} z)\}. \tag{B.3}$$

**Definition B.1.2.** The generalized fractal string $\eta$ (as in Definition 5.3.1) is said to be *languid* if its associated zeta function $\zeta_\eta$ satisfies certain growth conditions.[1] Specifically, let $\{T_n\}_{n\in\mathbb{Z}}$ be a sequence in $\mathbb{R}$ such that $T_{-n} < 0 < T_n$ for $n \geq 1$,

[1]We take $\zeta_\eta$ to be meromorphically continued to an open neighbourhood of $W$, as in Definition 5.3.3.

and

$$\lim_{n\to\infty} T_n = \infty, \lim_{n\to\infty} T_{-n} = -\infty, \text{ and } \lim_{n\to\infty} \frac{T_n}{|T_{-n}|} = 1. \tag{B.4}$$

For $\eta$ to be languid, there must exist real constants $M, c > 0$ and a sequence $\{T_n\}$ as described in (B.4), such that

**L1** For all $n \in \mathbb{Z}$ and all $\sigma \geq f(T_n)$,

$$|\zeta_\eta(\sigma + \mathbb{i}T_n)| \leq c \cdot (|T_n| + 1)^M \text{ , and} \tag{B.5}$$

**L2** For all $t \in \mathbb{R}$, $|t| \geq 1$,

$$|\zeta_\eta(f(t) + \mathbb{i}t)| \leq c \cdot |t|^M. \tag{B.6}$$

In this case, $\eta$ is said to be *languid of order* $M$.

**Definition B.1.3.** The generalized fractal string $\eta$ is said to be *strongly languid* if it satisfies **L1** and the condition **L2**$'$, which is clearly stronger than **L2**:

**L2**$'$ There exists a sequence of screens $S_m(t) = f_m(t) + \mathbb{i}t$ for $m \geq 1$, $t \in \mathbb{R}$, with $\sup S_m \to -\infty$ as $m \to \infty$, and with a uniform Lipschitz bound, for which there exist constants $a, c > 0$ such that

$$|\zeta_\eta(f(t) + \mathbb{i}t)| \leq c \cdot a^{|f_m(t)|}(|t| + 1)^M, \tag{B.7}$$

for all $t \in \mathbb{R}$ and $m \geq 1$.

*Remark* B.1.4. The general nature of the growth conditions (B.5)–(B.7) are being studied by Scot Childress currently. Indeed, there seems to be some deeper connections with the body of results collectively referred to as “Paley-Wiener Theorems”.

# Appendix C

# Definition and Properties of $\zeta_{\mathcal{T}}$

In this section, we confirm some basic properties of the geometric zeta function of a fractal spray $\zeta_{\mathcal{T}}$ defined in §4.5 and more generally in §5.4. However, we first require some facts about Mellin transformation. If $\varphi \in \mathbb{D} = C_c^\infty(0, \infty)$, it is elementary to check that for every $s \in \mathbb{C}$, the Mellin transform $\widetilde{\varphi}(s)$ is given by the well-defined integral (5.17) and satisfies $|\widetilde{\varphi}(s)| \leq |\widetilde{\varphi}|(\operatorname{Re} s) < \infty$. We will need additional estimates in what follows. We will also use the forthcoming fact that $\widetilde{\varphi}(s)$ is an entire function. This remains true when $\varphi$ is replaced by $h\varphi$, for any bounded function $h$.

**Lemma C.1.5.** *Suppose that $S \subseteq \mathbb{C}$ is horizontally bounded, so that $\inf_S \operatorname{Re} s$ and $\sup_S \operatorname{Re} s$ are finite. Let $K$ be a compact interval containing the support of $\varphi \in C_c^\infty(0, \infty)$. Then there is a constant $c_K > 0$ depending only on $K$ such that*

$$\sup_{s \in S} |\widetilde{\varphi}(s)| \leq c_K \|\varphi\|_\infty. \tag{C.1}$$

*This is the case, in particular, if $S$ is a screen as in Definition B.1.1. In* (C.1), *$\|\varphi\|_\infty$ is the supremum norm of $\varphi$.*

*Proof.* Let $K$ be a compact interval containing the support of $\varphi$. Since

$$|x^{s-1}| = x^{\operatorname{Re} s - 1} \leq \begin{cases} x^{\sup S - 1}, & x \geq 1 \\ x^{\inf S - 1}, & 0 < x < 1, \end{cases} \tag{C.2}$$

one can define a bound

$$b_K := \sup_{x \in K} \max\{x^{\sup S - 1}, x^{\inf S - 1}\}.$$

Note that $b_K$ is finite because the function $x \mapsto \max\{x^{\sup S-1}, x^{\inf S-1}\}$ is continuous on the compact set $K$, and hence is bounded. Then we use (C.2) to bound $\widetilde{\varphi}$ as follows:

$$\begin{aligned} |\widetilde{\varphi}(s)| &\leq \int_0^\infty |x^{s-1}| \cdot |\varphi(x)| \, dx \\ &= \int_K x^{\operatorname{Re} s - 1} |\varphi|(x) \, dx = \widetilde{|\varphi|}(\operatorname{Re} s) \qquad \text{(C.3)} \\ &\leq b_K \|\varphi\|_\infty \cdot length(K). \end{aligned}$$

□

**Corollary C.1.6.** *If $h$ is a bounded measurable function on $(0, \infty)$, and $\varphi$ and $K$ are as in Lemma C.1.5, then*

$$\sup_{s \in S} |\widetilde{h\varphi}(s)| \leq c_K \|h\|_\infty \|\varphi\|_\infty, \tag{C.4}$$

*where $c_K > 0$ depends only on $K$. In particular, $\widetilde{\kappa_{qi}\varphi}$ is always uniformly bounded on the screen $S$.*

*Proof.* The argument is identical to that of Lemma C.1.5. For each $i = 0, \ldots, d$, $\kappa_{qi}(\varepsilon)$ is bounded for $\varepsilon \leq g$ and constant for $\varepsilon > g$ (see Definition 4.4.2). Thus $\kappa_{qi}$ is globally bounded and the corollary applies. □

*Remark* C.1.7. The exact counterpart of Lemma C.1.5 and Cor. C.1.6 holds if $\widetilde{\varphi}(s)$ or $\widetilde{h\varphi}(s)$ is replaced by a translate $\widetilde{\varphi}(s - s_0)$ or $\widetilde{h\varphi}(s - s_0)$, for any $s_0 \in \mathbb{C}$. Therefore, under the same assumptions as in Cor. C.1.6, we have

$$\sup_{s \in S} |\widetilde{h\varphi}(s - s_0)| \leq c_{K,s_0} \|h\|_\infty \|\varphi\|_\infty, \tag{C.5}$$

where $c_{K,s_0} := b_{K,s_0} \cdot length(K)$, and

$$b_{K,s_0} := \sup_{x \in K} \max\{x^{\sup S - \operatorname{Re} s_0 - 1}, x^{\inf S - \operatorname{Re} s_0 - 1}\} < \infty. \tag{C.6}$$

In particular, for any compact interval $K$ containing the support of $\varphi$, and for each fixed integer $k \geq 0$,

$$\sup_{s\in S} |\widetilde{\kappa_{qi}\varphi}(s-d+k+1)| \leq c_{K,k}\|\varphi\|_\infty, \tag{C.7}$$

where $c_{K,k}$ is a finite and positive constant, independent of $q$ and $i$.

**Lemma C.1.8.** *Suppose that $(X,\mu)$ is a measure space, and define an integral transform by $F(s) = \int_X f(x,s)\,d\mu(x)$ where*

$$|f(x,s)| \leq G(x), \quad \text{for } \mu\text{-a.e. } x \in X,$$

*for some $G \in L^1(X,\mu)$, and for all $s$ in some neighbourhood of $s_0 \in \mathbb{C}$. If the function $s \mapsto f(x,s)$ is holomorphic for $\mu$-a.e. $x \in X$, then $F(s)$ is well-defined and holomorphic at $s_0$.*

The proof is a well-known application of Lebesgue's Dominated Convergence Theorem. We use Lemma C.1.8 and Cor. C.1.6 to obtain the following corollary, which is used to prove Theorem 5.4.5 and Theorem C.1.12.

**Corollary C.1.9.** *For $\varphi \in C_c^\infty(0,\infty)$, $\widetilde{\varphi}(s)$ is entire. Further, if $h(x)$ is a bounded measurable function, then $\widetilde{h\varphi}(s)$ is also entire. In particular, $\widetilde{\kappa_{qi}\varphi}(s)$ is entire for all $q = 1,\ldots,Q$ and $i = 0,\ldots,d$.*

*Proof.* Fix $s_0 \in \mathbb{C}$. If $s$ is in a compact neighbourhood of $s_0$, then $\operatorname{Re} s$ is bounded, say by $\alpha \in \mathbb{R}$. Then for almost every $x > 0$,

$$\left|x^{s-1}h(x)\varphi(x)\right| \leq x^{\alpha-1}\|h\|_\infty\|\varphi\|_\infty\chi_\varphi, \tag{C.8}$$

where $\chi_\varphi$ is the characteristic function of the compact support of $\varphi$. Upon application of Lemma C.1.8, one deduces that $\varphi$ is holomorphic at $s_0$. $\square$

Note that this does not combine with Lemma C.1.5 (or Cor. C.1.6) to imply that $\widetilde{\varphi}$ (or $\widetilde{h\varphi}$) is constant; indeed, Liouville's Theorem does not apply because $s$ is restricted to $S$ in these two propositions.

**Definition C.1.10.** For $T(\varepsilon,s)$ to be a *weakly meromorphic distribution-valued function* on $W$, there must exist

(i) a discrete set $\mathcal{P}_T \subseteq \mathbb{C}$, and

(ii) for each $\omega \in \mathcal{P}_T$, an integer $n_\omega < \infty$,

such that $\Psi(s) = \langle T(\varepsilon, s), \varphi(\varepsilon)\rangle$ is a meromorphic function of $s \in W$, and each pole $\omega$ of $\Psi$ lies in $\mathcal{P}_T$ and has multiplicity at most $n_\omega$.

To say that the distribution-valued function $T : W \to \mathbb{D}'$ given by $s \mapsto T(\varepsilon, s)$ is *(strongly) meromorphic* means that, as a $\mathbb{D}'$-valued function, it is truly a meromorphic function, in the sense of the proof of Lemma C.1.11. Recall that we are working with the space of distributions $\mathbb{D}'$, defined as the dual of the space of test functions $\mathbb{D} = C_c^\infty(0, \infty)$.

**Lemma C.1.11.** *If $T$ is a weakly meromorphic distribution-valued function, then it is a meromorphic distribution-valued function.*

*Proof.* For $\omega \notin \mathcal{P}_T$, note that as $s \to \omega$,

$$\frac{T(\varepsilon, s) - T(\varepsilon, \omega)}{s - \omega} \tag{C.9}$$

converges to a distribution (call it $T'(\varepsilon, \omega)$) in $\mathbb{D}'$, by the Uniform Boundedness Principle for a topological vector space such as $\mathbb{D}$; see [Rud, Thm. 2.5 and Thm. 2.8]. Hence, the $\mathbb{D}'$-valued function $T$ is holomorphic at $\omega$.

For $\omega \in \mathcal{P}_T$, apply the same argument to

$$\lim_{s \to \omega} \frac{1}{(n_\omega - 1)!} \left(\frac{d}{ds}\right)^{n_\omega - 1} \Big((s - \omega)^{n_\omega} T(\varepsilon, s)\Big), \tag{C.10}$$

which must therefore define a distribution, i.e., exist as an element of $\mathbb{D}'$. Thus $T$ is truly a meromorphic function with values in $\mathbb{D}'$, and with poles contained in $\mathcal{P}_T$. □

**Theorem C.1.12.** *Under the hypothesis of Theorem 5.4.5 or Theorem 5.5.1, the geometric zeta function of a fractal spray or tiling*

$$\begin{aligned} \zeta_{\mathcal{T}}(\varepsilon, s) &= \sum_{i=0}^{d} \sum_{q=1}^{Q} g_q^s \zeta_\eta(s) \frac{\varepsilon^{d-s}}{s - i} \kappa_{qi}(\varepsilon) \\ &= \langle \vec{g}(s) \zeta_\eta(s), \mathcal{E}(\varepsilon, s)\rangle_{\boldsymbol{\kappa}(\varepsilon)} \end{aligned} \tag{C.11}$$

*is a (strongly) distribution-valued meromorphic function on $W$, with poles contained in $\mathcal{D}_{\mathcal{T}}$.*

*Proof.* Let $\mathcal{P}_T = \mathcal{D}_{\mathcal{T}}$ and note that

$$\begin{aligned}\langle \zeta_{\mathcal{T}}(\varepsilon, s), \varphi(\varepsilon) \rangle_{\boldsymbol{\kappa}} &= \sum_{q,i} \int_0^\infty g_q^s \zeta_\eta(s) \frac{\varepsilon^{d-s}}{s-i} \kappa_{qi}(\varepsilon) \varphi(\varepsilon)\, d\varepsilon \\ &= \sum_{q,i} g_q^s \zeta_\eta(s) \frac{\widetilde{\kappa_{qi}\varphi}(d-s+1)}{s-i}. \end{aligned} \tag{C.12}$$

By Cor. C.1.9, this is a finite sum of meromorphic functions and hence meromorphic on $W$, for any test function $\varphi$. Applying Lemma C.1.11, one sees that $\zeta_{\mathcal{T}}$ is a meromorphic function with values in $\mathbb{D}'$. □

*Remark* C.1.13. Note that for each $\varphi \in \mathbb{D}$, the poles of the $\mathbb{C}$-valued function

$$s \mapsto \langle \zeta_{\mathcal{T}}(\varepsilon, s), \varphi(\varepsilon) \rangle \tag{C.13}$$

are contained in $\mathcal{D}_{\mathcal{T}}$. Further, if $m_\omega$ is the multiplicity of $\omega \in \mathcal{D}_{\mathcal{T}}$ as a pole of $\zeta_\eta(s)$, then the multiplicity of $\omega$ as a pole of (C.13) is bounded by $m_\omega + 1$.

**Corollary C.1.14.** *The residue of $\zeta_{\mathcal{T}}$ at a pole $\omega \in \mathcal{D}_{\mathcal{T}}$ is a well-defined distribution.*

*Proof.* This follows immediately from the second part of the proof of Lemma C.1.11, with $\mathcal{P}_T = \mathcal{D}_{\mathcal{T}}$. □

**Corollary C.1.15.** *The sum of residues appearing in Theorem 5.4.5 and Theorem 5.5.1 is distributionally convergent, and is thus a well-defined distribution.*

*Proof.* In view of the proof of Theorem C.1.12, this comes by applying the Uniform Boundedness Principle to an appropriate sequence of partial sums, in a manner similar to the proof of Lemma C.1.11. Again, see [La-vF4, Rem. 5.21]. □

# Appendix D

# The Error Term and Its Estimate

Recall the tube formula for fractal sprays given earlier as Theorem 5.4.5:

**Theorem D.1.16.** *Let $\eta$ be a fractal spray on generators $\{G_q\}_{q=1}^Q$, with generating inradii $g_q = \rho(G_q) > 0$. Assume that $\zeta_\eta$ is languid on a screen $S$ which avoids the dimensions $\mathcal{D}_\mathcal{T}(W)$, and that each generator is Steiner-like (as in Definition 4.4.2). Then for test functions in $C_c^\infty(0,\infty)$, the $d$-dimensional volume of the inner tubular neighbourhood of the spray is given by the following distributional explicit formula:*

$$V_\mathcal{T}(\varepsilon) = \sum_{\omega \in \mathcal{D}_\mathcal{T}(W)} \operatorname{res}\left(\zeta_\mathcal{T}(\varepsilon, s); \omega\right) + \mathcal{R}(\varepsilon). \tag{D.1}$$

*Here, the error term $\mathcal{R}(\varepsilon)$ is given by*

$$\mathcal{R}(\varepsilon) = \frac{1}{2\pi\mathbb{i}} \int_S \zeta_\mathcal{T}(\varepsilon, s)\, ds, \tag{D.2}$$

*and estimated by*

$$\mathcal{R}(\varepsilon) = O(\varepsilon^{d-\sup S}), \qquad \text{as } \varepsilon \to 0^+. \tag{D.3}$$

As promised, we give a proof of the expression for the error term (D.2) (in Theorem D.1.21), and its estimate (D.3) (in Theorem D.1.23). First, however, we require some preliminary results about the primitives and Mellin transforms of distributions.

**Definition D.1.17** (Primitives of distributions)**.** Let $T_\eta$ be a distribution defined by a measure as

$$\langle T_\eta, \varphi \rangle := \int \varphi \, d\eta.$$

Then the $k^{\text{th}}$ *primitive* (or $k^{\text{th}}$ antiderivative) of $T_\eta$ is defined by

$$\langle T_\eta^{[k]}, \varphi \rangle := (-1)^k \langle T_\eta, \varphi^{[k]} \rangle, \tag{D.4}$$

where $\varphi^{[k]}$ is the $k^{\text{th}}$ primitive of $\varphi \in C_c^\infty(0, \infty)$ that vanishes at $\infty$ together with all its derivatives. For $k \geq 1$, for example,

$$\langle T_\eta^{[k]}, \varphi \rangle = \int_0^\infty \int_y^\infty \frac{(x-y)^{k-1}}{(k-1)!} \varphi(x) \, dx \, d\eta(y). \tag{D.5}$$

**Theorem D.1.18.** *The Mellin transform of the $k^{th}$ primitive of a test function is given by $\widetilde{\varphi^{[k]}}(s) = \tilde{\varphi}(s+k)\psi_k(s)$, where $\psi_k$ is the meromorphic function*

$$\psi_k(s) := \sum_{j=0}^{k-1} \frac{\binom{k-1}{j}(-1)^j}{(k-1)!(s+j)}. \tag{D.6}$$

*Proof.* By direct computation,

$$\begin{aligned}
\widetilde{\varphi^{[k]}}(s) &= \int_0^\infty \varepsilon^{s-1} \int_\varepsilon^\infty \frac{(x-\varepsilon)^{k-1}}{(k-1)!} \varphi(x) \, dx \, d\varepsilon \\
&= \frac{1}{(k-1)!} \int_0^\infty \int_\varepsilon^\infty \sum_{j=0}^{k-1} \binom{k-1}{j} x^{k-1-j} (-\varepsilon)^j \varepsilon^{s-1} \varphi(x) \, dx \, d\varepsilon \\
&= \sum_{j=0}^{k-1} \frac{\binom{k-1}{j}(-1)^j}{(k-1)!} \int_0^\infty \int_\varepsilon^\infty x^{k-1-j} \varepsilon^{s+j-1} \varphi(x) \, dx \, d\varepsilon \\
&= \sum_{j=0}^{k-1} \frac{\binom{k-1}{j}(-1)^j}{(k-1)!} \int_0^\infty x^{k-1-j} \varphi(x) \int_0^x \varepsilon^{s+j-1} \, d\varepsilon \, dx \\
&= \sum_{j=0}^{k-1} \frac{\binom{k-1}{j}(-1)^j}{(k-1)!(s+j)} \int_0^\infty x^{s+k-1} \varphi(x) \, dx \qquad \text{(D.7)} \\
&= \tilde{\varphi}(s+k)\psi_k(s).
\end{aligned}$$

Again, the formula (D.6) for $\psi_k$ is valid for $\operatorname{Re} s > k$ by (D.7), but then extends to being valid for $s \in \mathbb{C}$ by meromorphic continuation. $\square$

**Corollary D.1.19.** *We also have* $\left|\widetilde{\kappa_{qi}\varphi^{[k]}}(s)\right| \leq |\widetilde{\kappa_{qi}\varphi}(s+k)\psi_k(s)|$.

*Proof.* Repeat the proof of Theorem D.1.18 with $\kappa_{qi}$ in the integrand, or follow (D.20) below, with $a = 1$. $\square$

*Remark* D.1.20. For $s \in S$, we also have

$$|\psi_k(s)| \leq \frac{c_\psi}{|t|^k}, \quad \text{for } t = \operatorname{Im} s \text{ and } c_\psi > 0. \tag{D.8}$$

We are now in a position to provide the proofs previously promised.

**Theorem D.1.21.** *As stated in* (5.27) *of Theorem 5.4.5, the error term is given by*

$$\mathcal{R}(\varepsilon) = \frac{1}{2\pi \mathbb{i}} \int_S \zeta_{\mathcal{T}}(\varepsilon, s)\, ds, \tag{D.9}$$

*and is a well-defined distribution.*

*Proof.* Applying (5.17) to (5.47) for $i = 0, \ldots, d$ gives[1]

$$\langle \mathcal{R}, \varphi \rangle_{qi} = \frac{1}{2\pi \mathbb{i}} \int_S g_q^s \zeta_{\mathfrak{s}}(s) \int_0^\infty \kappa_{qi}(\varepsilon) \frac{\varepsilon^{d-s}}{s-i} \varphi(\varepsilon)\, d\varepsilon\, ds. \tag{D.10}$$

To see that this gives a well-defined distribution $\mathcal{R}$, we apply the descent method, as described in [La-vF4, Rem. 5.20]. See also Remark 2.4.1 and the discussion following (2.35). The first step is to show that $\left\langle \mathcal{R}^{[k]}, \varphi \right\rangle_{qi}$ is a well-defined distribution for sufficiently large $k$; specifically, for any integer $k > M$, where $M$ is as in Definition B.1.2. Note that we can break the integral along the screen $S$ into two pieces and work with each separately:

$$\left\langle \mathcal{R}^{[k]}, \varphi \right\rangle_{qi} = \frac{(-1)^k}{2\pi \mathbb{i}} \int_{|\operatorname{Im} s| > 1} g_q^s \zeta_{\mathfrak{s}}(s) \int_0^\infty \kappa_{qi}(\varepsilon) \frac{\varepsilon^{d-s}}{s-i} \varphi^{[k]}(\varepsilon)\, d\varepsilon\, ds \tag{D.11}$$

[1] In the proof of Theorem 5.4.5, the quantity (D.10) was denoted by $\langle \mathcal{R}_{qi}, \varphi \rangle$, so that $\mathcal{R}$ could easily be written (formally) as a function in (5.48). Since we work with test functions, this quantity is instead denoted by $\langle \mathcal{R}, \varphi \rangle_{qi}$ throughout this proof.

$$+ \frac{(-1)^k}{2\pi \mathbb{i}} \int_{|\operatorname{Im} s| \leq 1} g_q^s \zeta_{\mathfrak{s}}(s) \int_0^\infty \kappa_{qi}(\varepsilon) \frac{\varepsilon^{d-s}}{s-i} \varphi^{[k]}(\varepsilon)\, d\varepsilon\, ds. \qquad \text{(D.12)}$$

Here and throughout the rest of this appendix, it is understood that such integrals (as in (D.11)–(D.12)) are for $s \in S$. Since the screen avoids the integers $0, \ldots, d$ by assumption, the quantity $|s-i|$ is bounded away from 0. Recall from the proof of Cor. C.1.6 that $\kappa_{qi}$ is bounded on the support of $\varphi$ by some constant $c_{qi} > 0$. Since the screen avoids the poles of $\zeta_{\mathfrak{s}}$ by hypothesis, $\zeta_{\mathfrak{s}}(s)$ is continuous on the compact set $\{s \in S \,\vdots\, |\operatorname{Im} s| \leq 1\}$. Therefore, it is clear that (D.12) is a well-defined integral. We focus now on (D.11):

$$\begin{aligned}
&\left| \frac{1}{2\pi \mathbb{i}} \int_{|\operatorname{Im} s| > 1} g_q^s \zeta_{\mathfrak{s}}(s) \int_0^\infty \kappa_{qi}(\varepsilon) \frac{\varepsilon^{d-s}}{s-i} \varphi^{[k]}(\varepsilon)\, d\varepsilon\, ds \right| \\
&\quad \leq \frac{1}{2\pi} \int_{\operatorname{Im} s > 1} \left| \frac{g_q^s \zeta_{\mathfrak{s}}(s)}{s-i} \right| \cdot \left| \widetilde{\kappa_{qi} \varphi^{[k]}}(s-d+1) \right| ds \\
&\quad \leq c_1 \int_1^\infty |t|^{M-1} \cdot |\widetilde{\kappa_{qi}\varphi}(s-d+k+1)| \cdot |\psi_k(s-d+1)|\, dt \\
&\quad \leq c_1 \int_1^\infty |t|^{M-1} \cdot c_K c_{qi} \|\varphi\|_\infty \cdot \frac{c_\psi}{|t|^k}\, dt, \\
&\quad = C\|\varphi\|_\infty \int_1^\infty |t|^{M-1-k}\, dt,
\end{aligned} \qquad \text{(D.13)}$$

which is clearly convergent for $k > M$. The second inequality in (D.13) comes by (B.6) and Cor. D.1.19. Also, recall that for $s \in S$, the real part of $s$ is given by a function $f$ which is Lipschitz, and hence is almost every differentiable and has bounded derivatives on the support of $\varphi$. The third comes by Cor. C.1.6, or rather, inequality (C.7) of Remark C.1.7, along with Remark D.1.20. This establishes the validity of $\left\langle \mathcal{R}^{[k]}, \varphi \right\rangle_{qi}$ and thus shows that $\mathcal{R}^{[k]}$ defines a linear functional on $\mathbb{D}$.

To check that the action of $\mathcal{R}^{[k]}$ is continuous on $\mathbb{D}$, let $\varphi_n \to 0$ in $\mathbb{D}$, i.e., suppose $K$ is a compact set which contains the support of every $\varphi_n$, and $\|\varphi_n\|_\infty \to 0$. Then

$$\left| \langle \mathcal{R}^{[k]}, \varphi_n \rangle \right| \leq C \cdot |\widetilde{\varphi}_n(s-d+k+1)| \leq c_K \|\varphi_n\|_\infty \xrightarrow{n\to\infty} 0, \qquad \text{(D.14)}$$

by following (D.13) and then applying Lemma C.1.5, along with its extensions as stated in Remark C.1.7. Thus, $\mathcal{R}^{[k]}$ is a well-defined distribution. If we differentiate it distributionally $k$ times, we obtain $\mathcal{R}$. This shows that $\mathcal{R}$ is a well-defined distribution and concludes the proof. $\square$

Before finally checking the error estimate, we define what is meant by the expression $T(x) = O(x^\alpha)$ as $x \to \infty$, when $T$ is a distribution.

**Definition D.1.22.** When $\mathcal{R}(x) = O(x^\alpha)$ as $x \to \infty$ (as in (5.16)), we say as in [La-vF4, §5.4.2] that $\mathcal{R}$ is of *asymptotic order at most* $x^\alpha$ as $x \to \infty$. To understand this expression, first define

$$\varphi_a(x) := \tfrac{1}{a}\varphi\left(\tfrac{x}{a}\right), \tag{D.15}$$

for $a > 0$ and for any test function $\varphi$. Then "$\mathcal{R}(x) = O(x^\alpha)$ as $x \to \infty$" means that

$$\langle \mathcal{R}, \varphi_a \rangle = O(a^\alpha), \qquad \text{as } a \to \infty,$$

for every test function $\varphi$. The implied constant may depend on $\varphi$. Similarly, the expression "$\mathcal{R}(x) = O(x^\alpha)$ as $x \to 0^+$" (as in (5.29)) is defined to mean that

$$\langle \mathcal{R}, \varphi_a \rangle = O(a^\alpha), \qquad \text{as } a \to 0^+,$$

for every test function $\varphi$.

**Theorem D.1.23** (Error estimate)**.** *As stated in Theorem 5.4.5, the error term* $\mathcal{R}(\varepsilon)$ *in* (D.9) *is estimated by*

$$\mathcal{R}(\varepsilon) = O(\varepsilon^{d-\sup S}), \qquad \textit{as } \varepsilon \to 0^+. \tag{D.16}$$

*Proof.* As in the proof of Theorem D.1.21, we use the descent method and begin by splitting the integral into two pieces. Since $\langle \mathcal{R}^{[k]}, \varphi_a \rangle = (-1)^k \langle \mathcal{R}, (\varphi_a)^{[k]} \rangle$, we work with

$$\left\langle \mathcal{R}, (\varphi_a)^{[k]} \right\rangle_{qi} = \frac{1}{2\pi\mathbb{i}} \int_{|\operatorname{Im} s|>1} g_q^s \zeta_{\mathfrak{s}}(s) \int_0^\infty \kappa_{qi}(\varepsilon) \frac{\varepsilon^{d-s}}{s-i} (\varphi_a)^{[k]}(\varepsilon)\, d\varepsilon\, ds \tag{D.17}$$

$$+ \frac{1}{2\pi\mathbb{i}} \int_{|\operatorname{Im} s|\le 1} g_q^s \zeta_{\mathfrak{s}}(s) \int_0^\infty \kappa_{qi}(\varepsilon) \frac{\varepsilon^{d-s}}{s-i} (\varphi_a)^{[k]}(\varepsilon)\, d\varepsilon\, ds. \tag{D.18}$$

The $k^{\text{th}}$ primitive of $\varphi_a$ is given by

$$
\begin{aligned}
(\varphi_a)^{[k]}(\varepsilon) &= \int_\varepsilon^\infty \frac{(u-\varepsilon)^{k-1}}{(k-1)!} \tfrac{1}{a}\varphi\left(\tfrac{u}{a}\right)\, du \\
&= \int_{\varepsilon/a}^\infty \frac{(au-\varepsilon)^{k-1}}{(k-1)!}\varphi(u)\, du. \qquad \text{(D.19)}
\end{aligned}
$$

By following the same calculations as in Theorem D.1.18, one observes that

$$
\begin{aligned}
&\left| \int_0^\infty \kappa_{qi}(\varepsilon) \frac{\varepsilon^{d-s}}{s-i} \int_{\varepsilon/a}^\infty \frac{(au-\varepsilon)^{k-1}}{(k-1)!}\varphi(u)\, du\, d\varepsilon \right| \\
&= \left| \int_0^\infty \int_0^{au} \frac{\kappa_{qi}(\varepsilon)}{s-i} \sum_{j=0}^{k-1} \frac{\binom{k-1}{j}(-1)^j}{(k-1)!} (au)^{k-1-j} \varepsilon^{d-s+j} \varphi(u)\, d\varepsilon\, du \right| \\
&\le \frac{1}{|s-i|} \sum_{j=0}^{k-1} \frac{\binom{k-1}{j}(-1)^j}{(k-1)!} \int_0^\infty \left|(au)^{k-1-j}\varphi(u)\right| \int_0^{au} \left|\kappa_{qi}(\varepsilon)\varepsilon^{d-s+j}\, d\varepsilon\right|\, du \\
&\le \frac{c_{qi}}{|s-i|} \psi_k(d-\operatorname{Re} s+1) \int_0^\infty (au)^{k-1-j} (au)^{d-\operatorname{Re} s+j+1} |\varphi(u)|\, du \\
&= a^{d-\operatorname{Re} s+k} \frac{c_{qi}}{|s-i|} \psi_k(d-\operatorname{Re} s+1) \widetilde{|\varphi|}(d-\operatorname{Re} s+k). \qquad \text{(D.20)}
\end{aligned}
$$

Using (D.8) for $\psi_k$ and (C.3) for $\widetilde{|\varphi|}$ (see Remark C.1.7), we bound (D.17) by

$$
\begin{aligned}
&\frac{c_{qi}}{2\pi} \int_{|\operatorname{Im} s|>1} a^{d-\operatorname{Re} s+k} \cdot \frac{|g_q^s \zeta_{\mathfrak{s}}(s)|}{|s-i|} \cdot \frac{c_\psi}{|t|^k} \cdot c_K \|\varphi\|_\infty\, ds \qquad \text{(D.21)} \\
&\le a^{d-\sup S+k} \left( C \int_1^\infty |t|^{M-1-k}\, dt \right), \qquad \text{(D.22)}
\end{aligned}
$$

for any $0 < a < 1$, as in (D.13). Since the integral in (D.22) clearly converges for $k > M$, we have established the estimate for $\mathcal{R}^{[k]}$, along the part of the integral where $|\operatorname{Im} s| > 1$. Recall that all our contour integrals are taken along the screen $S$. The proof for (D.18), where $|\operatorname{Im} s| > 1$, readily follows from the corresponding argument in the proof of Theorem D.1.21. Thus we have established that

$$
\left|\langle \mathcal{R}^{[k]}(\varepsilon), \varphi_a(\varepsilon)\rangle\right| \le a^{d-\sup S+k} c_k, \quad \text{for all } 0 < a < 1. \qquad \text{(D.23)}
$$

In (D.23)–(D.25), the constants $c_k$ are allowed to depend on the test function $\varphi$.[2]

By iterating the following calculation:

$$\begin{aligned}\left|\langle \mathcal{R}^{[k-1]}(\varepsilon), \varphi_a(\varepsilon)\rangle\right| &= \left|\langle \mathcal{R}^{[k]}(\varepsilon), \left(\tfrac{1}{a}\varphi\left(\tfrac{\varepsilon}{a}\right)\right)'\rangle\right| \\ &= \left|\tfrac{1}{a}\langle \mathcal{R}^{[k]}(\varepsilon), (\varphi')_a(\varepsilon)\rangle\right| \\ &\leq a^{d-\sup S+k-1} c_{k-1},\end{aligned} \tag{D.24}$$

one sees that

$$|\langle \mathcal{R}(\varepsilon), \varphi_a(\varepsilon)\rangle| \leq a^{d-\sup S} c_0, \quad \text{for all } 0 < a < 1. \tag{D.25}$$

By Definition D.1.22, this implies that $\mathcal{R}(\varepsilon) = O(\varepsilon^{d-\sup S})$ as $\varepsilon \to 0^+$. $\square$

[2]Note that $c_{k-1}$ does not correspond to $c_k$ when $k$ is replaced by $k-1$; rather, $c_{k-1}$ depends on the support of $\varphi'$. The notation is just used to indicate the analogous roles the constants $c_k$ play.

# Bibliography


[BeGo] M. Berger and B. Gostiaux, *Differential Geometry: Manifolds, Curves and Surfaces*, English transl., Springer-Verlag, Berlin, 1988.

[Fal1] K. J. Falconer, *Fractal Geometry — Mathematical Foundations and Applications*, John Wiley, Chichester, 1990.

[Fal2] K. J. Falconer, On the Minkowsi measurability of fractals, *Proc. Amer. Math. Soc.* **123** (1995), 1115–1124.

[Fed] H. Federer, Curvature measures, *Trans. Amer. Math. Soc.* **93** (1959), 418–491.

[Fra] M. Frantz, Minkowski measurability and lacunarity of self-similar sets in $\mathbb{R}$, preprint, December 2001.

[Fu1] J. H. G. Fu, Tubular neighbourhoods in Euclidean spaces, *Duke Math. J.* **52** (1985), 1025–1046.

[Fu2] J. H. G. Fu, Curvature measures of subanalytic sets, *Amer. J. Math.* **116** (1994), 819–880.

[Gat] D. Gatzouras, Lacunarity of self-similar and stochastically self-similar sets, *Trans. Amer. Math. Soc.* **352** (2000), 1953–1983.

[Gr] A. Gray, *Tubes (second ed.), Progress in Math 221*, Birkhäuser, Boston, 2004.

[HaLa] B. M. Hambly and M. L. Lapidus, Random fractal strings: Their zeta functions, complex dimensions and spectral asymptotics, *Trans. Amer. Math. Soc.* (2005), *in press*.

[HeLa1] C. Q. He and M. L. Lapidus, Generalized Minkowski content and the vibrations of fractal drums and strings, *Mathematical Research Letters* **3** (1996), 31-40.

[HeLap2] C. Q. He and M. L. Lapidus, Generalized Minkowski content, spectrum of fractal drums, fractal strings and the Riemann zeta-function, *Memoirs Amer. Math. Soc.* No. 608 **127** (1997), 1-97.

[HLW] D. Hug, G. Last, W. Weil, A local Steiner-type formula for general closed sets and applications, *Mathematische Zeitschrift.* **246** (2004), 237–272.

[Hut] J. E. Hutchinson, Fractals and self-similarity, *Indiana Univ. Math. J.* **30** (1981), 713–747.

[KLSW] R. Kenyon, J. Li, R. S. Strichartz and Y. Wang, Geometry of self-affine tiles II, *Indiana Univ. Math. J.* 1 **48** (1999), 25–42.

[Kig] J. Kigami, *Analysis on Fractals*, Cambridge University Press, Cambridge, 1999.

[KlRo] Daniel A. Klain, Gian-Carlo Rota, *Introduction to Geometric Probability*, Accademia Nazionale dei Lincei, Cambridge University Press, Cambridge, 1999.

[L] S. P. Lalley, Packing and covering functions of some self-similar fractals, *Indiana Univ. Math. J.* **37** (1988), 699–709.

[La1] M. L. Lapidus, Fractal drum, inverse spectral problems for elliptic operators and a partial resolution of the Weyl–Berry conjecture, *Trans. Amer. Math. Soc.* **325** (1991), 465–529.

[La2] M. L. Lapidus, *Spectral and fractal geometry: From the Weyl–Berry conjecture for the vibrations of fractal drums to the Riemann zeta-function,* in: Differential Equations and Mathematical Physics (C. Bennewitz, ed.), Proc. Fourth UAB Internat. Conf. (Birmingham, March 1990), Academic Press, New York, 1992, pp. 151–182.

[La3] M. L. Lapidus, *Vibrations of fractal drums, the Riemann hypothesis, waves in fractal media, and the Weyl–Berry conjecture,* in: Ordinary and Partial Differential Equations (B. D. Sleeman and R. J. Jarvis, eds.), vol. IV, Proc. Twelfth Internat. Conf. (Dundee, Scotland, UK, June 1992), Pitman Research Notes in Math. Series, vol. 289, Longman Scientific and Technical, London, 1993, pp. 126–209.

[LaMa] M. L. Lapidus and H. Maier, The Riemann hypothesis and inverse spectral problems for fractal strings, *J. London Math. Soc.* (2) **52** (1995), 15–34.

[LaPe1] M. L. Lapidus and E. P. J. Pearse, A tube formula for the Koch snowflake curve, with applications to complex dimensions, *J. London Math. Soc.,* in press, (2005). `arXiv: math-ph/0412029`

[LaPe2] M. L. Lapidus and E. P. J. Pearse, Tube formulas and complex dimensions of self-similar tilings, preprint, May 2006, 61 pages. `arXiv: math.DS/0605527`

[LaPe3] M. L. Lapidus and E. P. J. Pearse, Tube formulas for generators of self-similar tilings, in preparation.

[LaPe4] M. L. Lapidus and E. P. J. Pearse, Fractal curvature measures and local tube formulas, in preparation.

[LaPo1] M. L. Lapidus and C. Pomerance, The Riemann-zeta function and the one-dimensional Weyl–Berry conjecture for fractal drums, *Proc. London Math. Soc.* (3) **66** (1993), 41–69.

[LaPo2] M. L. Lapidus and C. Pomerance, Counterexamples to the modifed Weyl–Berry conjecture on fractal drums, *Math. Proc. Cambridge Philos. Soc.* **119** (1996), 167–178.

[La-vF1] M. L. Lapidus and M. van Frankenhuysen, *Fractal Geometry and Number Theory: Complex dimensions of fractal strings and zeros of zeta functions, 2nd ed.*, Birkhäuser, Boston, 2000.

[La-vF2] M. L. Lapidus and M. van Frankenhuysen, Fractality, Self-Similarity and Complex Dimensions, *Proc. Symp. in Pure Math.* (2000), 1–24.

[La-vF3] M. L. Lapidus and M. van Frankenhuysen, Complex dimensions of self-similar fractal strings and Diophantine approximation, *J. Experimental Mathematics* 1 **42** (2003), 43–69.

[La-vF4] M. L. Lapidus and M. van Frankenhuijsen, *Fractal Geometry, Complex Dimensions and Zeta Functions: geometry and spectra of fractal strings*, Springer Mathematical Monographs, Springer-Verlag, New York, in press. (To appear in July 2006.).

[LlWi] M. Llorente and S. Winter, A notion of Euler characteristic for fractals, in press. To appear in: *Math. Nachr.* (2005).

[Man] B. B. Mandelbrot, *The Fractal Geometry of Nature*, rev. and enl. ed., W.H. Freeman, New York, 1983.

[Mat] P. Mattila, *Geometry of Sets and Measures in Euclidean Spaces (Fractals and Rectifiability)*, Cambridge Univ. Press, Cambridge, 1995.

[Mu] J. R. Munkres, *Topology*, 2nd ed., Prentice Hall, Upper Saddle River, NJ, 2000.

[Pe] E. P. J. Pearse, Canonical self-similar tilings by IFS, preprint, Nov. 2005, 18 pages. `arXiv: math.MG/0606111`

[Rud] W. Rudin, *Functional Analysis* (2nd ed.), McGraw-Hill, New York, 1991.

[Schn1] R. Schneider, Curvature measures of convex bodies, *Ann. Mat. Pura Appl.* IV **116** (1978), 101–134.

[Schn2] R. Schneider, *Convex Bodies: The Brunn-Minkowski Theory*, Cambridge University Press, Cambridge, 1993.

[Sch] L. Schwartz, *Théorie des Distributions*, rev. and enl. ed., Hermann, Paris, 1966.

[Sta] L. L. Stacho, On curvature measures, *Acta Sci. Math.* **41** (1979), 191–207.

[StWa] R. S. Strichartz and Y. Wang, Geometry of self-affine tiles I, *Indiana Univ. Math. J.* 1 **48** (1999), 1–23.

[Tr] C. Tricot, *Curves and Fractal Dimensions*, Springer-Verlag, New York, 1995.

[We] H. Weyl, On the volume of tubes, *Amer. J. Math.* **61** (1939), 461–472.

[Wi] S. Winter, Curvature measures and fractals, Ph. D. Dissertation, Friedrich-Schiller-Universität Jena, 2006.

[Zä1] M. Zähle, Integral and current representation of Federer's curvature measures, *Arch. Math.* **46** (1986), 557–567.

[Zä2] M. Zähle, Curvatures and currents for unions of sets with positive reach, *Geom. Dedicata* **23** (1987), 155–171.

[Zy] A. Zygmund, *Trigonometric Series*, Cambridge University Press, Cambridge, 1959.

# List of Symbols

Page numbers in bold indicate the main definition

| | |
|---|---|
| $T$ | isometry of $\mathbb{R}^d$, rigid motion, 90, 94 |
| $T'$ | distributional derivative of $T \in \mathbb{D}'$, **172** |
| $T^{[k]}$ | $k^{\text{th}}$ primitive of the distribution $T \in \mathbb{D}'$, **175** |
| $T_\eta$ | distribution defined by integration with respect to a measure $\eta$ , **175** |
| $T_k$ | tileset, i.e., closure of the $k^{\text{th}}$ generation of tiles, **50**, **65** |
| $\mathcal{T}$ | self-similar tiling, **52**, 100 |
| $V_A(\varepsilon)$ | inner tube formula for the set $A$, **77** |
| $V_G(\varepsilon)$ | generator tube formula, 89, 90 |
| $V_\eta(\varepsilon)$ | tube formula for a (generalized) string $\eta$ , 111 |
| $V_{\mathbf{Kc}}(\varepsilon)$ | Koch tube formula, 6, 12, 20, 29, 33, 34 |
| $\widetilde{V}_{\mathbf{Kc}}(\varepsilon)$ | preliminary Koch tube formula, **19**, 20, 22, 29 |
| $V_L(\varepsilon)$ | volume of $\varepsilon$-neighborhood, 2 |
| $V_{\mathcal{L}}(\varepsilon)$ | tube formula for a fractal string $\mathcal{L}$ , 2, 4, 101 |
| $V_{\mathcal{T}}(\varepsilon)$ | inner tube formula for a tiling $\mathcal{T}$ , 75, **78**, 101, 102 |
| $V_q$ | the part of $V_{\mathcal{T}}$ corresponding to $G_q$, 116 |
| $W$ | window, 108, **165** |
| $w$ | word of length $k$, **48** |
| $w(\varepsilon)$ | width of a rectangle in an error block, in computing the Koch tube formula, 23 |
| $\xi$ | complex parameter; often set to $\frac{1}{2} + \frac{\mathrm{i}}{2\sqrt{3}}$, 13, 53, 137, 144 |
| $\psi_k$ | a certain meromorphic function relating $\widetilde{\varphi^{[k]}}(s)$ to $\widetilde{\psi}(s+k)$, 176 |
| $\zeta_L$ | zeta function of a string viewed as a 1-dimensional tiling, **131** |
| $\zeta_\eta$ | (scaling) zeta function of a fractal spray, 108, **113** |
| $\zeta_{\mathfrak{s}}$ | scaling zeta function, 7, **84**, 128 |
| $\zeta_{\mathcal{L}}$ | geometric zeta function of a fractal string, **3**, 73, **73**, 74, 102, 112, 130, 131 |
| $\zeta_{\mathcal{T}}$ | geometric zeta function of a tiling or spray, 7, **97**, 98, 114, 126 |

# Index